UCRL-TR-209923

FY04 Engineering Technology Reports

Laboratory Directed Research and Development

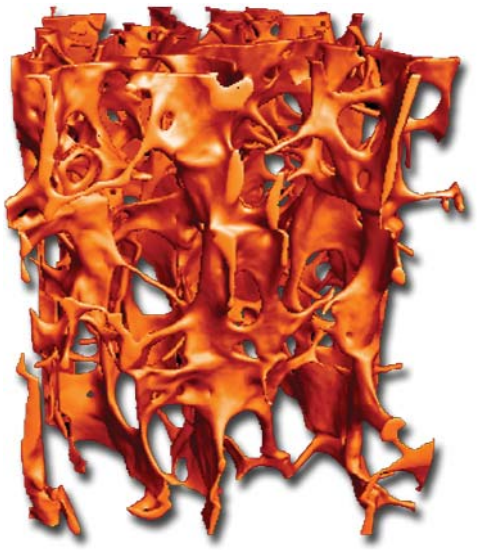

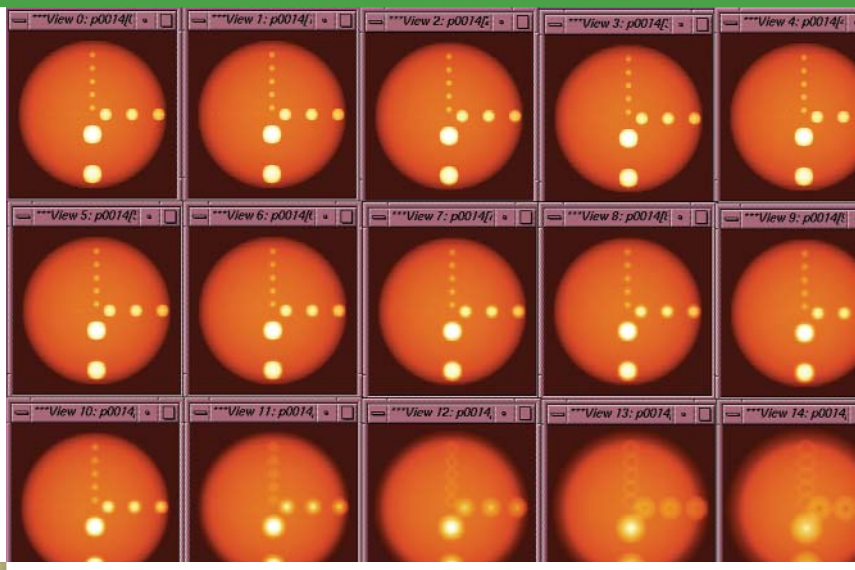

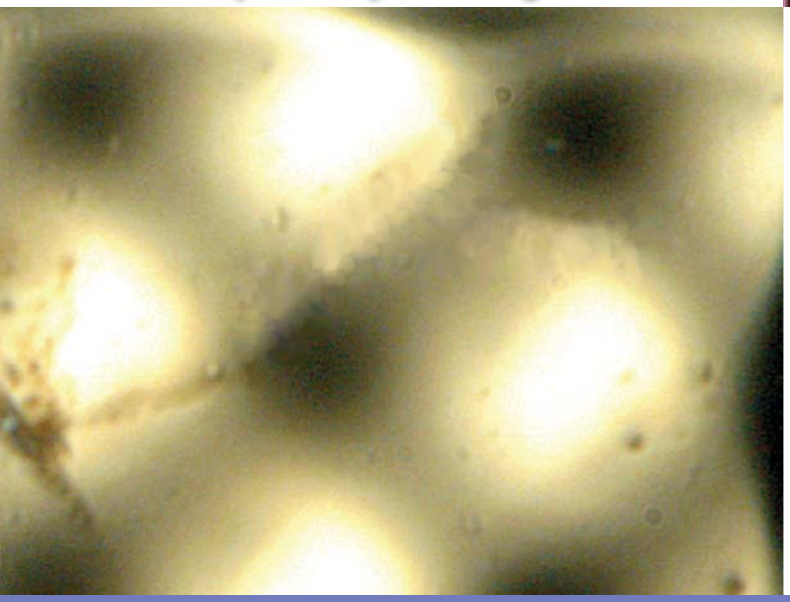

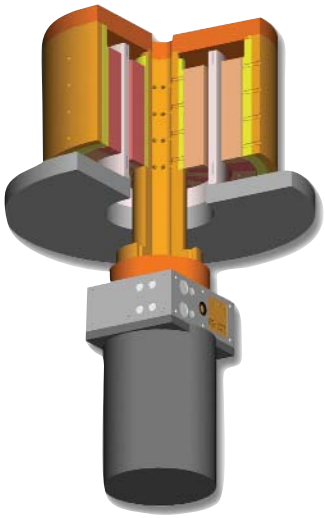

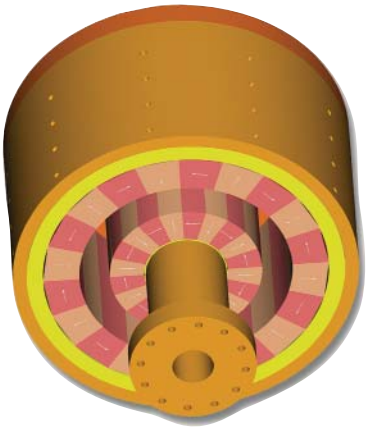

APRIL
2005
Lawrence Livermore National Laboratory

ENGINEERING X

Pushing engineering science to the Xtreme

Acknowledgments

Scientific Editing
Camille Minichino

Graphic Design
Irene J. Chan

Art Production/Layout
Jeffrey Bonivert
Lucy Dobson
Kathy J. McCullough
Debbie A. Ortega

Cover:
Graphics representing LDRD projects from Engineering's five Centers and other technologies.

FY04 Engineering Technology Reports

Laboratory Directed Research and Development

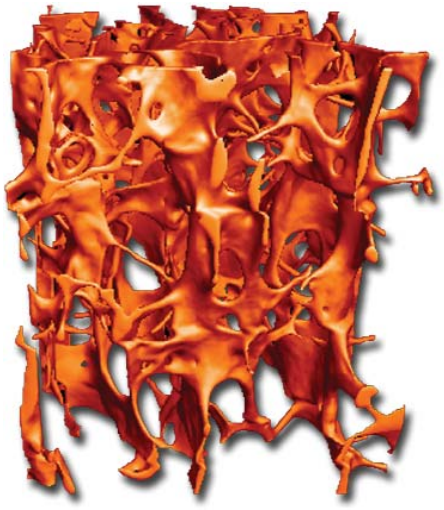

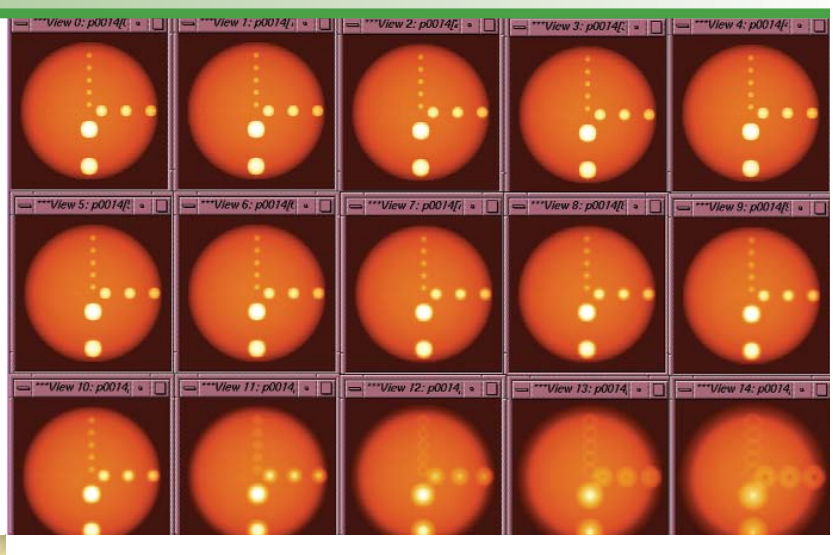

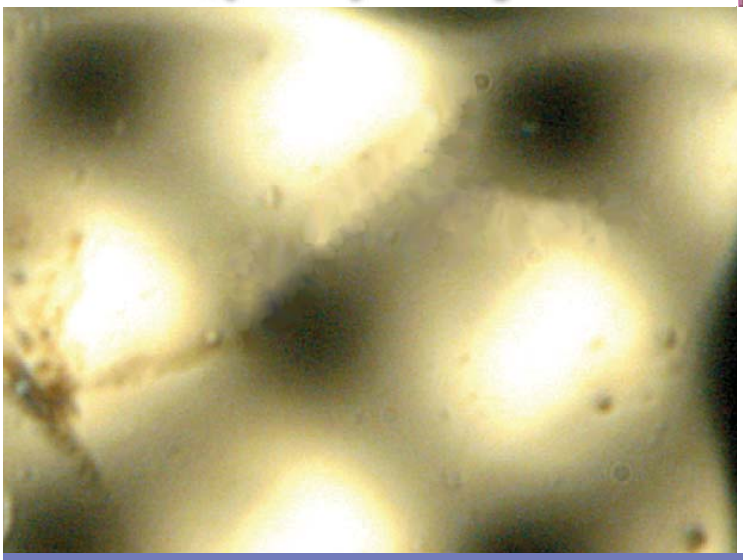

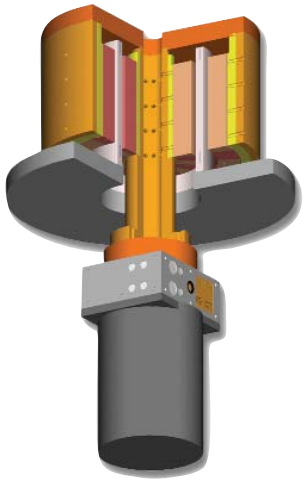

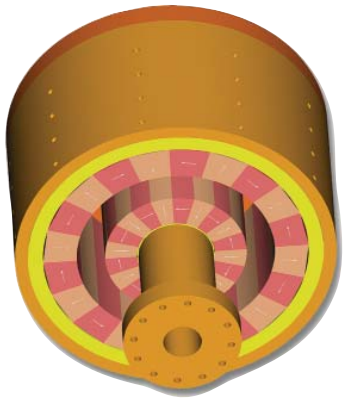

APRIL
2005

Contents

A Message from

Steven R. Patterson,
Associate Director for Engineering

This report summarizes the science and technology research and development efforts in Lawrence Livermore National Laboratory's Engineering Directorate for FY2004, and exemplifies Engineering's more than 50-year history of developing the technologies needed to support the Laboratory's missions. Engineering has been a partner in every major program and project at the Laboratory throughout its existence and has prepared for this role with a skilled workforce and the technical resources developed through venues like the Laboratory Directed Research and Development Program (LDRD). This accomplishment is well summarized by Engineering's mission: "Enable program success today and ensure the Laboratory's vitality tomorrow."

Engineering's investment in technologies is carried out through two programs, the "Tech Base" program and the LDRD program.

LDRD is the vehicle for creating those technologies and competencies that are cutting edge. These require a significant level of research or contain some unknown that needs to be fully understood. Tech Base is used to apply technologies to a Laboratory need. The term commonly used for Tech Base projects is "reduction to practice." Therefore, the LDRD report covered here has a strong research emphasis. Areas that are presented all fall into those needed to accomplish our mission.

For FY2004, Engineering's LDRD projects were focused on mesoscale target fabrication and characterization, development of engineering computational capability, material studies and modeling, remote sensing and communications, and microtechnology and nanotechnology for national security applications.

Engineering's five Centers, in partnership with the Division Leaders and Department Heads, are responsible for guiding the long-term science and technology investments for the Directorate. The Centers represent technologies that have been identified as critical for the present and future work of the Laboratory, and are chartered to develop their respective areas. Their LDRD projects are the key resources to attain this competency, and, as such, nearly all of Engineering's portfolio falls under one of the five Centers. The Centers and their Directors are:

- **Center for Computational Engineering:** Robert M. Sharpe
- **Center for Microtechnology and Nanotechnology:** Raymond P. Mariella, Jr.
- **Center for Nondestructive Characterization:** Harry E. Martz, Jr.
- **Center for Precision Engineering:** Keith Carlisle
- **Center for Complex Distributed Systems:** Gregory J. Suski, Acting Director

FY2004 Center Highlights

The **Center for Computational Engineering** orchestrates the research, development and deployment of software technologies to aid in many facets of the Laboratory's engineering mission. Computational engineering has become a ubiquitous component throughout the engineering discipline. Current activities range from fundamental improvements for modeling full-scale DOE and DoD systems performing at their limits to advances for treating photonic and micro-fluidic systems.

Highlights of the Center's LDRD projects for this year include advances in finite-element methods, and modeling and simulation tools; integration of electromagnetic capabilities with structural mechanics solutions; nonlinear materials treatments for photonic systems; and propagation models for comunication systems performance. The Center continues to offer a real-world computing capability that opens the door to solving a wide variety of fluid, solid, and electromagnetic interaction problems in homeland defense, stockpile stewardship, and key infrastructure settings.

The mission of the **Center for Microtechnology and Nanotechnology** is to invent, develop, and apply microscale and nanoscale technologies to support the Laboratory missions in Stockpile Stewardship, Homeland Security, Nonproliferation, and other programs. The research topics for this Center cover materials, devices, instruments, and systems that require microfabricated components, including microelectromechanical systems (MEMS), electronics, photonics, micro- and nanostructures, and micro- and nanoactuators.

This year's projects include a microfluidic system for solution-array-based bioassays, and tools to perform a virtual electronic polymerase chain reaction.

The **Center for Nondestructive Characterization** researches and develops nondestructive characterization measurement technology to significantly impact the manner in which the Laboratory inspects, and through this, designs and refurbishes systems and components. The Center plays a strategic and vital role in the research and development of scientific and engineering NDC technologies, such as acoustic, infrared, microwave, ultrasonic, visible and x-ray imaging, to enable Engineering in the far- to mid-term to incorporate the successful technologies into Laboratory and DOE programs.

This year's LDRD projects include concealed threat detection at multiple frames/second; phase effects on mesoscale object x-ray absorption images; nanoscale fabrication of mesoscale objects; precision x-ray optics development; and ultrasonic NDE of multilayered structures.

The **Center for Precision Engineering** advances the Laboratory's high-precision capabilities in manufacturing, dimensional metrology, and assembly, to meet the future needs of the Laboratory and DOE programs. Precision engineering is a multi-disciplinary systems approach to achieve an order of magnitude greater accuracy than currently achievable. Essential to the Center's success are its core technologies, which are the building blocks for the machines, systems, and processes that will be required for future programs. Our LDRD portfolio is driven to support this goal.

Highlights for this year include a high-bandwidth fast tool servo for single-point turning in high-energy-density physics targets; a high-stiffness hybrid passive/active magnetic bearing for precision engineering applications; and our work with the other Centers on fabrication projects.

The **Center for Complex Distributed Systems** was formed to promote technologies essential to the analysis, design, monitoring and control of large-scale, complex systems. Given the ubiquitous nature of large systems, CDS obviously covers a very broad technical area. This includes development of integrated sensing, communication and signal processing systems for efficient gathering of the data essential for real-time system monitoring. The Center also promotes the development of new methodologies for combining measured data with computer simulations in order to achieve enhanced characterization and control of complex systems.

As reported in this volume, the Center has projects in security sensor systems, seismic arrays and wave propagation, and communications. Particular emphasis is on technologies applicable to national security missions.

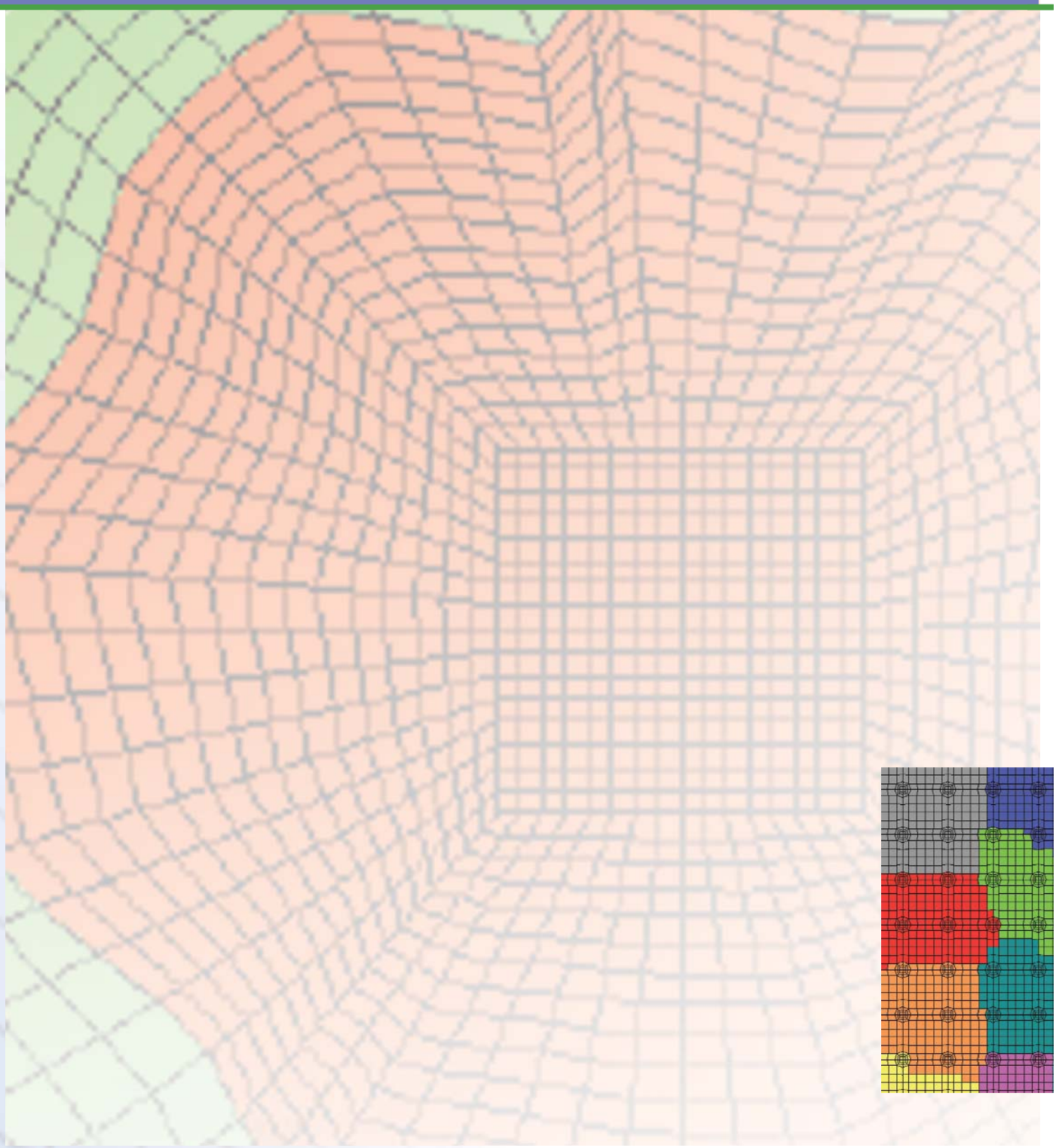

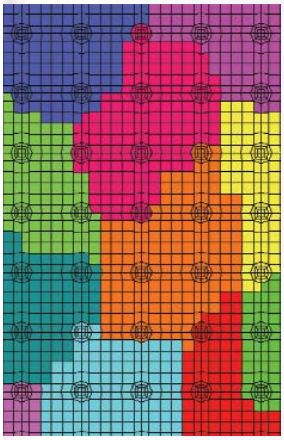

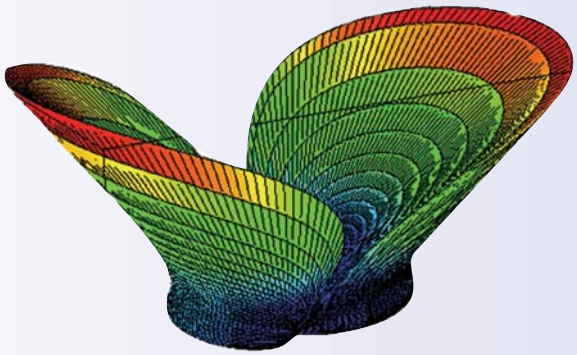

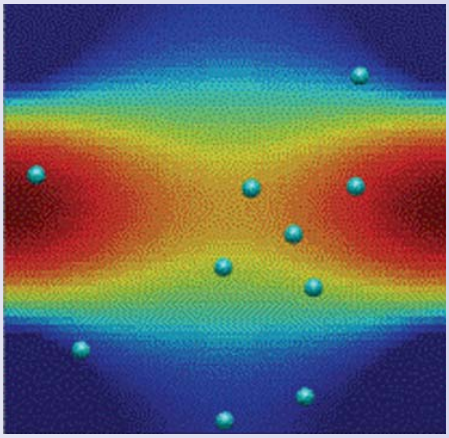

Center for Computational Engineering

LDRD

A New "Natural Neighbor" Meshless Method for Modeling Extreme Deformations and Failure

For more information contact **Michael Puso**
(925) 422-8198, puso1@llnl.gov

The objective of this project is to develop a fully Lagrangian analysis approach, based on a "natural neighbor" discretization technique, to model extreme deformation and failure for analyses such as earth penetration and dam failure. The method is related to finite elements, except that arbitrary polyhedral elements are defined by Laplace shape functions. A free Lagrange approach can then be exploited such that mesh connectivity is redefined on the fly to eliminate mesh tangling. No remapping of quantities will be required since they will be computed and stored at the node points. The method is more stable than SPH methods, is faster than EFG meshless methods and circumvents the advection required by ALE. The method will be effectively meshless (nodes, and not connectivity, will define the model) and will be incorporated into DYNA3D.

Project Goals

If successful, the new approach will provide an improved method for modeling extreme events. For example, since the method is fully Lagrangian, better descriptions of anisotropic material damage for concrete can be applied, whereas Eulerian/ALE techniques have difficulties with these models due to advection. Water spilling over the damaged dam could be modeled with this approach. SPH is also fully Lagrangian but has stability issues and isn't suitable for implicit type problems such as static gravity loading of a dam. Because it is "meshless," the approach could be used for applications where nondestructive evaluations are required, such as as-built weapons analysis or biomechanics. In short, a much larger class of problems could then be solved.

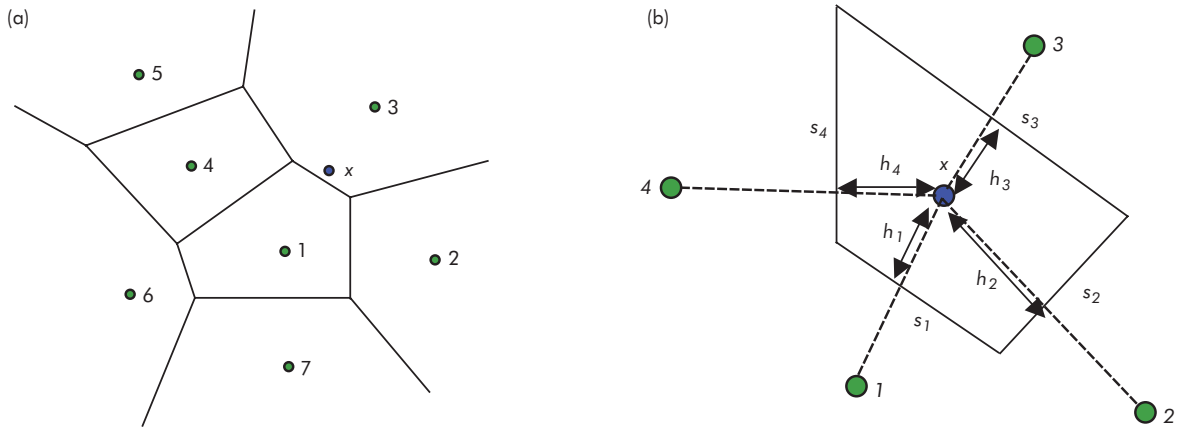

Figure 1. (a) Cloud of seven points and associated Voronoi diagram. Considering the arbitrary location, x, in (a), a secondary local Voronoi cell (b) can be formed about this location, x, using its "nearest neighbors," points 1 to 4.

Relevance to LLNL Mission

The proposed approach treats solid and fluid mechanics and is applicable to some important LLNL problems. Analyses of earth penetration, and terrorist vulnerability evaluation of infrastructures are target applications for this new approach. As-built x-ray tomography of NIF targets and *in-vivo* MRI imaging for biomechanics create "point clouds" and are good examples where some form of meshless method could be exploited for expediting stress analyses.

FY2004 Accomplishments and Results

In mid-FY2004, we began definition of data structures and code module development for the NIKE3D/DYNA3D implementation. This included the following tasks: 1) set up general, ragged-type data structures to handle arbitrary connectivity of a cloud of points; 2) implement Voronoi techniques for identifying nearest neighbors and discerning surface boundaries necessary for defining the integration domain; and 3) implement Laplace interpolation modules.

The natural neighbor method uses the Laplace shape functions defined from a Voronoi diagram of the cloud of points. Consider the 2-D cloud of points and the associated Voronoi diagram in Fig. 1 (a). The shape function N_i for node i = 1,4 evaluated at the location x, is computed from this local Voronoi cell in Fig. 1 (b) about the point x, using the length s_i (the length of the edge) and h_i (the distance between x and p_i) through the following equation:

$$N_i(\boldsymbol{x}) = \frac{s_i/h_i}{\sum_{j=1}^{5} s_j/h_j}$$

A stabilized nodal integration technique is then exploited to integrate the weak form of the equations of motion. In this approach, an average strain is computed at node i by integrating the strain field calculated from the shape functions, over the Voronoi cell of node i. By definition, the Voronoi diagram is unbounded and must be "trimmed" at the perceived surface boundaries (see Fig. 2). So, for example, the cloud of points in Fig. 3 (a) produces the "trimmed" Voronoi diagram in Fig. 3 (b).

We now have most of the parts of a serial implementation in NIKE3D completed.

FY2005 Proposed Work

FY2005 will be dedicated to finishing the NIKE3D/DYNA3D small deformation implementation and extending the work to handle large deformations and damage. Tasks include further evaluating different approaches for determining surface definition from a cloud of points; evaluating the free Lagrange approach for doing large deformations; and exploring different damage models.

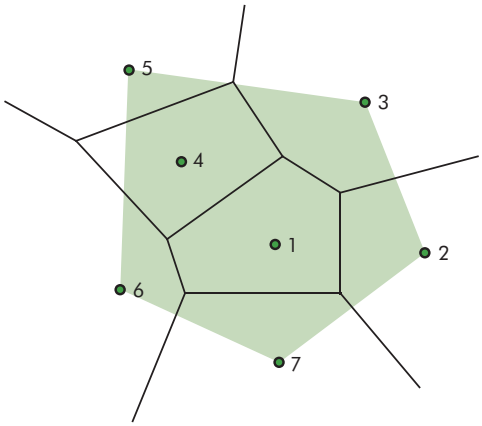

Figure 2. Unbounded Voronoi diagram "trimmed" by perceived surface boundaries. Shaded area defines integration domain for weak form of equations of motion.

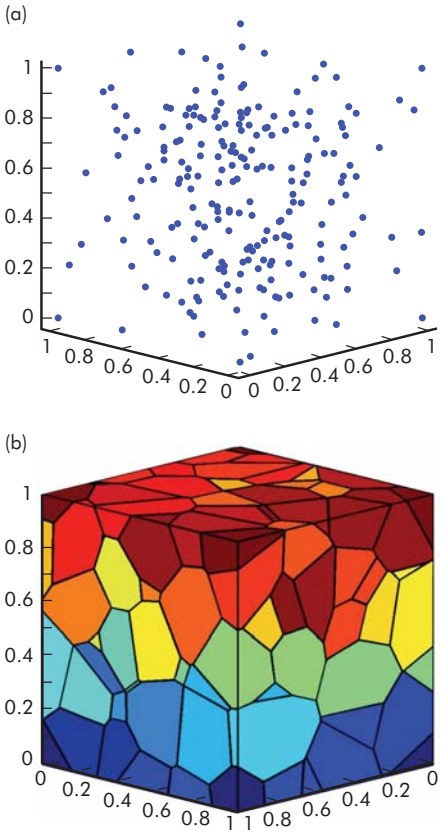

Figure 3. (a) Cloud of 216 points. (b) Voronoi diagram trimmed by surface definition.

Adaptive Mesh-Refinement Algorithms for Parallel Unstructured Finite-Element Codes

For more information contact **Dennis Parsons**
(925) 422-5208, parsons14@llnl.gov

At LLNL, the state-of-the-art solvers used for solid mechanics and electromagnetic simulations have sufficient architectural and functional maturity to benefit from the introduction of appropriate adaptive mesh-refinement (AMR) strategies. These new tools will enable analysts to conduct more reliable simulations at reduced cost, both in terms of analyst and computer time. Previous academic research in AMR has focused on error estimators and demonstration problems. Relatively little progress has been made on producing efficient implementations suitable for large-scale problem solving on state-of-the-art computer systems.

Research issues that we will consider include: effective error estimators for nonlinear structural mechanics and electromagnetics problems, local meshing at irregular geometric boundaries, and constructing efficient software for parallel computing environments.

Project Goals

The objective of this research is to implement AMR algorithms in unstructured finite-element codes used for solving nonlinear structural and electromagnetics problems on ASC-class, multiprocessor parallel (MPP) computers

Relevance to LLNL Mission

Many programmatic problems will be solved with greater precision and accuracy using the new AMR technology. Successful completion of this project will position LLNL as a leader in parallel finite-element technology by providing capabilities not present in other analysis systems.

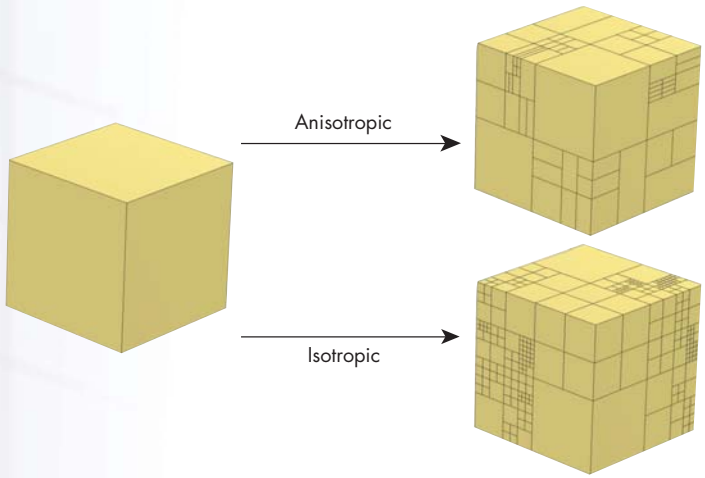

Figure 1. Meshes generated using isotropic and anisotropic *h*-refinement.

FY2004 Accomplishments and Results

To date, a serial AMR capability has been added to Diablo, a parallel structural analysis code. This includes the data structures and algorithms required to refine a user-defined mesh and error estimators based on patch recovery techniques and residual computations. Simple test problems have been constructed to confirm the correctness of the implementations.

The AMR implementation is able to perform both isotropic and anisotropic refinement as well as derefinement of a mesh (Fig. 1). Anisotropic refinement (i.e., refinement based on a directional error estimator) and derefinement are crucial for solving highly transient problems and implicit analysis, where the cost of solving equations can increase considerably with problem size.

Both residual- and patch-based error estimators are being developed for specific application to large-deformation solid mechanics problems with contact. A patch recovery scheme has already been implemented, and is undergoing testing. Two different kinds of residual-based schemes are now being implemented. Design of the parallel implementation is currently underway. Algorithm and software documentation are being produced using the UML that will form the basis of the abstraction of the AMR schemes. Coupled thermomechanics simulations have been conducted to demonstrate the capabilities of the current AMR implementation in Diablo (Fig. 2).

For electromagnetics, a global L2 projection-based error estimator has been developed and tested (Fig. 3), and a local patch recovery-based error estimator is currently under development. Both of these error estimators, at present, are limited to single material problems. Extension of these error estimators to multiple material problems will occur next year.

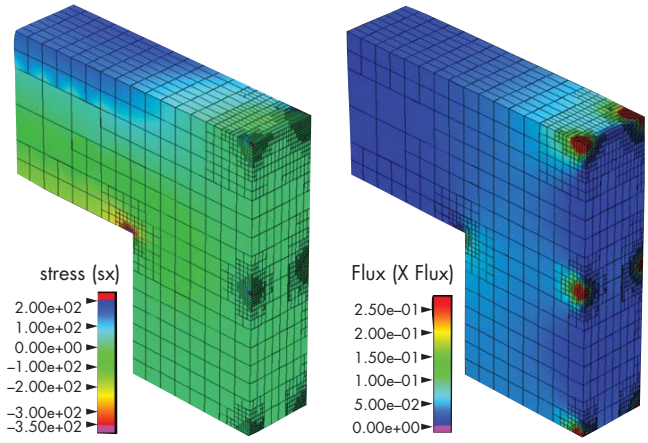

Figure 2. Stress and temperature gradient fields in a plate subjected to mechanical and thermal loads.

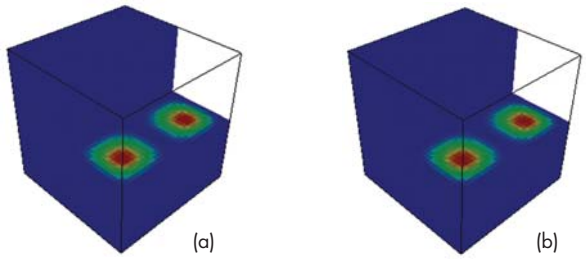

Figure 3. (a) Actual error and (b) estimated error showing the effectiveness of the error estimator for an electromagnetics demonstration problem.

FY2005 Proposed Work

The serial unstructured functionality developed for solid mechanics will be used to investigate the effectiveness of published algorithms for estimating discretization errors and for interpolating state variables to refined meshes. If necessary, improvements will be explored. The AMR functionality will be parallelized for efficient performance on MPP systems by introducing mesh-partitioning capabilities for allocating load-balanced subassemblies of a refined unstructured mesh to the available processors. The underlying data structures will be modified to account for the resulting additional interprocessor communications.

A hierarchical mesh-refinement capability will be combined with the error estimators to form an automatic AMR capability for electromagnetics. Optimization of the algorithm for parallel efficiency will also be conducted.

Dynamic Simulation Tools for the Analysis and Optimization of Novel Collection, Filtration, and Sample Preparation Systems

For more information contact **David S. Clague**
(925) 424-9770, clague1@llnl.gov

We are developing novel multiphysics simulation tools to address design and optimization needs in the general class of problems that involve air- and water-borne species and fluid (liquid and gas phases) transport through sieving media. This new capability will be specifically designed to characterize sub-system efficiencies, such as filter efficiency, based on the details of the microstructure, surface interactions, and environmental effects.

To accomplish this, we propose to develop new lattice-Boltzmann (LB) simulation tools that will include detailed microstructure descriptions, relevant surface interactions, and temperature effects, and be able to handle both liquid and gas phase systems. We are in the process of demonstrating the applicability of this new capability to transport problems relevant to homeland security, energy, and the environment.

Project Goals

The goal of this project is to equip scientists and engineers with the computational tools to analyze and optimize novel collection, filtration, and sample preparation systems.

Relevance to LLNL Mission

This capability will be directly applicable to Laboratory programs on weapons, energy and environment, medical technology, chemical and biological counter-proliferation, genomes, and homeland security. We are developing customers in the areas of aerosol transport, adhesion and re-suspension, and fluid and chemical transport in porous media.

FY2004 Accomplishments and Results

We have continued to study particle transport in viscous fluids through complex, fibrous media. This new capability, viscousLB, includes media module and colloidal interactions. To test this, we have continued our characterization of convective transport through ordered fibrous media. Figure 1 shows that our results exhibit very good agreement with those of Reference 2. The differences are due to their use of spheres to construct their

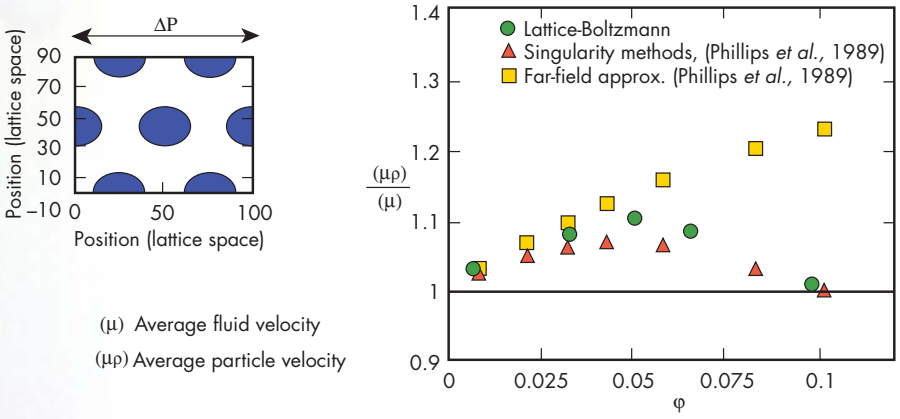

Figure 1. Comparison of convective transport coefficients predicted using the new lattice-Boltzmann capability (viscousLB) and the results of Reference 2.

cylinders, while we used cylinders directly. In addition to inclusion of the colloidal interactions module, we have expanded the capability to include Brownian forces on colloidal particles.

We have developed a gas phase fluid and particle simulation capability to enable characterization of flow and aerosol transport in complex porous media. A fourth order aerosol particle tracking routine was also developed and incorporated (Fig. 2).

To enhance the inclusion of colloidal interactions and external electric fields, we are coupling a fast multipole electromagnetic solver with viscousLB to rigorously solve the Poisson-Boltzmann equation and to include rigorous time-dependent electric fields. We are validating the aerosol transport module and the new Brownian Dynamics module, and testing the inclusion of colloidal forces in cylindrical pores for the porous membrane. Additionally, we have developed appropriate boundary conditions for gas flows, particles, and porous media. We are developing a customer base in the areas of aerosol dynamics and adhesion, flow in porous media, and flow in microenvironments with electric fields.

Related References

1. Clague, D. S., B. D. Kandhai, R. Zhang, and P. M. A. Sloot, "Hydraulic Permeability of (Un)bounded Fibrous Media Using the Lattice-Boltzmann Method," *Phys. Rev. E,* **61,** (1), pp. R1-985, 2000.

2. Phillips, R. J., W. M. Deen, and J. F. Brady, "Hindered Transport of Spherical Macro-Molecules in Fibrous Membranes and Gels," *AIChE J.,* **35,** (11), 1989.

3. Baron, P. A., and K. Willeke, Eds., Aerosol Measurement: Principles, Techniques, and Applications, Wiley Inter-Science, 2001.

FY2005 Proposed Work

Our plans are to: finalize the hybridization of the LB and Fast QR E&M capabilities and compare results with existing theory and experiment; extend our media module to incorporate filter/collector microstructures relevant to programmatic designs for a computational tool; perform analysis of filter/collector efficiencies with and without environmental temperature effects; finalize inclusion of the shear-thinning model and explore the implementation of unstructured grids to optimize physical resolution in desired domains; and apply Brownian motion capability to characterize particle petitioning and transport in nanoporous membranes, with colloidal interactions.

Factors affecting transport:
- media geometry (ordered, random)
- solid volume fraction (ϕ)
- ratio of fiber/particle size (λ)
- Knudsen number

Factors affecting surface capture:
- ratio of colloidal/aerodynamic forces
- surface charge density
- particle size

Aerosol flux calculation in an ordered filtration medium (φ = 0.05, λ = 10, Kn~0).

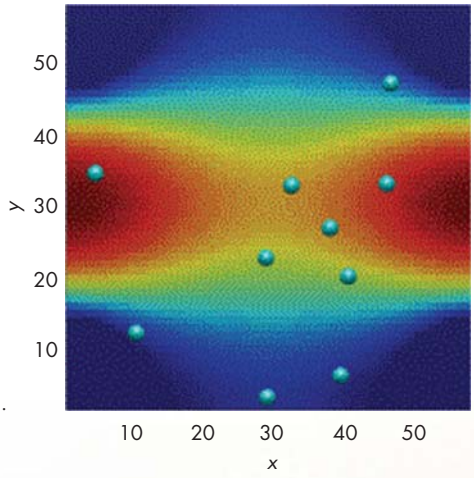

Figure 2. 2-D cross-section at a particular height of aerosol transport through a regular array of cylinders. The colors represent the magnitude of the fluid velocity. The cylinder quarters are in each corner of the periodic simulation cell.

Electro-Thermal-Mechanical Simulation Capability

For more information contact **Daniel A. White**
(925) 422-9870, white37@llnl.gov

LNL has long been a world leader in the area of computational mechanics, and recently several mechanics codes have become "multiphysics" codes with the addition of fluid dynamics, heat transfer, and chemistry. However, these multiphysics codes do not incorporate the electromagnetics that is required for a coupled electro-thermal-mechanical (ETM) simulation. There are numerous applications for an ETM simulation capability, such as explosively-driven magnetic flux compressors, electromagnetic launchers, inductive heating and mixing of metals, MEMS, and biophysics.

Project Goals

The purpose of this project is to research and develop numerical algorithms for 3-D ETM simulations. A simplified illustration of the coupling mechanisms is shown in Fig. 1. We will use an *H (curl)*-conforming finite-element method for the electromagnetics equations, and this will be coupled with existing finite-element thermal-mechanics codes, ALE3D and Diablo. Specific research issues that will be addressed include advection of electromagnetic quantities, continuity of electrical quantities in the context of contact, and Green's Function approaches for air/vacuum regions. The product will be a suite of ETM simulation software, designed for large-scale parallel simulation, and compatible with existing LLNL Engineering and DNT code frameworks.

Figure 1. Illustration of the proposed coupling mechanisms. The mechanics module computes the stress, strain, velocity (*V*), and position (*U*), of the geometry. The thermal module computes the temperature (*T*). The electromagnetics module computes the fields and currents, and provides the Joule heating $J \bullet E$ and the magnetic force $J \times B$ to the other modules.

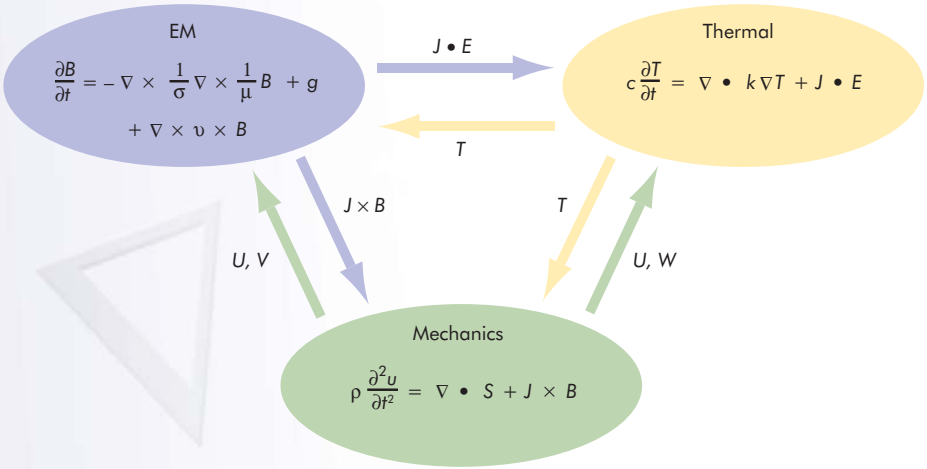

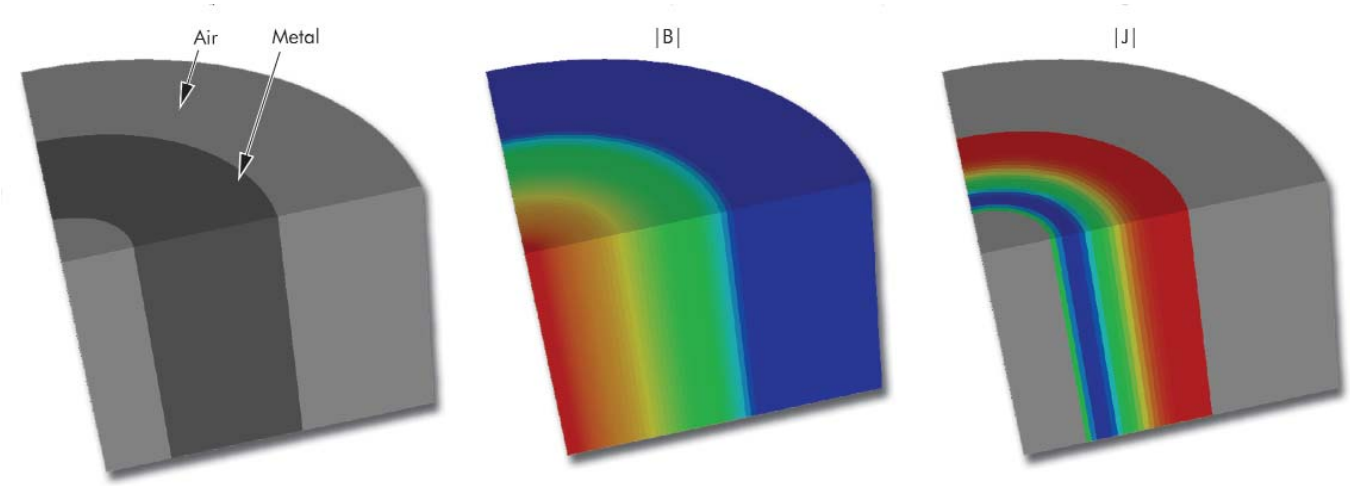

Figure 2. An example problem that has been used to benchmark our prototype finite-element electromagnetic diffusion equation algorithm. The problem consists of a metal cylinder (dark gray), with air (light gray) on the inside and outside. This is a 3-D time-dependent simulation. The middle picture shows a snapshot of the B-field magnitude, and the right picture shows a snapshot of the z-component of the current density. While the computational mesh is 3-D, with appropriate boundary conditions the computed results can be compared to the analytical solution for eddy currents in an infinite metal cylinder.

Relevance to LLNL Mission

Large-scale scientific simulation is a core-competency of LLNL. This project builds upon and enhances our expertise in multiphysics simulations. We will develop a novel simulation capability that is not available commercially, from academia, or from the other national Laboratories. With this capability, LLNL will have an unprecedented ability to simulate, design, and optimize ETM systems. A robust ETM simulation capability will enable LLNL physicists and engineers to better support current DOE pulse-power programs, as well as future programs, and will prepare LLNL for exciting long-term DoD opportunities.

FY2004 Accomplishments and Results

This project started in mid-FY2004. We are currently investigating different finite-element formulations for the electromagnetics equations, *i.e.* field-based vs. potential-based formulations. While the ultimate goal is to develop a simulation for dynamic (moving, deforming) geometry, we are currently evaluating alternative formulations in the context of motionless geometry, since there are numerous benchmark solutions that can be used as metrics.

In Fig. 2 we show a preliminary simulation of a 3-D eddy current problem. In the eddy current problem, a time-varying magnetic field diffuses into a conductor and induces electrical currents, which in turn generate an induced magnetic field. This particular example is of a finite metal cylinder, with the external magnetic field due to a current on the z-axis. This simulation uses an *H (curl)*-conforming finite-element discretization of the *E*-field vector diffusion equation, with implicit Crank-Nicholson time stepping. The *H (curl)*-conforming discretization properly models the discontinuity of fields and currents across material interfaces, and also maintains the divergence-free character of the fields and currents.

FY2005 Proposed Work

In FY2005 we will continue to research finite-element discretization methods for electromagnetics. We will evaluate an *E*-field formulation, an *H*-field formulation, and an *A*-field formulation. For each formulation an *H (curl)* finite element discretization will be used and the same Crank-Nicholson time stepping can be used. The difference in these formulations is manifested in different source terms and boundary conditions. We will develop a software module that can be incorporated into both the Diablo and ALE3D codes. Coupling the electromagnetics with the mechanics is the primary task for FY2005. We will also begin to research issues associated with advection, dynamic contact, and air/vacuum regions.

Broadband Radiation and Scattering

For more information contact **Robert M. Sharpe**
(925) 422-0581, sharpe1@llnl.gov

We will enhance our computational electromagnetics (CEM) capability in the area of broadband radiation and scattering. Broadband analyses include electromagnetic interference and electromagnetic compatibility noise analysis, broadband radar, and accelerator wakefield calculations. LLNL analysis codes are limited by the accuracy of radiation boundary conditions (RBCs), which truncate space. We will develop improved RBCs by extending the perfectly matched layer (PML) approach to non-Cartesian meshes, and by developing discrete-time-domain, boundary-integral techniques, which are compatible with high-accuracy, finite-element methods and capable of arbitrary accuracy. We will compare the two approaches for accuracy and efficiency for a variety of radiation and scattering problems.

Project Goals

The ultimate deliverable is an enhanced CEM capability that can provide accurate and efficient computational solutions to broadband radiation and scattering problems. The algorithms for improved RBCs will be incorporated into LLNL's existing EMSolve code. The result will be a 10- to 1000-fold improvement in the accuracy of simulations. Improved algorithms and our existing high-performance computer hardware will place LLNL's CEM activity among the top capabilities in the world.

This research and the resulting capability will be documented in appropriate peer-reviewed publications.

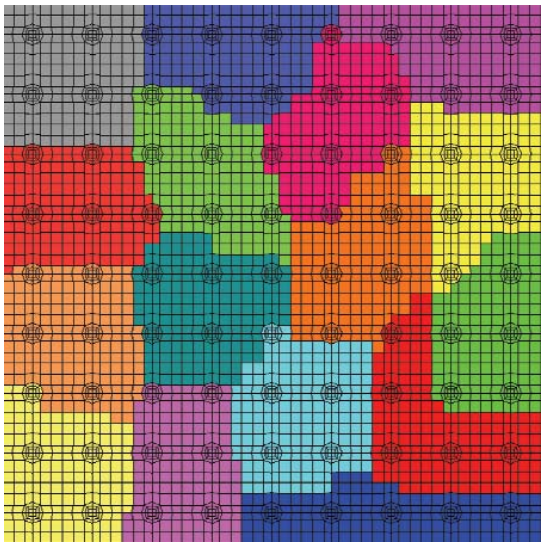

Figure 1. Computational mesh for a parallel simulation of a photonic bandgap structure. The colors denote the parallel partitioning. This is an unstructured hexahedral mesh using higher-order curved elements for the dielectric rods.

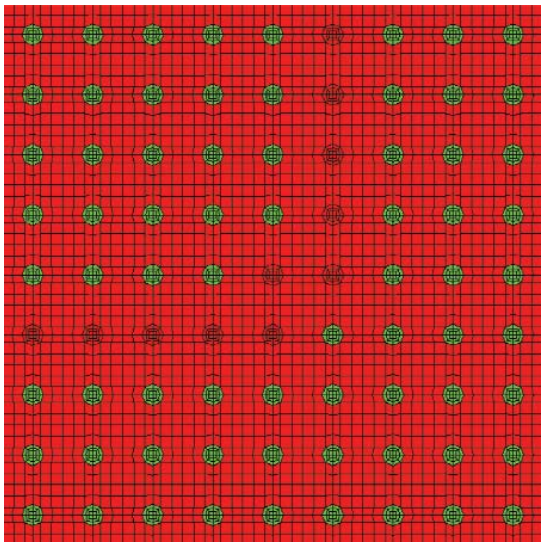

Figure 2. Computational mesh for a photonic bandgap simulation. The structure is an artificial crystal consisting of dielectric rods (green) in a bulk dielectric (red). The structure is designed to prohibit light waves of a prescribed wavelength. A photonic waveguide is constructed by removing rods. In this example the waveguide makes a 90° bend.

Relevance to LLNL Mission

Electromagnetics is a truly ubiquitous discipline that touches virtually every major LLNL program. Our work supports the national security mission by reducing the time and money spent in building and testing existing programs. It will enable computer simulations for new devices and systems, performance analysis of systems critical to nonproliferation efforts, and the design of micropower impulse radar and other microwave systems.

FY2004 Accomplishments and Results

Figures 1 to 4 are sample results for our CEM work.

We extended the PML concept to higher-order unstructured grids and analyzed the performance of this approach. We performed novel higher-order photonics simulations that would not have been possible without these extensions to the PML concept. Results were presented at a 2004 IEEE conference, and a manuscript has been submitted to *The Journal of Computational Physics*. On the boundary integral task, we developed a prototype code used to evaluate various boundary integral formulations. Significant effort was spent on investigation of numerical instabilities. We determined that temporal basis functions (as opposed to temporal differencing) are required for stability.

FY2005 Proposed Work

The stability and accuracy of the boundary integral approach depends critically on the integration, or quadrature rules. We will continue to research singularity extraction, polar integration, and Duffy transformation-based quadratures. We are collaborating with a professor at the University of Washington, an expert on time-domain integral equations, and will collaborate closely with him also on time integration methods and the hybrid finite-element boundary element formulation. We expect to have a fully functioning, although not fully optimized, time-domain boundary integral code working by the end of FY2005. This will enable the full hybridization with finite elements in FY2006.

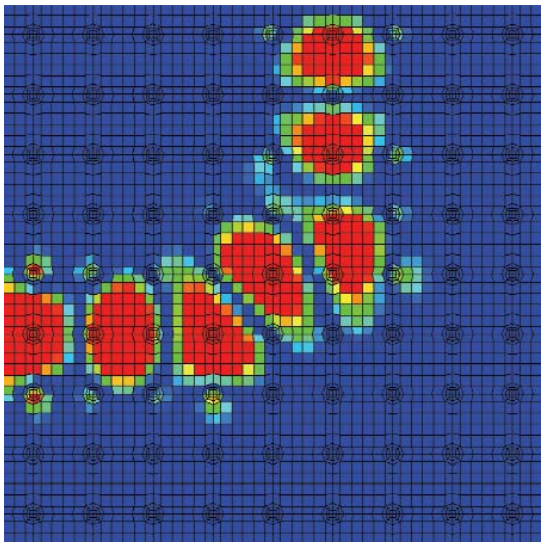

Figure 3. Snapshot of the computed electric field intensity. Note how the light makes a 90° bend, which is not possible with conventional dielectric waveguide technology. This simulation used third-order finite-element basis functions to eliminate numerical dispersion effects. The mesh was terminated with a single-layer third-order PML to absorb the outgoing waves.

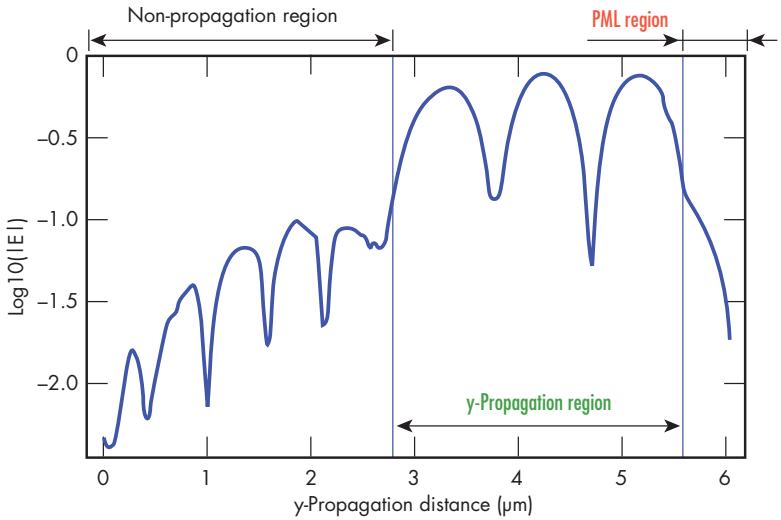

Figure 4. "Line-out" plot of the electric field intensity. This plot clearly shows the outgoing wave being absorbed by the third-order PML region.

Propagation Models for Predicting Communication System Performance in Tunnels, Caves, and Urban Canyons

For more information contact **Hsueh-Yuan Pao**
(925) 424-9744, pao2@llnl.gov

This project addresses the problem of characterizing the propagation of electromagnetic fields in the adverse environments that are encountered in enclosures such as caves and tunnels, where rough surface can compromise the quality of signals.

Project Goals

We have investigated the propagation physics; developed the mathematical models; derived the statistical descriptors, specialized to radio communication in tunnels and caves; and selected the models/methods best suited to the parameter space describing enclosures of interest.

Relevance to LLNL Mission

A military or emergency response commander must see, understand, and interact with complex environments such as caves and tunnels in "real time," and both receive and feed tactical data among the individual soldier, policeman, firefighter, and command post. This must be done from local or remote sensors. It is not possible to predict when wireless communications systems will be useful and when they will fail. A predictive tool is needed, to allow planning and preparation of communications systems.

To do this, we need to go beyond oversimplified empirical models of RF propagation in complex environments. Such models base their statistics on experiments without sufficient underlying theory to enable generalization to environments other than those in which the experiments were conducted.

The Yucca Mountain Repository Project, for example, requires reliable wireless communications systems for 300 years at the underground structure. This project is intended to fulfill this requirement.

An accurate model for a wireless propagation channel matches both the national security and the energy missions of the Laboratory.

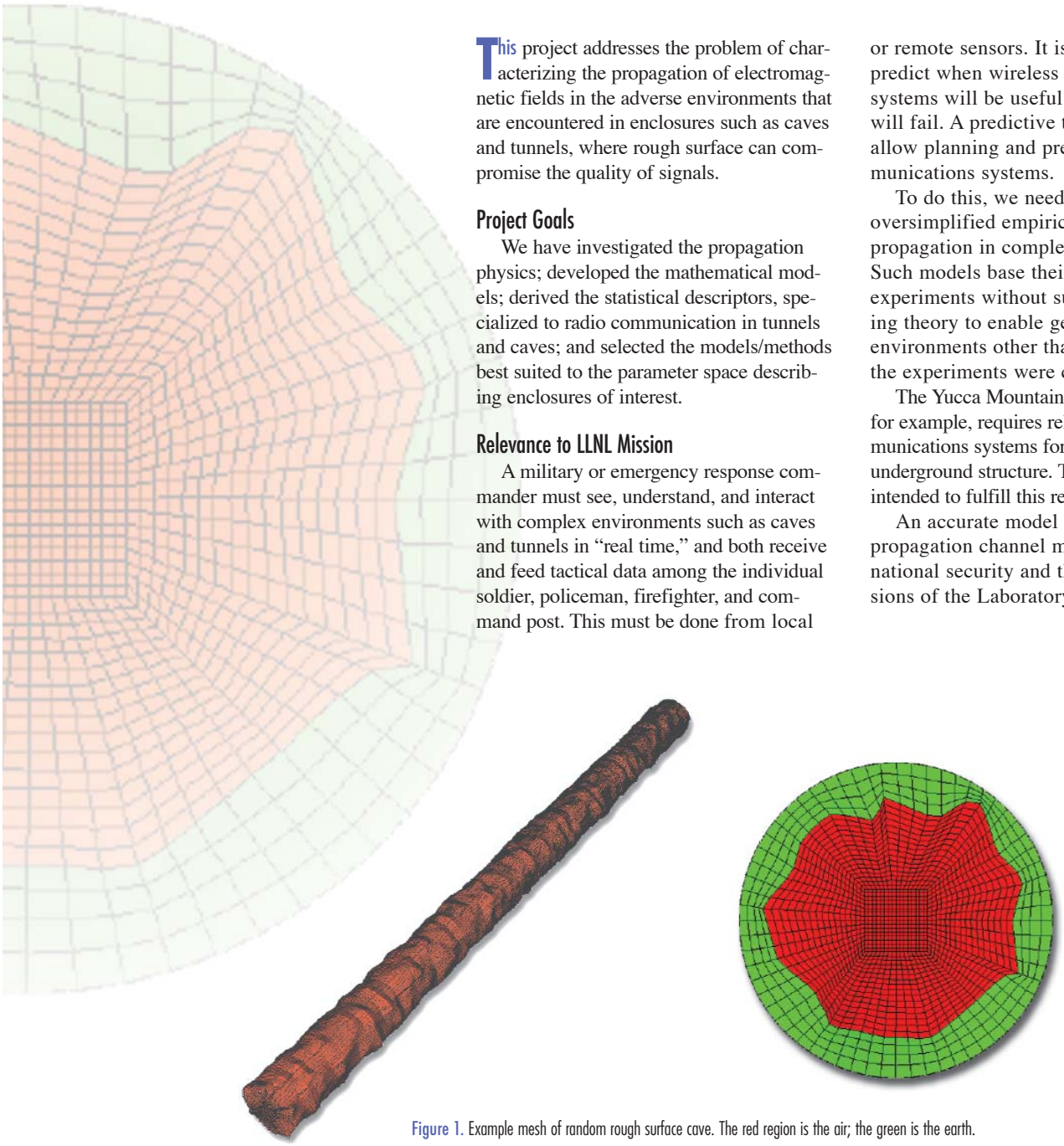

Figure 1. Example mesh of random rough surface cave. The red region is the air; the green is the earth.

FY2004 Accomplishments and Results

Our analytical work during FY2004 focused on specific problems: investigating the excitation and propagation of electromagnetic fields excited by sources situated within straight caves and tunnels that have rough walls (see Fig. 1); deriving the statistical characteristics of the fields and signals of RF in straight, perfect electrical conductor (PEC) rough wall tunnels; and extracting the wireless communication channel model in the tunnel from the physics-based models.

The principal results are as follows.

First, the field is shown to comprise the sum of a coherent or deterministic part and a zero-mean incoherent or random part. The latter is described by the appropriate correlation functions. Representative analytical and numerical results for the case in which the source is an electric-current loop show that the random part of the axial magnetic field is proportional to the deterministic part of this field, and is bound to the rough wall of the tunnel. The tightness of the binding is dependent on the signal frequency, the tunnel radius, and the power spectral density of the wall roughness.

Second, the probability density function for single-mode field-amplitude propagating in a straight PEC rough wall cave or tunnel is Ricean. Its distribution function is given by the analytic form consisting of exponential, power and modified Bessel function. The probability density function for the phase of single-mode field in the cave or tunnel is of analytic form as well. The expected values of the single-mode field-amplitude and intensity are derived. They represent the deterministic parts of single-mode field amplitude and intensity, respectively, and have very simple mathematical forms.

Third, the probability density function for total field amplitude in the cave or tunnel are Gaussian distributed. The probability distribution functions are the error functions. The average total field amplitude and intensity are of simple analytic mathematic forms.

Figures 2 and 3 show representative probability functions.

Fourth, field strength versus axial distance in tunnels can be divided into two regions. For near distances, the model has an axial dependence on z. For greater distances, the model produces an exponential axial fall-off, where the rate of decay is governed by the wavenumber of the dominant guided wave mode.

Our work has led to numerous presentations and publications.

Related References

1. Dudley, D. G., "Wireless Propagation in Circular Tunnels," *IEEE Transactions on Antennas and Propagation*, in press.

2. Pao, H., "Probability Density Function for Wave Propagation in a Straight PEC Rough Wall Tunnel," *Microwave and Optical Technology Letters*, in press.

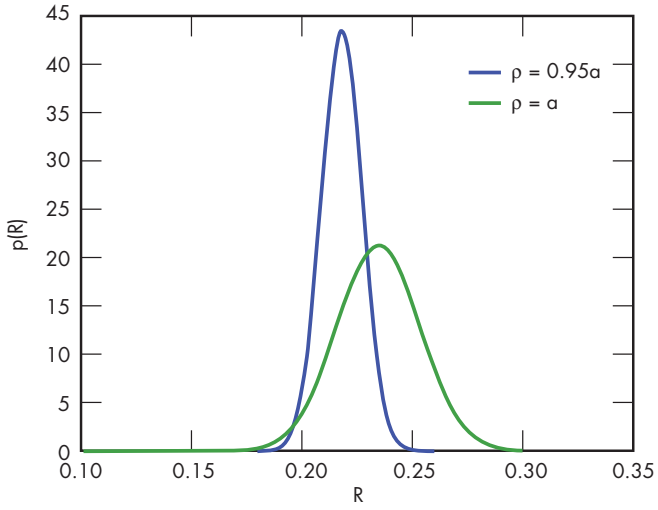

Figure 2. Probability density function for TE_{11} and TM_{01} modes at different radial locations.

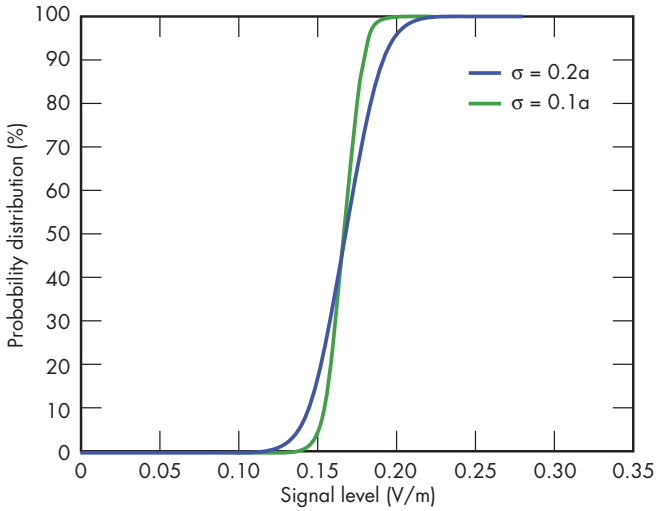

Figure 3. Cumulative probability distribution function for the amplitude of single-mode random, field at different wall roughness.

Three-Dimensional Vectorial Time-Domain Computational Photonics

For more information contact **Jeffrey S. Kallman**
(925) 423-2447, kallman1@llnl.gov

Demand from customers with needs in secure data transmission, computer networking, and high-bandwidth instrumentation is pushing photonic integrated circuit (PIC) technology. Compact (LSI to VLSI), low-latency (sub-ps), wide-bandwidth (THz), ultrafast (100 Gb/s), miniaturized digital-logic, transmission, and sensor systems are potentially feasible.

Despite the strong photonic modeling capability at LLNL, new numerical methods are necessary as more complex photonic devices, materials, and configurations are devised. Three-dimensional time-domain design tools are fundamental to enabling and accelerating technologies for the realization of all-optical logic systems for data generation, transmission, manipulation, and detection.

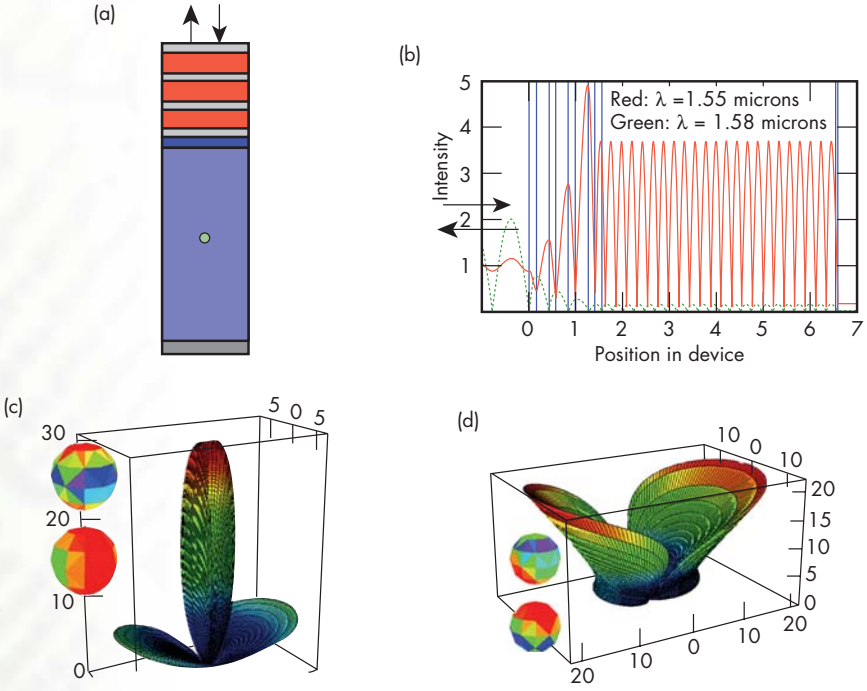

Figure 1. Scattering in semiconductor Fabry-Perot interferometer. (a) The device: a metal-mirror-backed semiconductor cavity with a λ/4 stack on top and a 0.1-μm-radius scatterer; (b) the intensity of the electric field through the device on- and off-resonance (red and green traces, respectively); (c) and (d) the scattering pattern of the E field when the wavelength is, respectively, on- and off-resonance. In (d), the large central lobe is missing, and the maximum E field is reduced by 30 dB relative to the on-resonance case.

Project Goals

We are filling the gap between existing modeling tools and those needed for Laboratory missions by extending the state of the art in simulation for the design of 3-D PICs. We have defined challenges that must be addressed in our codes, such as models for optical gain and nonlinearities, as well as microscopic, nonuniform, inhomogeneous structures.

Relevance to LLNL Mission

The ability to model complex 3-D photonic devices in the time domain is essential to LLNL for a broad range of applications. These include: high-bandwidth instrumentation for NIF diagnostics; microsensors for weapon miniaturization within the DNT programs; encryption devices and circuits for secure communications for NAI surveillance applications; high density optical interconnects for high-performance computing (core of the ASCI mission); and the Chemical and Biological National Security Program detection devices.

FY2004 Accomplishments and Results

We have extended the Quench suite (a scalar 2-D narrow-bandwidth paraxial-propagation code used to model nonlinear optical devices) to model 3-D devices, and the EMSolve code (a vector 3-D broadband Maxwell's Equations solver used to model linear optical devices) to deal with carrier diffusion and time-varying material properties.

We have verified our nonlinear material models against literature results. We used our codes to model a steady-state off-bandgap Fabry-Perot interferometer with index perturbations (see Fig. 1). This was useful for the design of the next generation of ultrafast, highly sensitive radiation sensors for NIF x-ray diagnostics. Results provide quantitative information about the magnitude of the scattering to be expected from a low-energy x ray hitting the sensor (both at and away from optical resonance), and showed the sensitivity of the device to the location of the x-ray absorption.

We coupled our 3-D carrier density decay-diffusion simulation to our bulk material models to generate complex refractive index distributions, which we then used in a 3-D BPM code to determine scattering from a carrier density distribution.

Related References

1. Bond, T. C., and J. S. Kallman, "Time-Domain Tools for the Investigation of Gain-Quenched Laser Logic," *International Semiconductor Device Research Symposium,* Washington, D. C., December 2003.

2. Koning, J. M., D. A. White, R. N. Rieben, and M. L. Stowell, "EMSolve: A Three Dimensional Time Domain Electromagnetic Solver," *5th Biennial Tri-Lab Engineering Conference,* Albuquerque, New Mexico, October 2003.

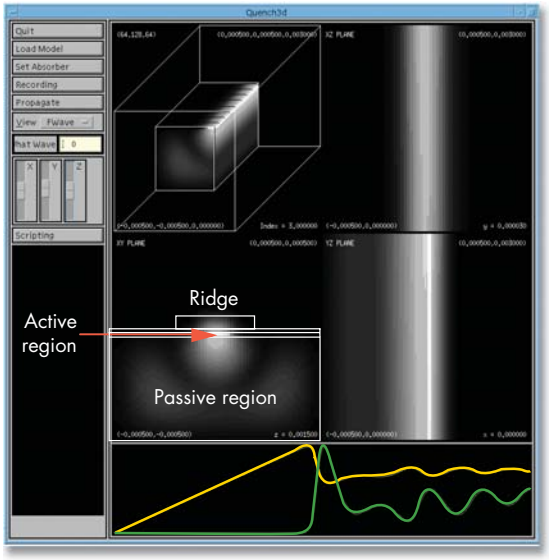

Figure 2. Output of the Quench3D program modeling a short laser. Upper left: three planes that are viewed in the other parts of the main image (this shows we are looking at approximately the center of the device). Upper right: XZ plane. Lower left: XY plane. Overlaid on the lower left image is an illustration of the design of the laser being modeled. Lower right: YZ plane. The graph at the bottom shows the time history of the laser output (green line) and the average carrier density (yellow line).

FY2005 Proposed Work

We will develop and incorporate gain and spontaneous emission algorithms into the EMSolve code and replace Quench3D's (see Fig. 2) scalar beam propagation solver with a vector finite-element beam propagation solver. The upgrade to EMSolve will allow us to model photonic crystal devices and semiconductor Fabry-Perot interferometers excited at the bandgap energy. The upgrade to Quench3D will allow us to examine the polarization dependence of the light emitted from semiconductor lasers. We will continue modeling devices for a variety of LLNL programs.

Virtual Polymerase Chain Reaction

For more information contact **Shea N. Gardner**
(925) 422-4317, gardner26@llnl.gov

The polymerase chain reaction (PCR) stands among the keystone technologies of our time for analysis of biological sequence data. It is used in virtually every laboratory doing molecular, cellular, genetic, ecologic, forensic, or medical research. Despite its ubiquity, we lack the precise predictive capability that would enable detailed optimization of the dynamics of PCR reactions.

In this project, we are developing tools to perform virtual PCR (vPCR) by building new computational methods (Fig. 1) to model the kinetic, thermodynamic, and biological processes of PCR reactions. These tools will allow us to predict the effects of primers and reaction conditions on PCR products, and thus to optimize these variables. For the first time, the algorithms we are building will enable simulation of a complete thermocycle (ramp and soak) and product prediction for multiple thermocycles (Fig. 2), which no other software package to-date can do.

Project Goals

The result of this project, a suite of programs that predict PCR products as a function of reaction conditions and sequences, will be used to address outstanding questions in pathogen detection, forensics and microarray applications, as well as to enable detailed examination of the effects of contaminants and PCR inhibitors on the PCR process.

vPCR should enable scientists to optimize PCR protocols, in terms of time, temperature, ion concentration, and primer sequences and concentrations, and to estimate products and error rates in advance of

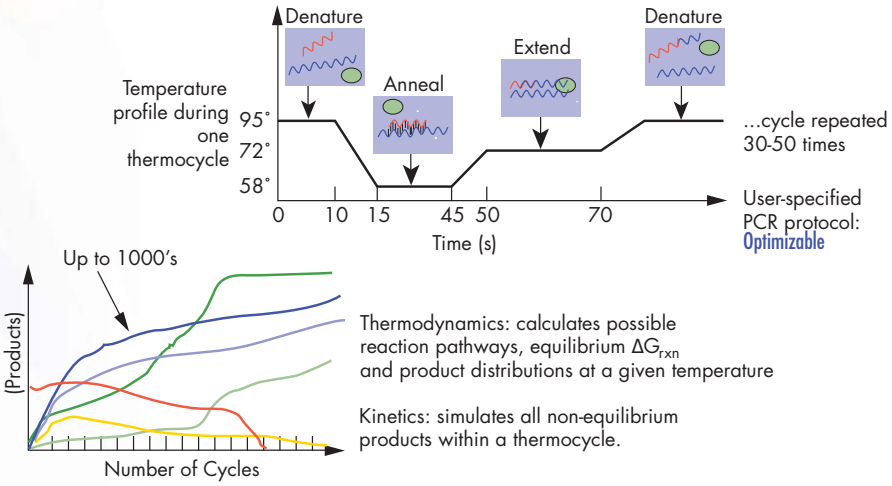

Figure 1. Flow chart showing how new capabilities will model important processes and predict the full spectrum of PCR products.

performing experiments. Our proposed capabilities are well ahead of all currently available technologies, which do not model non-equilibrium kinetics or polymerase extension, or predict PCR products. A provisional and a full patent application (IL-11192) have been filed.

Relevance to LLNL Mission

vPCR supports LLNL missions in homeland security, Genomes to Life (GtL), and human health. Any field that uses PCR, including bioforensics, biodetection, basic research in GtL, and disease research, such as cancer, will benefit. The challenges that vPCR can address include identification of genes and organisms present in complex microbial communities; optimization of DNA-polymerase-based gene synthesis; and forensic discrimination of closely related sequences.

FY2004 Accomplishments and Results

We have written the thermodynamics code to calculate reaction pathways and free energies, and have linked this with KINSOL, a nonlinear, simultaneous equation solver developed by CASC researchers, to solve the thermodynamic equations. We have developed the framework for efficient data transfer between the kinetic and thermodynamic modules. For the kinetic simulations we have developed the algorithms and written prototype code to perform Gillespie's formulation of stochastic chemical kinetic simulations for the PCR process. Currently, reaction probabilities are based on annealing probabilities in terms of rates of nucleation, proximity effects, and free energies of reaction.

Related References

1. Allawi, H. T., and J. Santalucia, Jr., "Thermodynamics and NMR of Internal GT Mismatches in DNA," *Biochem.*, **36,** pp. 10581-10594, 1997.

2. Gillespie, D., "A General Method for Numerically Simulating the Stochastic Time Evolution of Coupled Chemical Reactions," *J. Comp. Phys.*, **22,** pp. 403-434, 1976.

3. Gillespie, D., and L. R. Petzold, "Improved Leap-Size Selection for Accelerated Stochastic Simulation," *J. Chem. Phys.*, **119,** pp. 8229-8234, 2003.

4. Maheshri, N., and D. V. Schaffer, "Computational and Experimental Analysis of DNA Shuffling," *Proc. Natl. Acad. Sci. USA*, **100,** pp. 3071-3076, 2003.

5. Wetmur J. G., "DNA Probes: Applications of the Principles of Nucleic Acid Hybridization," *Crit. Rev. Biochem. Mol. Biol.*, **26,** pp. 227-59, 1991.

FY2005 Proposed Work

In the next fiscal year we plan to add polymerization (extension) to the kinetic and thermodynamic simulations; modify the collective capability to handle denaturation of primers during a thermocycle (the reverse reaction); develop the capability to dynamically handle reaction vessel temperature ramps; optimize parallelization at multiple levels; perform experiments using real-time PCR to test the models; and prepare a manuscript for submission to a peer-reviewed journal.

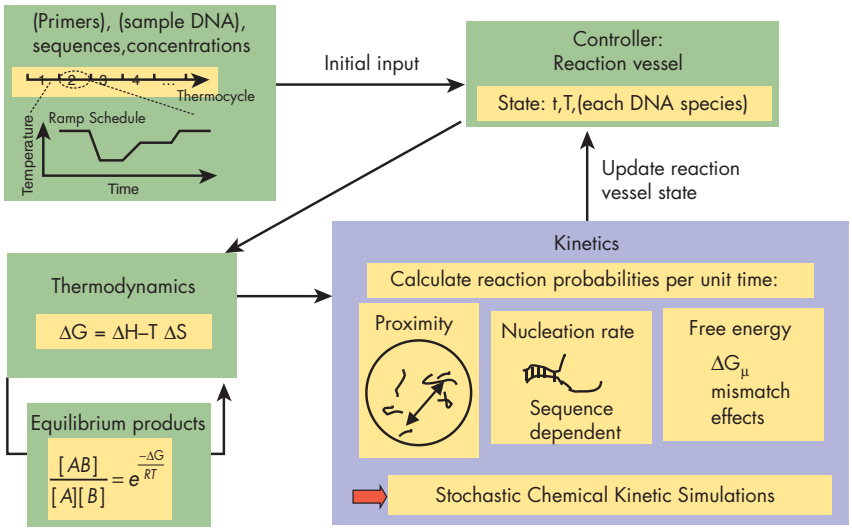

Figure 2. Flow chart showing how vPCR handles multiple cycles and adds kinetics to the simulation of the PCR process.

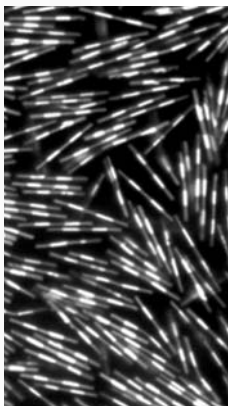

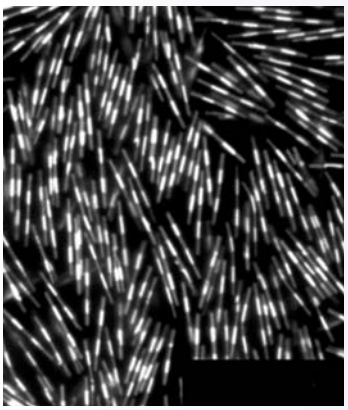

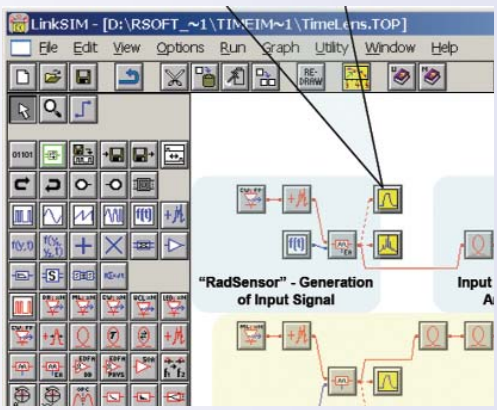

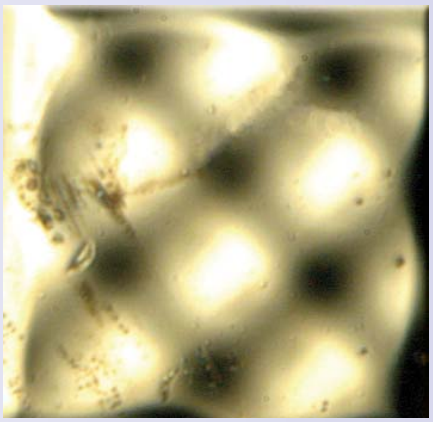

Center for
Microtechnology and Nanotechnology

LDRD

Microfluidic System for Solution-Array-Based Bioassays

For more information contact **George M. Dougherty**
(925) 423-3088, dougherty9@llnl.gov

We are developing an integrated, reconfigurable microfluidic system for performing user-specified multiplexed biomarker assays for the early detection of disease using solution array technology. Solution arrays are similar to gene and protein chips, but use surface functionalized particles in solution, rather than the binding of biomolecules to a fixed surface. Instead of correlating fluorescence with location, as in a chip format, the particles are encoded for identification. Results are read by examining particles for their encoded type and for the presence or absence of the fluorescence indicative of a positive binding event. The flexibility of solution arrays means that different types of functionalized particles can be added as desired by an end user, and particles for DNA, RNA, and protein detection can be used simultaneously in a single low-cost format.

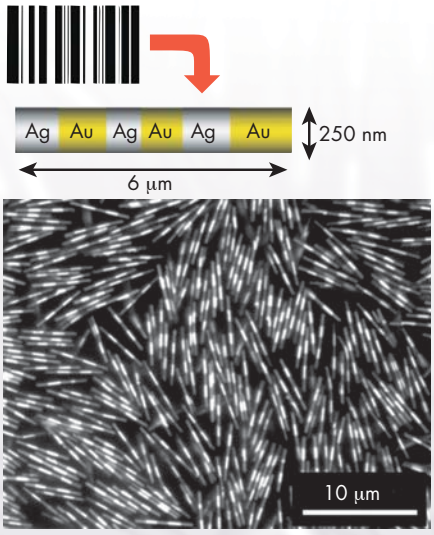

Figure 1. Optical microscope image of Nanobarcodes™ particles. The light and dark stripes are due to alternating bands of gold and silver metal, having different reflectivities at the observation wavelength.

The particles used in this project are Nanobarcodes™ particles (Fig. 1), short metallic nanowires that bear patterns of light and dark stripes analogous to the stripes in a supermarket barcode. These particles offer unique advantages in their ability to be identified using standard light microscopy, avoiding the need for complicated spectroscopic or flow cytometry methods. Surface functionalization of metal particles is understood, and the Nanobarcodes™ can be made with magnetic materials, opening up new possibilities for manipulating, transporting, and trapping the particles using magnetic and electric fields.

Project Goals

The goal of the project is to demonstrate a prototype bioassay system based on Nanobarcodes™ particles. This system will be capable of performing simultaneous assays for several biowarfare agent simulants. Along the way, we expect to achieve a number of important scientific goals, advancing the state of the art in particle-based biochemical assays and in the manipulation and control of metallic nanoparticles within aqueous solutions.

Relevance to LLNL Mission

Biodefense is a major research thrust at LLNL, in support of technology needs for homeland security and national defense. The technology developed in this project will also benefit medical diagnosis and treatment of disease.

FY2004 Accomplishments and Results

The project has made several important advancements in the past year. First, multiplex immunoassays have been successfully implemented in the Nanobarcodes™ format. The first implementation, using medical-grade cytokine antigens and anti-cytokine antibodies, demonstrated that the sensitivity of the Nanobarcodes™-based assay is similar to that of the best state-of-the-art immunoassays (Fig 2.). The second implementation used a panel of biowarfare agent simulants and demonstrated that the approach works with these types of reagents as well.

Progress was also made in the area of fluid transport and electromagnetic manipulation of the particles. Tests of functionalized particle transport through glass and silicone channels (Fig. 3) show minimal particle adhesion, and both experimental studies and computer modeling work have advanced our abilities to move and align particles using AC and DC electric fields as well as magnetic fields. In addition, experiments have revealed new, important data about the electrokinetic properties of functionalized metallic nanoparticles in aqueous suspension. Finally, we have demonstrated an effective means of using self-assembly to organize the Nanobarcodes™ particles into a 2-D array for improved optical readout.

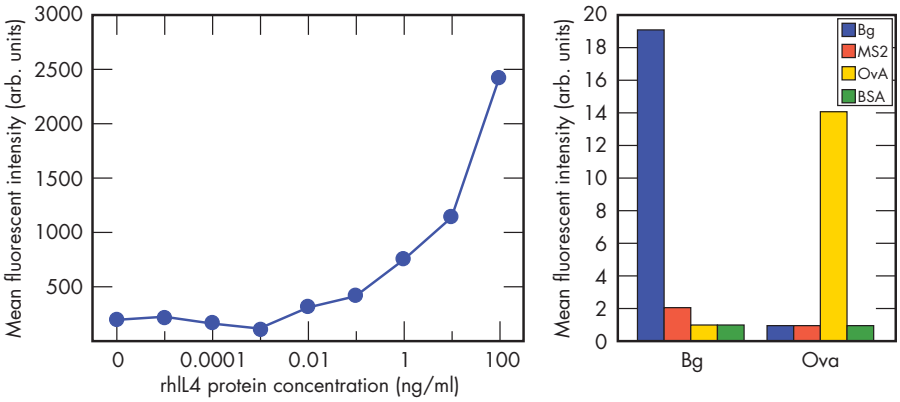

Figure 2. Nanobarcodes™-based bioassay results. (a) Plot of fluorescence signal vs. antigen concentration for a cytokine target, showing sensitivity in the 10 pg/ml range. (b) Plot of a four-plex biodetection panel showing the specificity of response to *Bacillus globigii*, a bacterial spore, and Ovalbumin, a soluble serum protein.

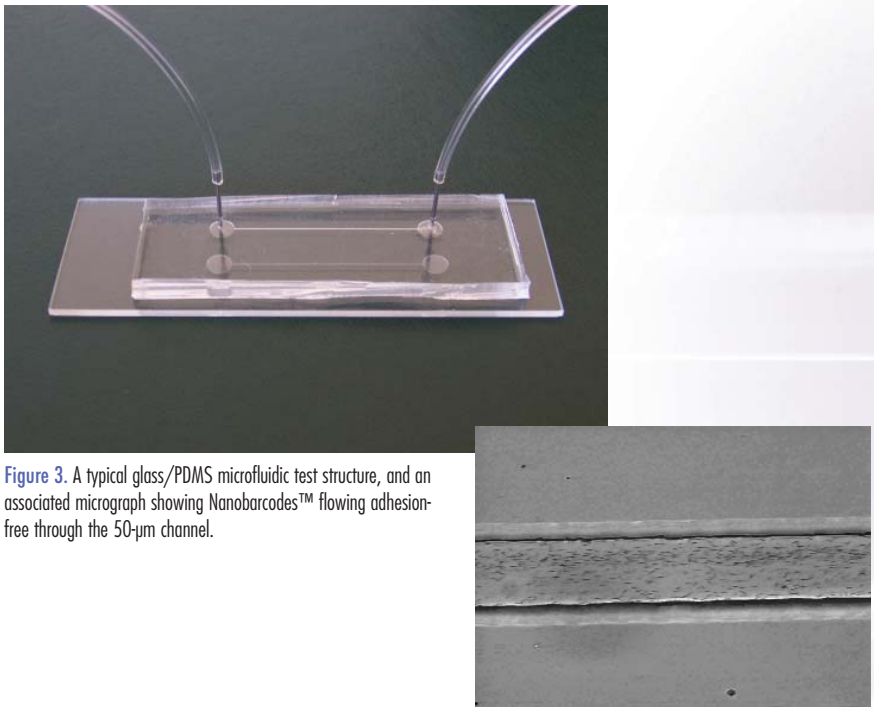

Figure 3. A typical glass/PDMS microfluidic test structure, and an associated micrograph showing Nanobarcodes™ flowing adhesion-free through the 50-μm channel.

Related References

1. Nicewarner-Pena, S. R., R. G. Freeman, B. D. Reiss, L. He, D. J. Pena, I. D. Walton, R. Cromer, C. D. Keating, and M. J. Natan, "Submicrometer Metallic Barcodes," *Science*, **294**, pp. 137-141, October 2001.

2. Keating, K. D., and M. J. Natan, "Striped Metal Nanowires as Building Blocks and Optical Tags," *Adv. Mater.*, **15**, pp. 451-454, 2003.

3. Dougherty, G. M., F. Chuang, K. Rose, S. Pannu, S. Penn, and M. Natan, "Multiplex Biodetection Using Solution Arrays Based on Encoded Nanowire Particles," *Materials Research Society Spring Meeting*, San Francisco, California April 12-16, 2004.

FY2005 Proposed Work

The final year of the project is devoted to integrating what we have learned into a working demonstration system that can carry out full biodetection tests using the Nanobarcodes™- particle-based solution assay. Work in the bioassay area will focus on optimizing the process performance within the microfluidic system. Electromagnetic manipulation and 2-D array formation will be included within the bioassay process flow. The complete system will be capable of performing biodetection assays, as well as extracting and reading Nanobarcodes™ particles from liquid suspensions for applications in forensics and other homeland security applications.

Nanoscale Fabrication of Mesoscale Objects

For more information contact **Raymond P. Mariella, Jr.**
(925) 422-8905, mariella1@llnl.gov

Neither LLNL nor any other organization has the capability to perform deterministic fabrication of mm-sized objects with arbitrary, μm-sized, 3-D features and with 20-nm-scale accuracy and smoothness. This is particularly true for materials such as high explosives and low-density aerogels.

In this project, we have, for the first time, combined the 1-D hydrocode "HYADES" with the 3-D molecular dynamics simulator "MDCASK" in our modeling studies. In FY2002 and FY2003, we investigated the ablation/surface-modification processes that occur on copper, gold, and nickel substrates with the use of sub-ps laser pulses. In FY2004, we investigated laser ablation of carbon, including laser-enhanced chemical reaction on the carbon surface for both vitreous carbon and carbon aerogels.

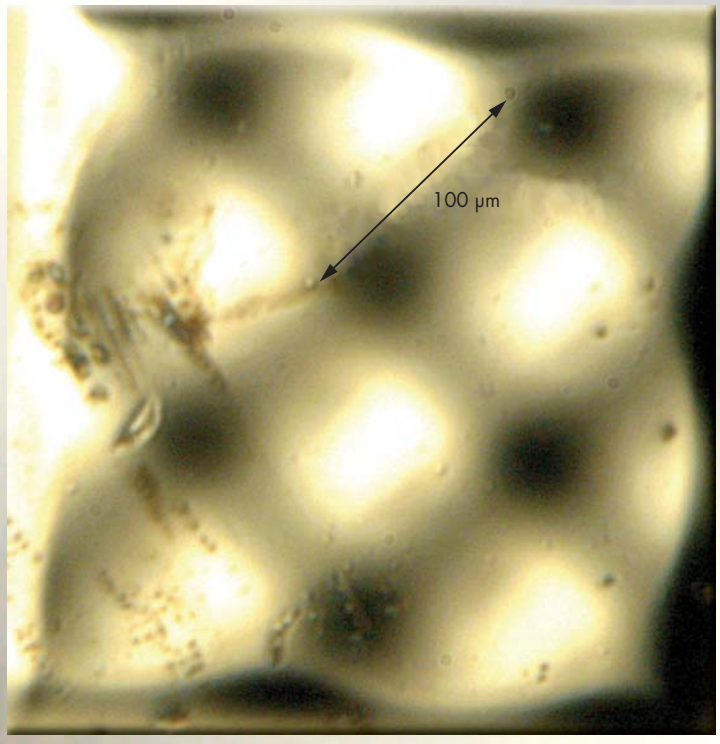

Figure 1. Optical micrograph of sinusoidal moguls, micromachined on vitreous carbon using reactive (oxygen) ion-beam milling.

Project Goals

The immediate impact of our investigation will be a much better understanding of the chemical and physical processes that influence materials that are exposed to fs laser pulses. More broadly, our goals are to develop the capability for fabricating and characterizing mesoscale objects using fs laser pulses and ion-beam etching for applications such as fabricating laser targets, developing miniature fuels cell, remote sensors, and medical technologies.

Relevance to LLNL Mission

These experiments will support the Laboratory's stockpile stewardship mission by providing data for corroborating the models in the improved physics codes for the Advanced Simulation and Computing Program, and developing new capabilities for the fabrication and characterization of mesoscale objects with nanoscale precision.

FY2004 Accomplishments and Results

In FY2004, using carbon substrates, we investigated the ablation processes that occur with the use of laser pulses to ablate the surface. We studied the process both in vacuum and in air. Our main effort used vitreous carbon, both

because it is readily available and because it was the easiest carbon to model. Through our collaboration with colleagues at Lawrence Berkeley Laboratory, we also showed that oxygen-ion beams could micromachine smooth features in vitreous carbon. We also studied laser ablation of carbon aerogels and were able to micromachine simple features in these aerogels. We submitted a manuscript to *Science* on our work on laser ablation of metals.

Figure 1 shows a vitreous-carbon sample with μm features. Figure 2 shows metrology plots for that sample.

Related References

1. Shirk, M. D., A. M. Rubenchik, G. H. Gilmer, B. C. Stuart, J. P. Armstrong, S. K. Oberhelman, S. L. Baker, A. J. Nikitin, and R. P. Mariella, Jr., "Mesoscale Laser Processing Using Excimer and Short-Pulse Ti:Sapphire Lasers," *ICALEO®*, Jacksonville, Florida, October 13-16, 2003.
2. Mariella, R. P., Jr., "MEMS-Based Sensor Systems," *NNSA Futures Conference,* Crystal City, Virginia, May 2004.
3. Gilmer, G. H., M. D. Shirk, A. M. Rubenchik, L. Zepeda-Ruiz, R. P. Mariella, Jr., T. Diaz de la Rubia, "Short-Pulse Laser Ablation Simulated by Molecular Dynamics, Void Nucleation and Cluster Ejection," *Third International Conference: Computational Modeling and Simulation of Materials,* Acireale, Sicily, Italy, May 30-June 4, 2004.
4. Gilmer, G. H., "Thin Film Deposition and Manipulation of Surfaces Using Laser Beams: Atomistic Modeling," *DOE-NSET Workshop on Artificially Structured Nanomaterials: Formation and Properties,* Gatlinburg, Tennessee, October 13-15, 2003.
5. Gilmer, G. H., "Short-Pulse Laser Ablation of Metals: Large-Scale Molecular Dynamics Simulations," *Second International Workshop on Strength and Fracture,* Berkeley, California, January 7-9, 2004.

FY2005 Proposed Work

We have made numerous interesting discoveries that merit further work. The ability to contour difficult materials needs to be placed into a more deterministic framework. That is, the quantitative relationship between the nominal fluence of the laser pulses and the micromachining needs to be better characterized, particularly in terms of the effect of pulse-to-pulse variability with variability in amount of material removed, and in the 3-D shape of the feature that is created in the substrate. Both chemically-assisted laser ablation as well as reactive-ion-beam etching of carbon warrant further investigations. For microfabricating 3-D objects of diamond, traditional machining will be ineffective, and lasers and ion beams will be the clear methods of choice. Diamond is being considered, for example, as a material that could serve as the ignition capsule on NIF.

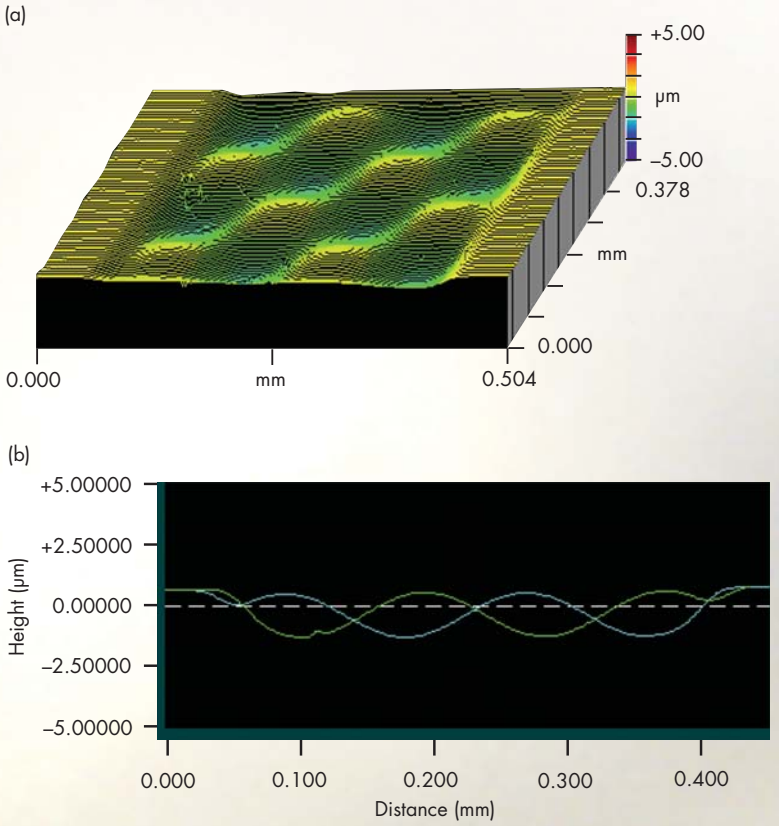

Figure 2. Optical-profilometer (a) image and (b) line scans of sinusoidal moguls, micromachined in the carbon substrate of Fig. 1.

Ultrafast Transient Recording Enhancements for Optical-Streak Cameras

For more information contact **Corey Bennett**
(925) 422-9394, bennett27@llnl.gov

Several experiments at LLNL will require hard x-ray and neutron diagnostics with temporal resolution of approximately 1 ps (or less) and a high dynamic range, particularly those experiments involving ignition. The Linac Coherent Light Source (LCLS) at the Stanford Linear Accelerator Center (SLAC) will need to measure timing and pulse shapes of its 100-fs fwhm x-ray pulse. These measurement requirements are far beyond existing solutions.

This project will develop a "time-microscope" front end for optical streak cameras. It will magnify signals having ultrafast optical detail so that they can be recorded with slower speed streak cameras with a much higher fidelity. The system will be compatible with a new class of ultrafast radiation detectors being developed, which produce a modulated optical carrier in response to ionizing radiation.

Figure 1. Comparison of (a) spatial and (b) temporal imaging systems. A time lens (c) is produced by mixing the input signal with a chirped optical pump pulse.

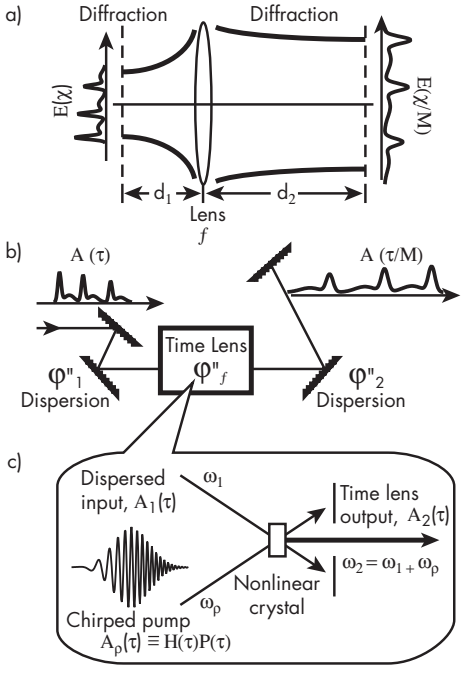

Project Goals

Temporal imaging is based on a space-time duality between how a beam of light spreads due to diffraction as it propagates in space, and how pulses of light spread as they propagate through dispersive media, such as grating systems or optical fiber (Fig. 1.) We have chosen to implement a "time lens" through sum-frequency generation (SFG) of a broadband-chirped optical pump with the input signal in a nonlinear crystal because of the improved resolution it produces.

This project will develop a temporal imaging system using fiber optic technologies. It will accept an optical signal at a 1550-nm wavelength that has around 600-ps duration and subpicosecond detail. The system will have a temporal resolution < 300 fs and will produce an output with 100 × temporal magnification, simultaneously shifting the signal to a 775-nm-center wavelength. The 300-fs input details, magnified to 30 ps at the output, will then be recorded with high fidelity on an optical streak camera.

Relevance to LLNL Mission

The success of NIF is critical to LLNL's stockpile stewardship mission. Our goal is to ensure delivery of the next-generation ultrafast diagnostics needed for critical experiments at NIF and other facilities, such as LCLS.

FY2004 Accomplishments and Results

We have performed an initial design of our temporal imaging system and modeled it in LinkSim (Fig. 2), with co-simulation in MATLAB. The model starts with a "RadSensor" generating an input pattern and a mode-locked laser, which is used to generate the chirped time lens pump pulse. Signals propagate through modulators, fibers, and amplifier modules containing the approximate characteristics of the intended components. They combine in a module that exports the data to MATLAB to simulate SFG in a nonlinear crystal. The simulation returns to LinkSim, propagates through the output dispersion module, and plots the output waveform. The input and output are plotted on 5 ps/div

and 0.5 ns/div scales, respectively, a 100 × magnification. The output is blurred slightly and has ripple to one side due to non-idealities in the input dispersion. This preliminary model will be revised as the design is improved and actual components are measured.

Precision dispersion measurement for each component is critical to understanding the cause of aberrations like that shown in Fig. 2. We have constructed such a measurement system and are currently using it to characterize all our components. With this information steps can be taken to remove the aberrations.

Construction of the temporal imaging system has begun with the time lens. Figure 3 shows the laser system and pulse picker.

Related References

1. Bennett, C. V., and B. H. Kolner, "Upconversion Time Microscope Demonstrating 103x Magnification of Femtosecond Waveforms," *Optics Letters,* **24,** (11), pp. 783-785, June 1, 1999.

2. Bennett, C. V., and B. H. Kolner, "Principles of Parametric Temporal Imaging-Part I: System Configurations," *IEEE J. Quantum Electronics,* **36,** (4), pp. 430-437, April 2000.

3. Bennett, C. V., and B. H. Kolner, "Principles of Parametric Temporal Imaging-Part II: System Performance," *IEEE J. Quantum Electronics,* **36,** (6), pp. 649-655, June 2000.

4. Bennett, C. V., and B. H. Kolner, "Aberrations in Temporal Imaging," *IEEE J. Quantum Electronics,* **37,** (1), pp. 20-32, January 2001.

FY2005 Proposed Work

We will proceed with completion of the time lens system. We will generate the required chirped pump pulse and design and implement the nonlinear crystal that will impart those characteristics through SFG with the input. An improved input dispersion design will be developed and implemented to remove the aberrations predicted in Fig. 2. We will also develop timing and triggering systems compatible with NIF.

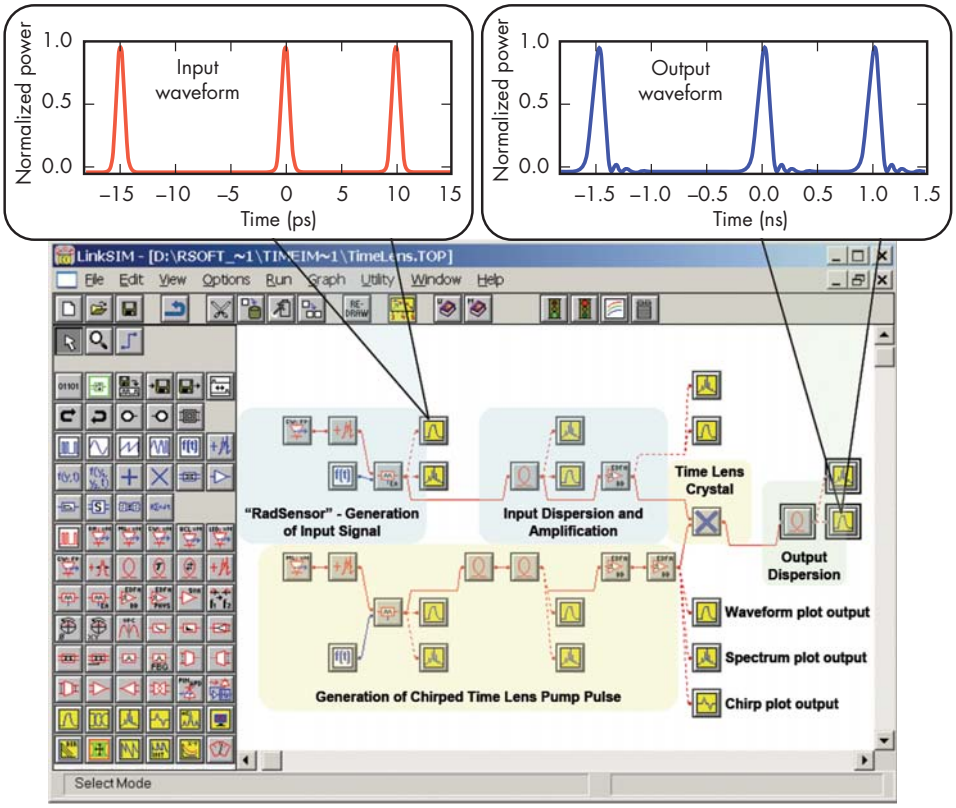

Figure 2. Layout of our initial system design in LinkSim along with input and output waveforms.

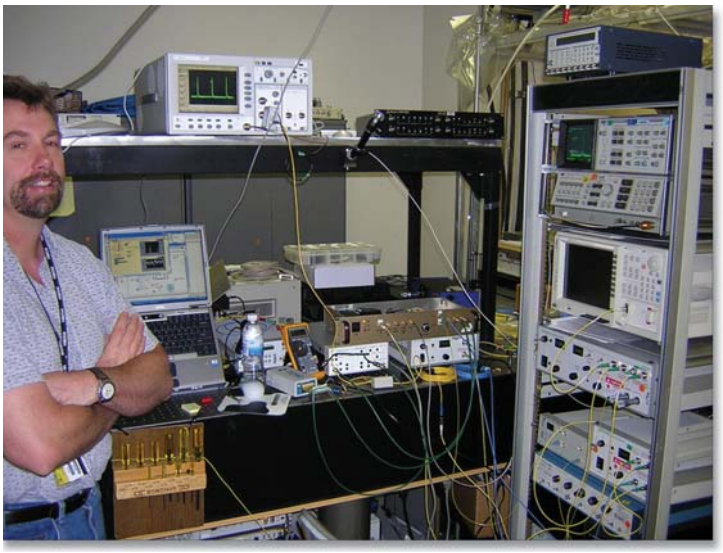

Figure 3. Bryan Moran optimizing the mode-locked fiber laser and pulse picking system. These are the initial components in the chain that generates the chirped time lens pump pulse.

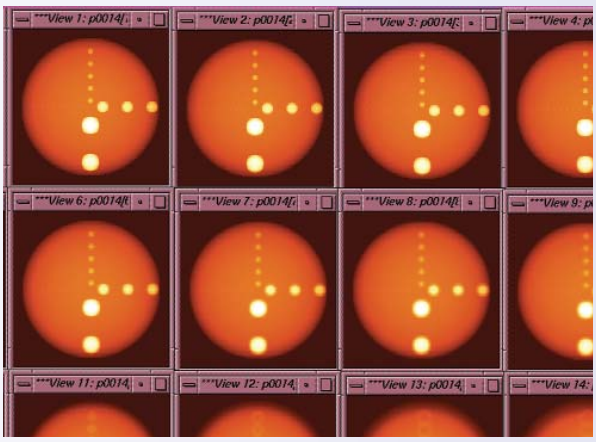

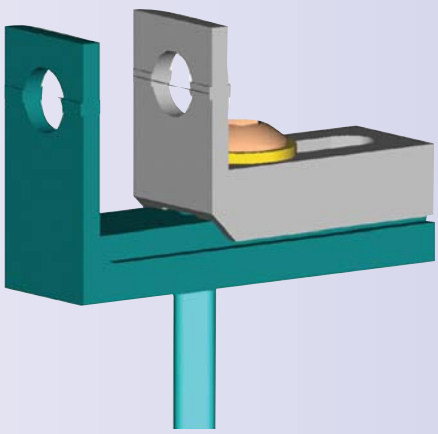

Center for Nondestructive Characterization

LDRD

Acoustic Characterization of Mesoscale Objects

For more information contact **Diane Chinn**
(925) 423-5134, chinn3@llnl.gov

Mesoscale is an emerging area of science and engineering that focuses on the study of materials with dimensions, features, and structures that range from a few millimeters down to a few micrometers. Mesoscale objects typically have embedded features that require resolutions on the order of a few micrometers. Mesoscale nondestructive characterization technologies are required that can, first, penetrate into or through a few millimeters of diverse materials and, second, provide spatial resolutions of about a micrometer.

An acoustic technique is attractive because it offers high sensitivity to features such as thickness and interface quality that are important to mesoscale objects. In addition to the resolution requirements, many mesoscale objects require a noncontact technique to avoid damaging fragile surfaces.

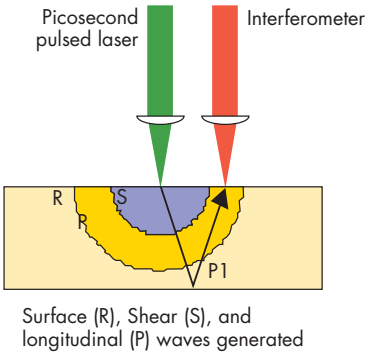

Figure 1. Schematic of Laser UT. Laser UT uses a pulsed laser as a source to generate acoustic waves, and a laser interferometer to detect them. The source and receiver can be on the same side (as shown) or on opposite sides of the object. The acoustic wave travels through the object before it is detected. Use of a pulsed laser gives temporal resolution to the detected signal.

Project Goals

The goal of this project is to research characterization of mesoscale objects using noncontact laser ultrasonic (UT) techniques (Fig. 1). Spatial resolution requirements in mesoscale objects require the use of frequencies from 100 MHz to 10 GHz to acoustically characterize features from 5 to 0.5 μm in size. At this time, laser UT in this frequency range does not exist (Fig. 2).

The three phases of this project are viability (FY2004), prototype (FY2005-FY2006) and demonstration (FY2006). The biggest challenge to this research, addressed in the viability phase, is the propagation distance attainable at GHz frequencies. Mesoscale objects usually have structures with thicknesses on the order of 25 to 200 μm. Inspection of these structures requires propagation distances of the same order. Propagation distance is governed by attenuation of the acoustic wave and is strongly dependent upon material.

Another challenge to this work is the identification of optimal laser parameters to mitigate ablative damage to the object upon acoustic wave generation.

Relevance to LLNL Mission

This proposal impacts the DNT, NIF, Engineering, and Chemistry and Materials Science Directorates through high-energy-density physics laser target fabrication and characterization. Other applications, such as fuel cells, biological cells, and tissue research, will benefit the Nonproliferation, Arms Control and International Security, and the Biology and Biotechnology Research Directorates.

FY2004 Accomplishments and Results

In FY2004, the viability of using GHz ultrasound in materials important to the Laboratory was demonstrated using a laser-based acoustic system at frequencies ranging from 500 MHz to 1 GHz. From these measurements, acoustic velocity and attenuation at 800 MHz are derived for some materials (see table). Also listed in the table are ablative and thermoelastic propagation distances. These propagation distances generally exceed the 200-μm nominal thickness of mesoscale objects. These results indicate that GHz laser UT is viable for characterization of mesoscale objects. Establishment of viability sets the stage for the design and construction of an acoustic characterization system for mesoscale materials.

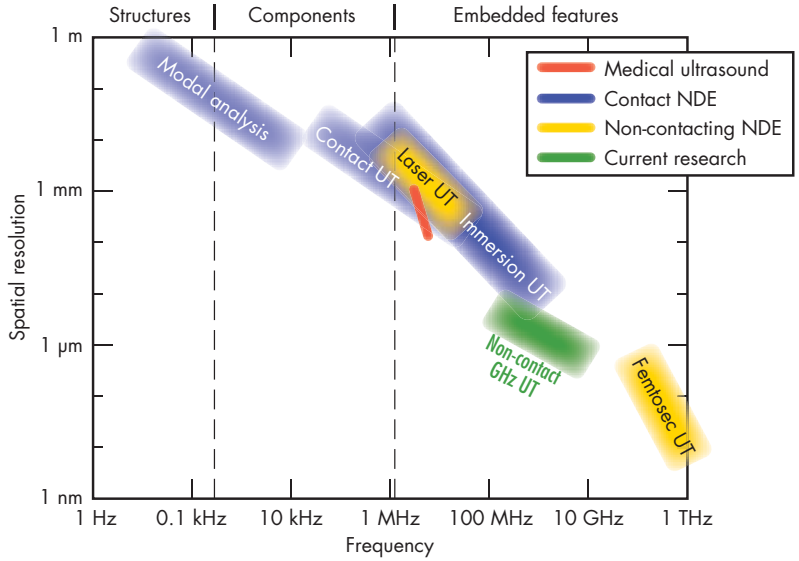

Figure 2. Chart showing two key parameters describing acoustic characterization: which systems exist, and the range of the particular technique.

Material	Approx. ablation energy (μJ)	Attenuation @ 0.8 GHz (dB/mm)	Wave speed (mm/μs)	Wavelength @ 0.8 GHz (μm)	Prop. distance, thermoelastic (μm)	Prop. distance, ablative (μm)
Aluminum	0.13	49.9	6.58	8.2	700	1100
Copper	0.14	77.8	4.07	5.1	225	525
Vanadium	0.13	52.3	5.88	7.4	225	825
Gold	0.16	58.6	3.25	4.1	200	250
Tantalum	0.15	69.6	4.26	5.3	100	200
Polystyrene	0.2*	68.7	2.05	2.6	350	—
Polycarbonate	0.2*	40.1	1.95	2.4	525	—
Polyamide	0.2*	60.5	1.89	2.4	150	—

*thermoelastic excitation only

Measured laser and acoustic parameters from the laser UT system, demonstrating the viability of GHz acoustics.

Related References

1. Chambers, D., D. Chinn, and R. Huber, "Optical Mapping of the Acoustic Output of a Focused Transducer," *Proceedings of the 147th Acoustical Society of America Meeting*, 2004.

2. Scruby, C., Laser Ultrasonics: Techniques And Applications, Adam Hilger, New York, New York, 1990.

FY2005 Proposed Work

In the FY2005 prototype phase, acoustic parameters measured in the viability phase will be used to model GHz laser UT. With this optoacoustic model we will determine resolution and penetration capability of GHz ultrasound in other materials; design the GHz acoustic system; study the onset of ablation and its effects on wave generation; and model the characterization of mesoscale objects.

Designs for the acoustic characterization system will be finalized, and construction of the system will begin. Testing of the system is scheduled to take place during the second half of FY2005. Extensive modeling of laser/material interaction will be undertaken to assist with modeling of the acoustic waves that are generated and then propagate through the material.

Advancing the Technology R&D of Tabletop Mesoscale Nondestructive Characterization

For more information contact **Harry E. Martz, Jr.**
(925) 423-4269, martz2@llnl.gov

This project will advance nondestructive characterization of mesoscale (mm-sized) objects, allowing μm resolution over the objects' entire volume. X-ray imaging will be developed that allows object characterization with materials that vary widely in composition, density, and geometry.

Project Goals

The overall goal is to research the science and engineering needed to nondestructively characterize and model mesoscale objects. The spatial resolution goal for this microscopy is roughly 1 μm^3 or better, while the contrast goal represents a signal-to-noise ratio of 1000:1.

Relevance to LLNL Mission

Specific LLNL programs that would benefit from this new capability include the development of novel sensors for NAI applications; the study of explosive samples for DoD and DOE; and high-energy-density physics and inertial confinement fusion experiments for NIF.

FY2004 Accomplishments and Results

We performed several types of modeling to better understand x-ray imaging of mesoscale objects. Characterization of the solid deuterium-tritium (D-T) fuel layer in an ICF capsule using a beryllium ablator requires phase-contrast imaging. We chose

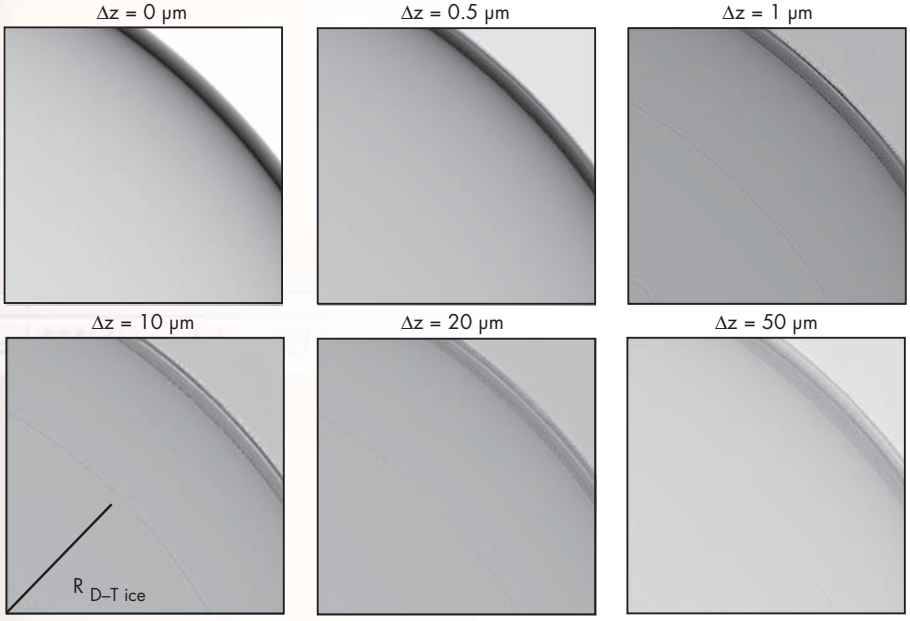

Figure 1. A perfect Wolter optic microscope simulation of a D-T ice layer inside a Be capsule. Exit-to-image-plane distances are labeled as Δz. The D-T ice gas layer is discernable for Δz ≥ 0.5 μm.

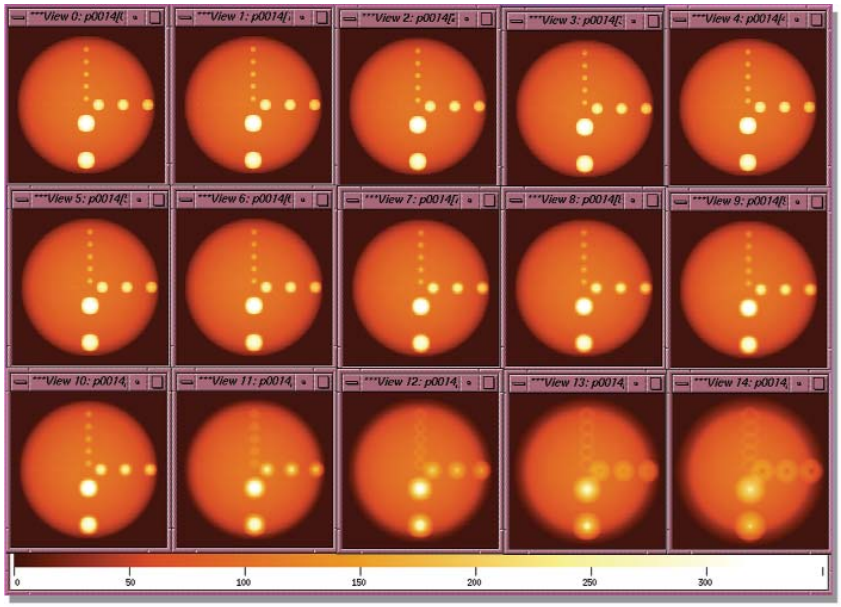

Figure 2. Simulated images of a 45-μm-diameter spherical object with a number of spherical inclusions on the center plane of the sphere. The first image has the center plane of the spherical object on the focal plane of a Wolter x-ray optic instrument. The succeeding images are the results of translations of the object toward the detector along the instrument axis. Images 2 to 10 are each 0.5 μm steps further from the focal plane (0.5 μm to 4.5 μm). The last five images are at 5, 10, 15, 20, 25 μm from the focal plane.

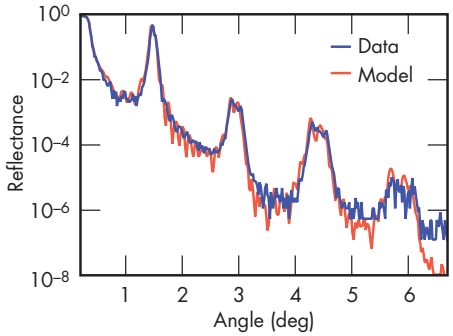

Figure 3. Measured reflectivity of the multilayer coating as a function of incident angle.

this as one example for our modeling work. We modeled projection imaging systems with a coherent parallel-beam and a point source, and a large-size source with a Wolter x-ray imaging optic (Fig. 1). These studies showed that imaging was possible with either approach.

Objects with geometric and x-ray properties comparable to an ICF capsule were used in initial experimental tests of the modeling results. These objects were successfully imaged using LLNL's KCAT system, Xradia's μXCT, and ANL's Advanced Photon Source.

We examined whether it is necessary to use the multislice method to solve the paraxial wave equation to simulate x-ray microscopy of mesoscale objects, or if ray tracing will suffice. Preliminary results reveal ray tracing was adequate for modeling the propagation of x rays through mesoscale objects of interest.

Additional modeling probed the imaging capability and limitations of a Wolter x-ray microscope system. This system was designed to characterize mesoscale objects to sub-μm spatial resolutions. A code has been developed to model the 2-D image formation in a Wolter x-ray microscope. A series of simulations using various objects were run to study the effects of the optics (Fig. 2). These simulations were analyzed using both laminographic and tomosynthesis methods.

One Wolter 8-keV x-ray optic was fabricated for the microscope, with two important results. First, the team developed a framework and methodology for the construction of high-precision optics for future efforts at LLNL. Second, we demonstrated both a laterally- and a depth-graded multilayer coating to maximize the throughput of the optic (Fig. 3).

Related References

1. Kozioziemski, B. J., J. A. Koch, A. Barty, H. E. Martz, W.-K. Lee, and K. Fezzaa, "Quantitative Characterization of Inertial Confinement Fusion Capsules Using Phase Contrast Enhanced X-Ray Imaging," submitted to *J. Appl. Phys.*, 2004.

2. Martz, Jr., H. E., and G. F. Albrecht, "Nondestructive Characterization Technologies for Metrology of Micro/Mesoscale Assemblies," *Proceedings of Machines and Processes for Microscale and Mesoscale Fabrication, Metrology, and Assembly,* ASPE Winter Topical Meeting, Gainesville, Florida, January 22-23, pp.131-141, 2003.

FY2005 Proposed Work

This initiative has evolved into two projects, one focusing on x-ray phase-effects characterization, the other on x-ray optics fabrication.

Concealed Threat Detection at Multiple Frames per Second

For more information contact **John T. Chang**
(925) 424-4624, chang16@llnl.gov

We are investigating the science and technology of real-time array imaging as a rapid way to detect hidden threats through obscurants such as smoke, fog, walls, doors, and clothing. Our purpose is to augment the capabilities of protective forces in concealed threat detection, including people as well as weapons.

Among other attributes, ultra-wideband (UWB) can penetrate and propagate through many materials, such as wood, some concretes, non-metallic building materials, and some soils, while maintaining high range resolution. We have built collaborations with university partners and government agencies. We have considered the impact of psychometrics on target recognition and identification. Specifically, we have formulated images in real-time that will engage the user's vision system in a more active way to enhance image interpretation capabilities.

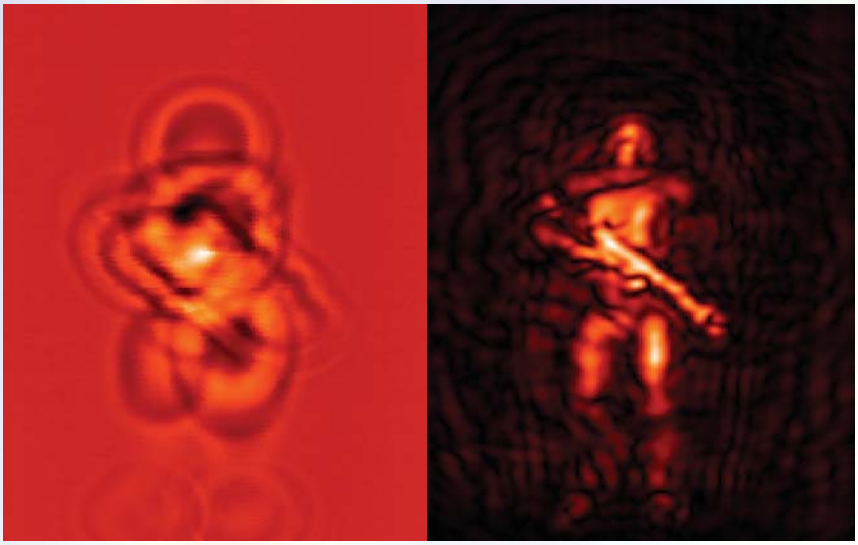

Figure 1. Sample frames from UWB radar imaging of a man holding a rifle 1 m down range. Left: image from simple Hugh transform. Right: image from a computationally intensive reconstruction algorithm.

Project Goals

We evaluated the ability of real-time UWB imaging for detecting smaller objects, such as concealed weapons that are carried by the obscured personnel. We also examined the cognitive interpretation process of real time UWB electromagnetic images. The specific goals included:

1. Develop/test a real-time array imaging simulation tool from existing static codes.
2. Research new image processing methodologies and potential algorithms that can be preformed in real-time, and demonstrate the benefits from real-time visualization.
3. Build one or more scaled-down laboratory arrays based on the most advanced field-programmable gate arrays (FPGAs).
4. Use the simulation tool to test the sensitivity of various array designs.
5. Measure the capability of human visual perception in real time versus static imaging, under various conditions.
6. Develop a plan for implementation of a full array for human perception studies and potential sponsor demonstrations.

Relevance to LLNL Mission

LLNL has an interest in improved weapons detection. A real-time radar camera will be an enabling scientific achievement because it will be unique in the world, and it will have enormous applicability.

FY2004 Accomplishments and Results

To meet our goals, we have developed a numerical imaging algorithm and implemented it to study UWB beam forming and steering. We have been successful in developing a computational simulator system to evaluate and predict the performance of the imaging system. The simulator is capable of generating impulse radar images of moving

targets with arbitrary trajectories. It is capable of facilitating parametric studies of the effects of transceiver element configuration. It has been used to guide us in anticipating and benchmarking what information the laboratory prototype system should be acquiring.

Further, we have been successful in building the laboratory prototype radar camera hardware, and we subsequently used it to study and characterize UWB image generation (see Fig. 1).

We have collaborated with the DoD in characterizing the behavior of UWB electromagnetic signals through various building materials, and to assess the capability of imaging through such materials. A provisional patent application has been put in place.

To evaluate the physical characteristics and limitations of using UWB signals for imaging, we further quantified and demonstrated the effects of UWB beam forming and focusing ability. Figure 2 shows a case comparison of the effect of bandwidth on the ability to focus UWB signals. It clearly demonstrates that a large bandwidth is not only desired, but also required to enable focusing.

We evaluated the effect of array configurations that will enable beam steering. Figure 3 demonstrates that an array configuration of interleaving transceivers suppresses sidelobe levels that in turn can enable a much better capability of image formation.

Two records of invention and associated patents have been filed: "Through Wall Motion Imaging, Tracking, and Discrimination of Multiple Human Heartbeats and Respiration Rates," and "Fast Framing, Through Obstacle, Electronically Steerable Dynamic Radar Imaging Array."

Related Reference

Chang, J., G. Azevedo, D. Chambers, P. Haugen, R. R. Leach, C. Paulson, C. E. Romero, A. Spiridon, M. Vigars, and J. Zumstein, "Ultrawideband Radar Methods and Techniques of Through Barrier Imaging," *IEEE International Symposium on Antennas, Propagation and USNC/URSI National Radio Science Meeting*, Monterey, California, June 20-26, 2004.

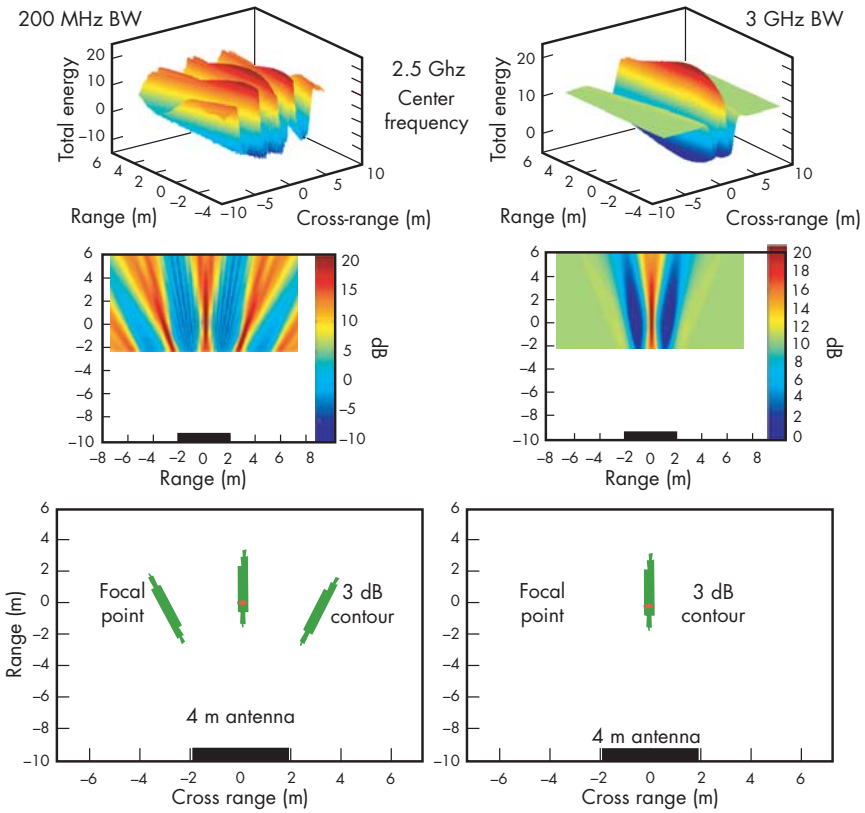

Figure 2. Example case comparison of the focusing ability of UWB signals as a function of bandwidth that will enable beam focus. Left column: narrow band signals cannot focus. Right column: UWB signals enhance focus.

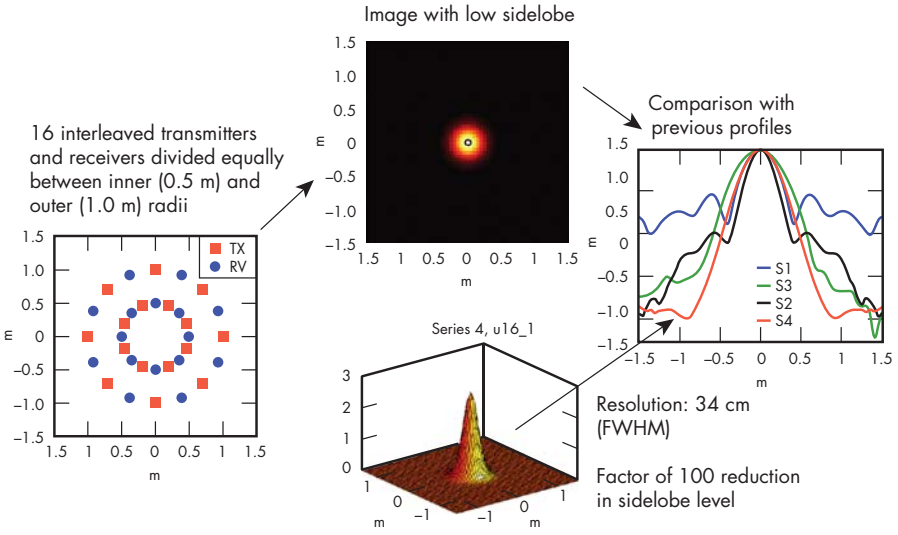

Figure 3. Example demonstrating the significance of array element distribution in suppressing the sidelobes that contribute to image quality degradations. S1 to S4 correspond to different element distributions of the antenna array. The configuration shown corresponds to S4.

IR Diagnostics for Dynamic Failure of Materials

For more information contact **Steven J. DeTeresa**
(925) 422-6466, deteresa1@llnl.gov

This project is exploratory research into the thermodynamics of dynamic deformation and failure of materials, using high-speed and spatially-resolved infrared (IR) temperature measurements. During deformation, mechanical work is converted to different forms of energy depending on the deformation process. For example, it can be dissipated as heat in purely plastic deformation, stored as strain energy in dislocations in metals and in oriented polymeric molecular structures, and expended during the generation of new surfaces during damage and fracture. How this work is converted into these various forms is not well understood. In fact, there is controversy for the relatively simple case regarding the amount of work dissipated as heat during uniform plastic deformation.

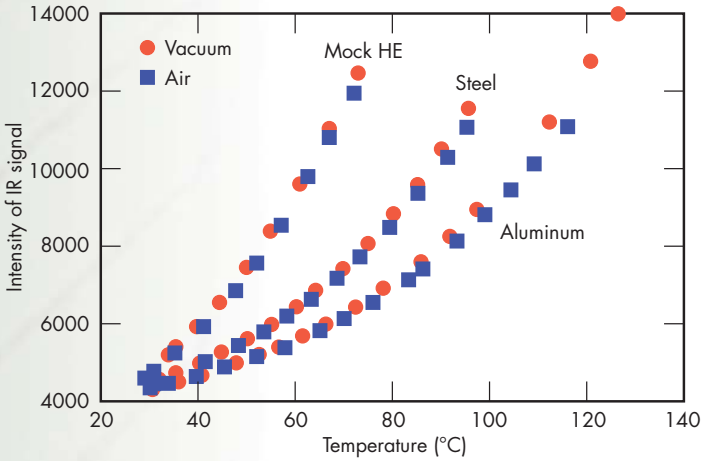

Figure 1. Comparison of IR temperature calibrations in air and vacuum for various materials.

Project Goals

The goals are to develop dynamic IR temperature measurement techniques and apply them to gain a better understanding of the dynamic failure processes in both metals and polymeric composite materials. The experimental results will be compared against predictions of existing constitutive models and guide the development of higher fidelity models if needed.

Relevance to LLNL Mission

The completion of this project will improve our competency in stockpile stewardship materials experiments. Future DOE applications of the IR temperature measurement technology include machining and safety aspects of explosives, verification of existing material models, and contributions to the development of new material models. The capabilities will be immediately applicable to the study of hazardous (radioactive, toxic, and explosive) materials that are unique to NNSA laboratories. The capability will also be beneficial to DoD for armor/anti-armor applications of materials; and to NNSA for penetrator case materials in the Robust Nuclear Earth Penetrator program, and for materials for explosive containment vessels.

FY2004 Accomplishments and Results

To resolve the controversy regarding the percentage of plastic work that is converted to heat for metals, we have completed a series of experiments.

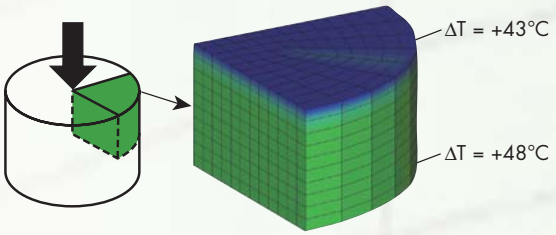

Figure 2. Spatial distribution of temperature rise in a top quadrant of a cylindrical metal specimen that is uniformly compressed to a true strain of 35% at a rate of 35 s^{-1}.

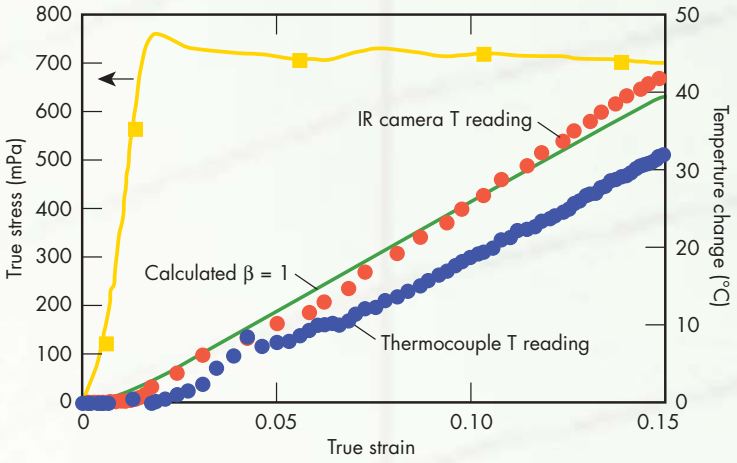

Figure 3. Stress-strain response and simultaneous temperature measurement during compression of pure Ta at a strain rate of 10 s^{-1}.

Calibrations of IR temperature measurement in controlled environments were performed using an environment chamber designed for this purpose and for controlling atmosphere during dynamic deformation. We have shown that there is no significant difference between calibrations performed in air or vacuum for metals and a mock high explosive (HE) (Fig. 1).

Repeated calibrations in air of both metals and mock HE to maximum temperatures expected during dynamic deformation (~100 °C above ambient) showed that emissivity did not change. This demonstrates that for these materials, surface oxidation does not occur or does not alter IR emissivity in this temperature range.

Thermomechanical modeling using LS DYNA was performed for the uniform compression of metals at different strain rates to determine when adiabatic conditions are met. At intermediate strain rates (~10 s^{-1}) most of the specimen is compressed adiabatically (Fig. 2).

Preliminary tests with Ta at intermediate strain rate yielded different values of temperature when measured using IR and a thermocouple. An example is shown in Fig. 3, where the Taylor-Quinney coefficient, β, which represents the fractional conversion of plastic work heat, is found to be 1.0 for IR measured temperature and 0.8 for thermocouple data. We are characterizing the emissivity of deformed specimens and the temperature response of the thermocouple on the specimen to resolve this discrepancy.

FY2005 Proposed Work

If we find that β is significantly less than 1—indicating that a significant fraction of work is stored as a change in internal energy—we will study how the remaining mechanical work is stored in a plastically deformed material. If β is found to be close to 1, we will have shown that plastic deformation is a completely dissipative process. We will also characterize the temperature gradients due to strain localization from shear bands in dynamic deformation experiments with metals using the high-speed detector acquired in FY2004. A key part of this work will be the measurement of the detector system spatial resolution in terms of a modulation transfer function determined using either line or edge broadening.

We will also continue the work with mock HE to determine the energy conversion and dissipation mechanisms under uniform dynamic deformation.

Phase Effects on Mesoscale Object X-Ray Absorption Images

For more information contact **Harry E. Martz, Jr.**
(925) 423-4269, martz2@llnl.gov

At Lawrence Livermore National Laboratory, we are placing particular emphasis on the NDC of "mesoscale" objects. We define mesoscale objects as objects that have mm extent with μm-sized features. Here we confine our discussions to x-ray imaging methods applicable to mesoscale object characterization.

Project Goals

Our goal is the development of object recovery algorithms, including phase, to enable emerging high-spatial-resolution x-ray imaging methods to "see" inside, or image, mesoscale-size materials and objects. To be successful, our imaging characterization effort must be able to recover the object function to 1 μm^3 or better spatial resolution over a few mm × mm field-of-view, with very high contrast.

Relevance to LLNL Mission

Specific LLNL programs that would benefit from this new capability include the development of novel sensors for NAI applications; the study of explosive samples for DoD, DOE; and high-energy-density physics and inertial confinement fusion experiments for NIF.

FY2004 Accomplishments and Results

Our approach includes the research, development, and validation of algorithms to model phase-contrast effects observed in x-ray systems, and to use these algorithms for quantitative object recovery. This requires three tasks.

First, we are modifying HADES to model phase effects for point projection imaging, and investigating whether multi-slice techniques within the object are needed to fully capture the physics seen in phase-contrast data. Second, we are developing several object recovery approaches using parameter-based and voxel-based techniques. Third, we are validating these simulations against x-ray systems using well-known objects. At the end of this R&D, we will have a set of validated x-ray codes for modeling and reconstructing objects, including the effects of phase.

We have extended HADES to be able to calculate both the x-ray attenuation and phase of complex objects, a capability that is already showing relevance to other LLNL projects.

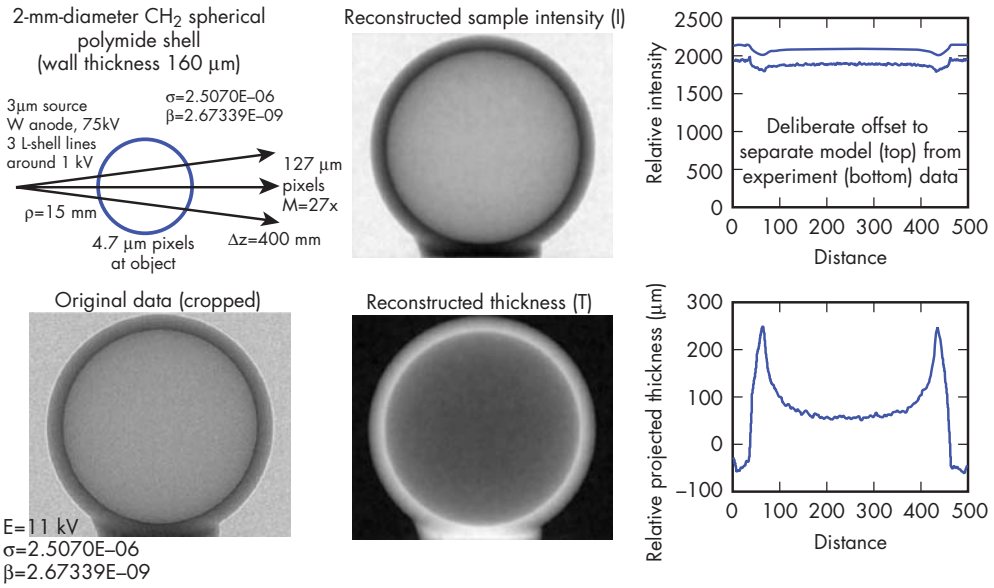

Figure 1. Application of the single-material reconstruction algorithm to LLNL's KCAT data of a polystyrene sphere.

We have reached the point in x-ray imaging where the spatial resolution and object dimensions could theoretically result in the wave diffraction effects within the sample becoming significant. We studied this possibility and determined that diffraction effects on the measured data will be insignificant.

Typically more than one image is required to separate the object phase and absorption structure. However, for the case of an object composed of a single material, both the projected phase and the amplitude through an object are directly related to the projected material thickness. This enables the object to be described in a single variable, the object thickness, as opposed to two variables, amplitude and phase. This in combination with the transport of intensity equation yields a strategy for reconstructing the object taking into account phase effects in the detected image. This approach has been implemented numerically (Fig.1).

Continued modeling has identified that there is a shift in position of key features within an object that can be explained only by incorporating phase effects into the system modeling (Fig. 2).

A key part of this proposed project is the validation of the simulation and object-recovery codes. Two things are required to validate x-ray simulation codes: the x-ray system being modeled, and a well-known object (also known as a phantom or reference standard). We have designed a multislice phantom that can be modeled and used to validate the simulations (Fig. 3).

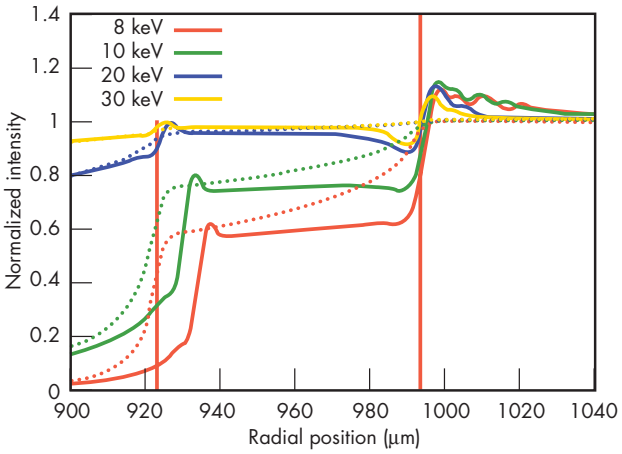

Figure 2. Simulated results for x-ray imaging of a CVD diamond shell coated on a SiN mandrel. The image shows the shift in position of the interface with energy. Results with phase effects included are shown by the solid lines. Results with no phase effects are shown by the dashed lines. Note the dramatic difference in the phase data as a function of energy (due to the change in refractive index) compared with the results for no phase.

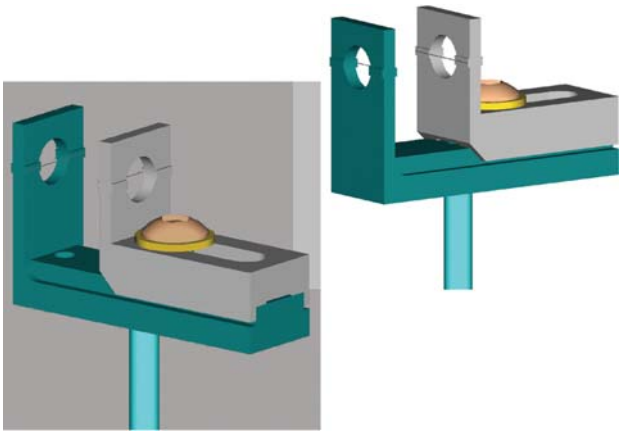

Figure 3. Phantom designed to validate the multislice (also known as the beam propagation) method to solve the paraxial wave equation to simulate x-ray microscopy of mesoscale objects and determine if ray tracing within the object will suffice. The phantom has two carbon fibers of 6-µm diameter that can be placed at different locations (0 to 10 mm) along the x-ray beam axis.

Related References

1. Aufderheide, M. B., D. M. Slone, and A. E. Schach von Wittenau, "HADES, A Radiographic Simulation Code," *Review of Progress in Quantitative Nondestructive Evaluation,* **20A,** *AIP Conference Proceedings,* **557**, pp. 507-513, 2000.

2. Aufderheide, M. B., A. Barty, and H. E. Martz, "Simulation of Phase Effects in Imaging for Mesoscale NDE," LLNL, UCRL-CONF-206263, submitted to *Review of Progress in Quantitative Nondestructive Evaluation,* 2004.

3. Barty, A., K. A. Nugent, A. Roberts, and D. Paganin, "Quantitative Phase Tomography," *Opts. Comm.,* **175**, pp. 329-336, 2000.

4. Martz Jr., H. E., and G. F. Albrecht, "Nondestructive Characterization Technologies for Metrology of Micro/Mesoscale Assemblies," *Proceedings of Machines and Processes for Microscale and Mesoscale Fabrication, Metrology, and Assembly*, ASPE Winter Topical Meeting, Gainesville, Florida, January 22-23, pp. 131-141, 2003.

FY2005 Proposed Work

We will focus on 2-D simulations and uniform object recovery. HADES incorporation of phase effects and the multislice code will be validated using phantoms. Object recovery algorithms will be investigated and validated for uniform single material objects and parametric reconstructions using HADES.

Ultrasonic NDE of Multilayered Structures

For more information contact **Michael J. Quarry**
(925) 422-2427, quarry1@llnl.gov

This project developed ultrasonic NDE based on guided and bulk waves in multilayered structures using arrays. First, a guided wave technique was developed by preferentially exciting dominant modes with energy in the layer of interest via an ultrasonic array. Second, we used Fermat's principle of least time, as well as wave-based properties, with a bulk wave technique, to reconstruct array data and image the multilayered structure.

Inspecting multilayered structures with a guided wave relies on exciting modes with sufficient energy in the layer of interest. Multilayered structures are modeled to determine the possible modes and their distribution of energy across the thickness.

Bulk wave imaging algorithms were developed to overcome the difficulties of multiple reflections and refractions at interfaces. Reconstruction algorithms were developed to detect and localize flaws.

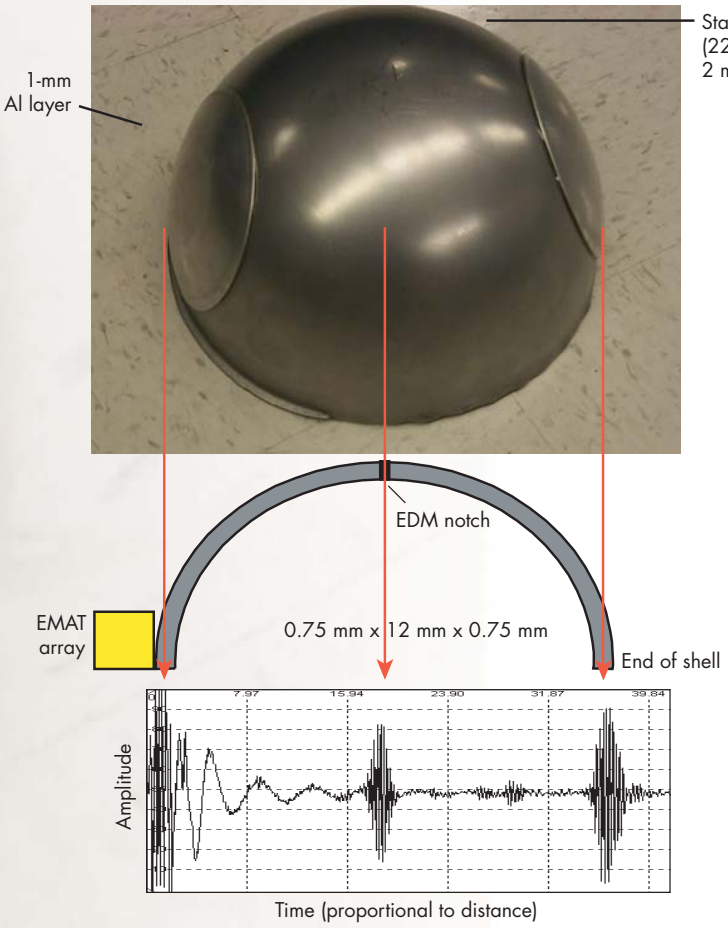

Figure 1. A sample RF waveform, showing the detection of an EDM notch using a guided wave on a curved stainless steel structure with A1 layers bonded at the sides with epoxy.

Project Goals

The goals of the guided wave technique were to detect a 20% through-wall notch in the bottom layer of a three-layer structure, and demonstrate the technique on curved structures. The project goal for the bulk wave technique was to detect a 1-mm drilled hole in the layer of interest.

Relevance to LLNL Mission

Both guided and bulk wave inspection techniques developed in this work will enhance LLNL's role in stockpile stewardship and inspecting weapons without disassembly. Experiments have also shown the scalability of guided waves to smaller curvatures, such as boiler tubing, and shows promise for application to NIF targets. In addition, the planar multilayer diffraction tomography reconstruction algorithms may image density distributions in explosives as well as shallow, near earth environments, to look for buried hazardous waste and covert trans-border tunnels.

FY2004 Accomplishments and Results

In FY2004, we evaluated the quantitative detection abilities of both techniques. Also, feasibility studies were conducted on programmatic-like structures. Experimental studies were conducted on tubes to analyze the scalability and range of applicable curvatures.

Multilayer plates of Al-epoxy-steel were constructed with notches of depths 10%, 20%, 30%, 50%, and 100% through-wall in the bottom layer. The guided wave technique showed sensitivity to detect the smallest (10%) flaw, exceeding our goal.

Electromagnetic acoustic transducer arrays were used to excite and detect an EDM notch at the pole of a curved multilayer structure, with excellent signal-to-noise (Fig. 1). Additional experiments were conducted on a stainless steel tube to show applicability to smaller curvatures. A through-wall crack and secondary cracking were created on a tube by bending it several times. A piezoelectric array excited a guided wave from one end of the tube and detected the cracks (Fig. 2).

For bulk waves, an Al-Cu planar sample was constructed with a side-drilled hole. Data were collected with a 5-MHz ultrasonic array. For the wave-based algorithm, the Green function was calculated to use diffraction tomography inversion algorithms that significantly simplify inversion. Both wave-based and bent-ray algorithms were used to reconstruct the data. Both images resulted in an accurate location and size of the hole. Holes of diameters 0.75 mm and 1.5 mm were later tested. The bent-ray algorithm imaged the 0.75-mm flaw, but the newer wave-based algorithm requires more work.

Related References

1. Quarry, M. J., "Phased Array Design Concepts for Lamb Wave Mode Tuning," *Nondestructive Characterization of Materials,* **XI,** pp. 81-87, 2003.
2. Quarry, M. J., "Guided Wave Inspection of Multilayered Structures," *Review of Progress in Quantitative Nondestructive Evaluation,* **23A,** pp. 246-253, 2004.
3. Lehman, S. K., "Hilbert Space Inverse Wave Imaging in a Planar Multilayer Environment," *Journal of the Acoustical Society of America,* in press.
4. Fisher, K. A., "Development of a Quantitative Multiview Time Domain Imaging Algorithm Using a Fermat Correction," *Journal of the Acoustical Society of America,* in press.

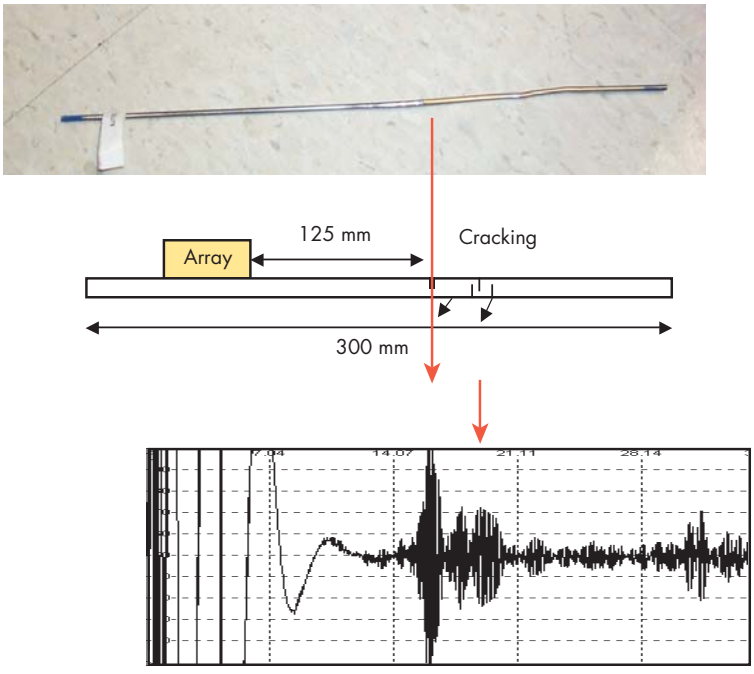

Figure 2. Sample results from an experiment on a stainless steel tube. Cracks in a 6-mm-diameter tube were detected by a guided wave with the array at 125 mm from the largest through-wall crack.

FY2005 Proposed Work

In our guided wave work, we will study incorporating time reversal techniques to improve resolution. Future bulk wave techniques will include shear waves and curvatures in the reconstruction algorithms to enhance signal-to-noise in images.

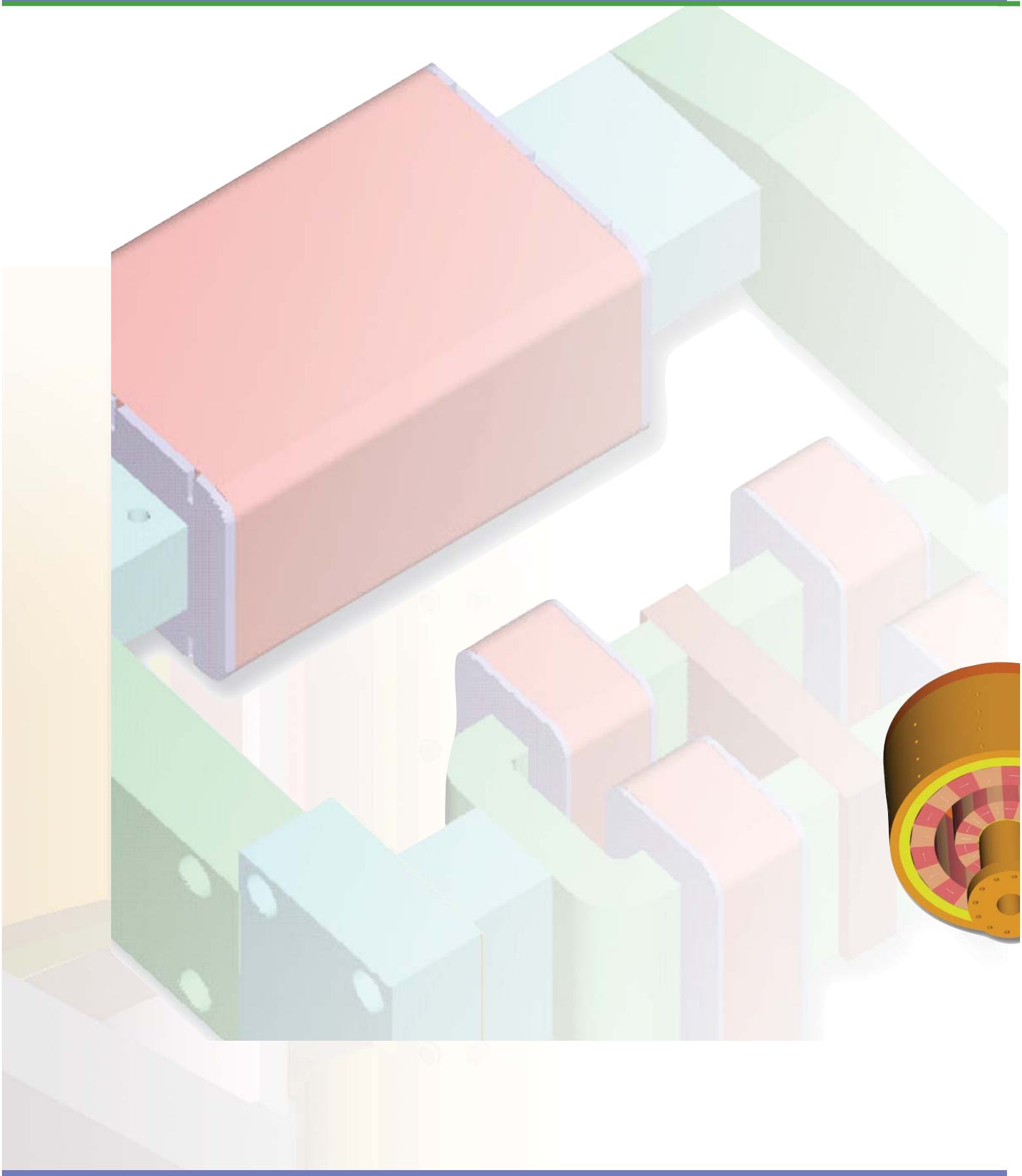

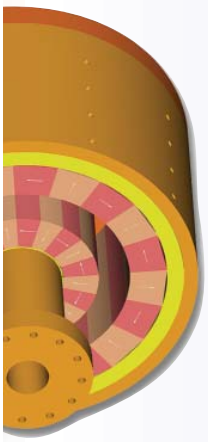

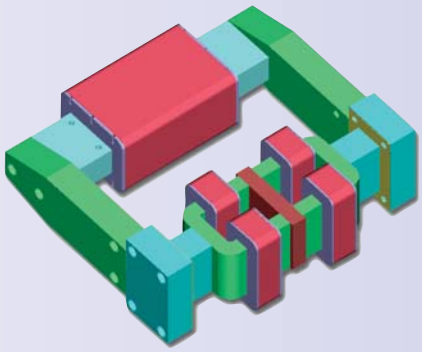

Center for
Precision Engineering

LORD

High-Stiffness Hybrid Passive/Active Magnetic Bearing for Precision Engineering Applications

For more information contact **Lisle Hagler**
(925) 423-8595, hagler3@llnl.gov

We intend to develop a dynamically stable, high-stiffness, hybrid passive/active magnetic bearing for the ultra-precise machining of parts. This bearing is to have low error motion so that it will be able to perform in this highly stringent application. Low error motion is defined to be 50 nm or less in this case. This study will show that, theoretically, the rotor error motions due to mass imbalance and internal/external excitation sources can be rendered negligible.

Additionally, we develop a methodology to initially align the rotor to meet our "error budget." At the same time, we must develop an active control scheme to take care of the residual rotor error motion.

Project Goals

The end result of this project will be the demonstration of the feasibility of our bearing concept. Also, we plan to have an initial design for a prototype of a hybrid passive/active magnetic bearing with the stiffness and stability for precision machining operations that will meet or exceed state-of-the-art tolerance limits.

Relevance to LLNL Mission

Applications of improved precision machining include mirrors for laser-optic systems, telescope mirrors for basic science and reconnaissance, and high-energy-density physics targets, all pertaining to key LLNL missions in national security. In particular, the goal of achieving inertial confinement fusion using lasers is dependent on the precision of the system's optical components.

FY2004 Accomplishments and Results

This study has shown, theoretically, that rotor error motions due to mass imbalance and internal/external excitation sources can be rendered negligible.

We also met our goal of developing a methodology to initially align the rotor to meet our error budget constraint. At the

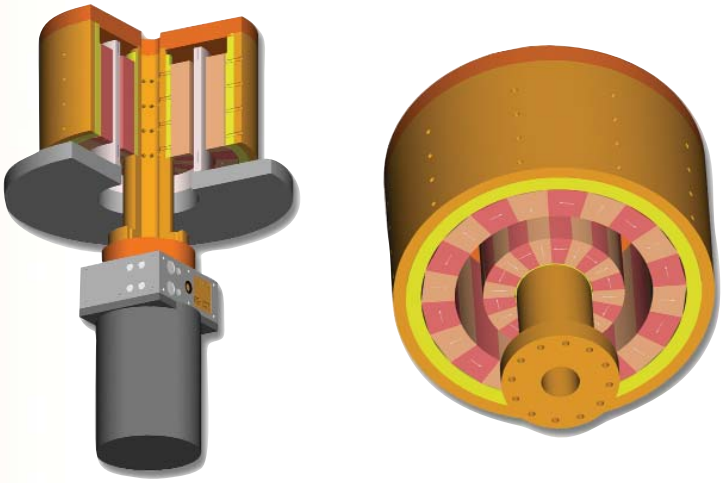

Figure 1. Views of the preliminary design of prototype hybrid passive/active magnetic bearing.

same time, we developed an active control scheme to take care of the residual rotor error motion. Our results indicate that it is possible to meet all error budget and design constraints. We conclude that it is quite feasible that the proposed bearing can be constructed and meet all design criteria. This has led to the preliminary design of a prototype machine using a hybrid magnetic bearing (see Fig. 1).

This prototype, because of the versatility of the Halbach design, is able to operate stably over a large range of spindle RPM (Ω) and spindle overhang (l_H). Stability is ensured whenever Re (λ) <0 (see Fig. 2).

Figure 3 is the Campbell diagram of the system. The red lines are sources of rotor excitation and the blue lines are whirl modes as a function of rotor RPM. At the RPM (Ω) where these lines cross, there is potential for large amplitude vibration. The Halbach array can easily be designed such that the system operates at a point where it is insensitive to these excitations.

In summary, this hybrid bearing will be capable of stable dynamic operation and high stiffness over a large range of rotor RPM. "Designing-in" insensitivity to internal or external excitation at operating speed allows for a low error-motion capability in the passive component. The active control system will then eliminate any residual error motion.

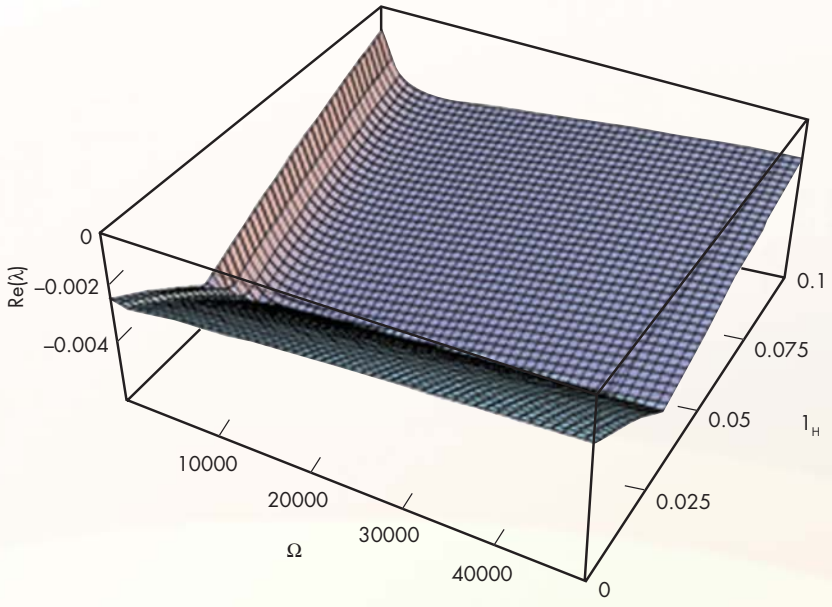

Figure 2. Rotor-dynamic stability diagram.

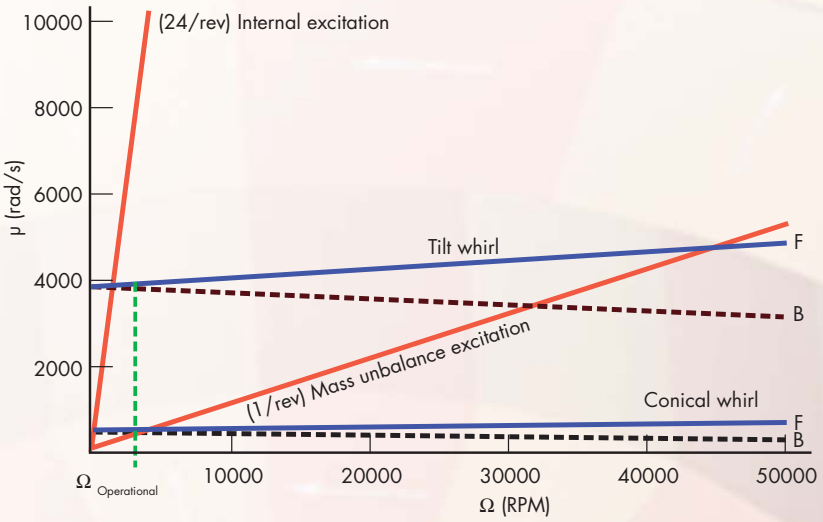

Figure 3. Campbell diagram.

Precision X-Ray Optics Development

For more information contact **John S. Taylor**
(925) 422-8227, taylor11@llnl.gov

Building on achievements of the EUVL Program, we have begun developing a long-term vision for manufacturing reflective x-ray optics that may lead to diffraction-limited performance (~100 Å). The feasibility of building a Wolter mirror with this spatial resolution raises significant system-level questions about detectors, reconstruction algorithms, and alignment that will also require similar levels of investment.

Project Goals

In the first three years of this program we set out to meet important goals: development and implementation of a complete process flow for the construction of reflective x-ray optics, improvement of metrology techniques, and fabrication of a replicated optic with 1 μm spatial resolution over a millimeter field of view.

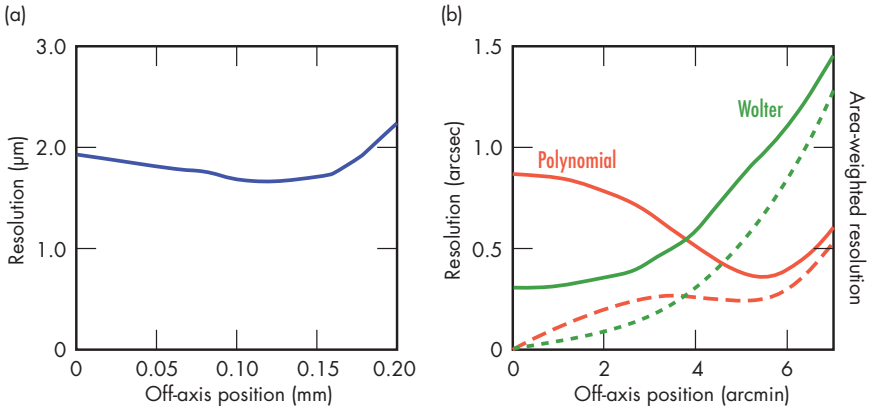

Figure 1. (a) Resolution vs. off-axis position for a standard Wolter optic designed to fulfill the imaging requirements for a 40-keV NIF backlighter experiment, assuming a figure error of 0.2 arcs. The field has been flattened by slightly shifting the position of the focal plane. (b) Comparison of a Wolter telescope with a design that incorporates additional polynomial terms to improve off-axis performance.

Relevance to LLNL Mission

Wolter systems fulfill demonstrated needs in a range of programmatic applications, including microscopy for high-Z NIF targets and imaging of NIF and EOS experiments. Figure 1 illustrates the combination of a Wolter optic with a 40-keV backlighter to perform a Ta foil experiment on NIF. Other applications include astronomical optics and manufacturing improvements that can be applied to synchrotron and LCLS beamline optics.

FY2004 Accomplishments and Results

Constructing an optical system that meets stringent resolution goals requires a detailed understanding of the process flow and an error budget that accurately captures limitations in manufacturing and metrology. As a test of key error sources in producing replicated optics, a flat test mandrel and replicated coupon are being fabricated. The process includes diamond turning a 2-in.-diameter flat; depositing electroless-nickel plating; diamond turning the nickel coating; polishing the diamond-turned nickel; and replicating the polished surface. Metrology is performed at each step to track the high ($\lambda < 100$ nm), mid (100 nm $< \lambda <$ 1 mm), and low ($\lambda >$ 1 mm) spatial frequency sources of error throughout the process. LLNL is performing all metrology and diamond turning. NASA MSFC is providing the polishing and replication.

Driving down the uncertainty in measurements will lead to more accurate maps of the surface, which can in turn be fed back into the process flow to improve the performance of the final optic. A major

challenge in inspecting x-ray optics is the interrelation of noncontact scan data with the optic's coordinate system.

Two options are being considered to provide this new capability. The first is based on the Phase-Shifting Diffraction Interferometer (PSDI) developed during the EUV Lithography Program. It appears that current PSDI designs can be used in a grazing incidence configuration to measure Wolter-type shells—singly or nested—as well as the convex replication mandrels themselves. The basic concept is sketched in Fig. 2.

The second approach is an integration of an optical profiling instrument with a coordinate measuring machine (CMM) that would lead to the measurement of an entire surface from a discrete set of sub-aperture scans. Candidates for the optical profiler include the well-known "Takacs Long-Trace Profiler" and a sub-aperture version of the PSDI that would provide both figure and finish information. Combining the PSDI with LLNL's Large Optic Diamond Turning Machine (LODTM), used as a CMM, opens the possibility of normal-incidence surface measurements of more complex shells and mandrels, thus increasing our capability beyond standard conic-shaped optics.

One difficult challenge is simultaneously meeting the stringent figure and finish specifications, as polishing usually leads to the degradation of figure. A novel solution to this problem takes advantage of the magnetron sputtering capabilities developed for the EUVL Program, where the precision of the figure control of the deposited layers was maintained to less than 0.1 nm rms (see Fig. 3).

Related References

1. Martz Jr., H. E., and G. F. Albrecht, "Nondestructive Characterization Technologies for Metrology of Micro/Mesoscale Assemblies," *Proceedings of Machines and Processes for Microscale and Mesoscale Fabrication, Metrology, and Assembly,* ASPE Winter Topical Meeting, Gainesville, Florida, January 22-23, pp. 131-141, 2003.

2. Burrows, C. J., R. Burg, and R. Giacconi, "Optimal Grazing Incidence Optics and Its Application to Widefield X-Ray Imaging," *Astrophysics Journal,* **392**, p. 760, 1992.

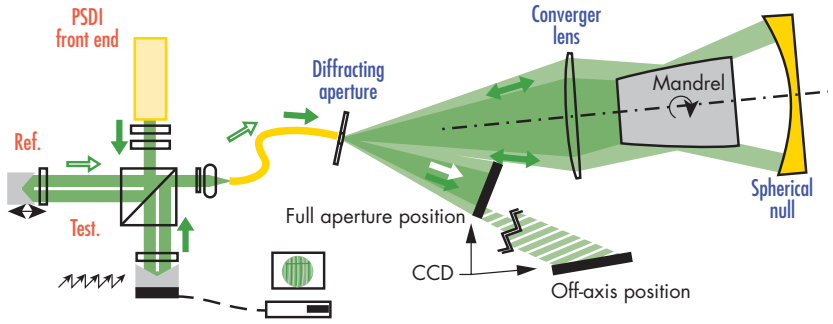

Figure 2. Sketch depicting the basic concepts of a PSDI design intended for grazing incidence metrology. The interferometer components are labeled in red, optical elements in purple, and detector elements in black.

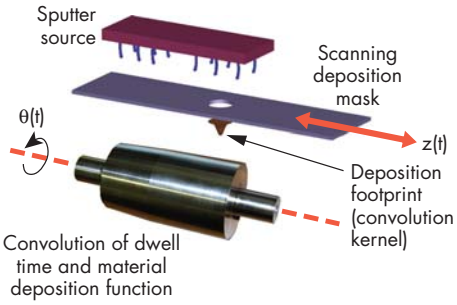

Figure 3. Extension of the EUV deposition technology envisioned for post-polishing figure correction. The mandrel rotates underneath a sputtering target configured with a small mask. Surface maps based on metrology techniques determine the rate the aperture mask moves across the mandrel face.

FY2005 Proposed Work

We propose to develop optical designs that meet the requirements of specific NIF/EOS diagnostics, and also of a target characterization microscope. A production process will be designed that can achieve optical surface errors consistent with sub-micron imaging resolution. Proof-of-principle developments will begin in optical fabrication and metrology for constructing and characterizing Wolter-type optics and mandrels.

Short-Stroke Rotary Fast Tool Servo for Single-Point Turning High-Energy-Density Physics Targets

For more information contact **Richard C. Montesanti**
(925) 422-7361, montesanti1@llnl.gov

This project developed a 10-kHz rotary fast tool servo (FTS) capable of 10-μm peak-to-peak (PP) motion at low frequencies and 2.5-μm PP motion at 10 kHz (500 g). A FTS provides a diamond-turning machine with a high-speed axis that allows the production of non-axisymmetric or textured surfaces on a workpiece that is rotating on a spindle at relatively high speeds. Our 10-kHz rotary FTS leverages on proof-of-principle from our successful 2-kHz rotary FTS developed during the previous years of this project.

The heart of the 10-kHz FTS is a normal-stress variable reluctance actuator having a flexure-guided rotor with an integral tool holder. The actuator is designed to produce a magnetic force-density an order of magnitude higher than the force density of a typical Lorentz-force actuator or shear-stress variable reluctance actuator. We merged the moving masses of our actuator and the payload into a single moving mass by attaching the tool arm directly to the rotating element of the actuator. This avoids the usual uncoupled-mode resonance of a servo system, and sets a relatively higher frequency non-rigid body mode of the moving mass as the lowest frequency uncontrollable mechanical resonance. Placing the displacement feedback sensor directly behind the tool, and careful design of the support structure, allow hiding certain flexible modes of the system to further improve high-frequency performance. When combined with a high-force-density actuator, the merged mass approach provides the high torque-to-inertia ratio needed for a 500-g tool-tip acceleration. Adjusting well-understood design parameters in future versions will allow achieving 1000 g and beyond.

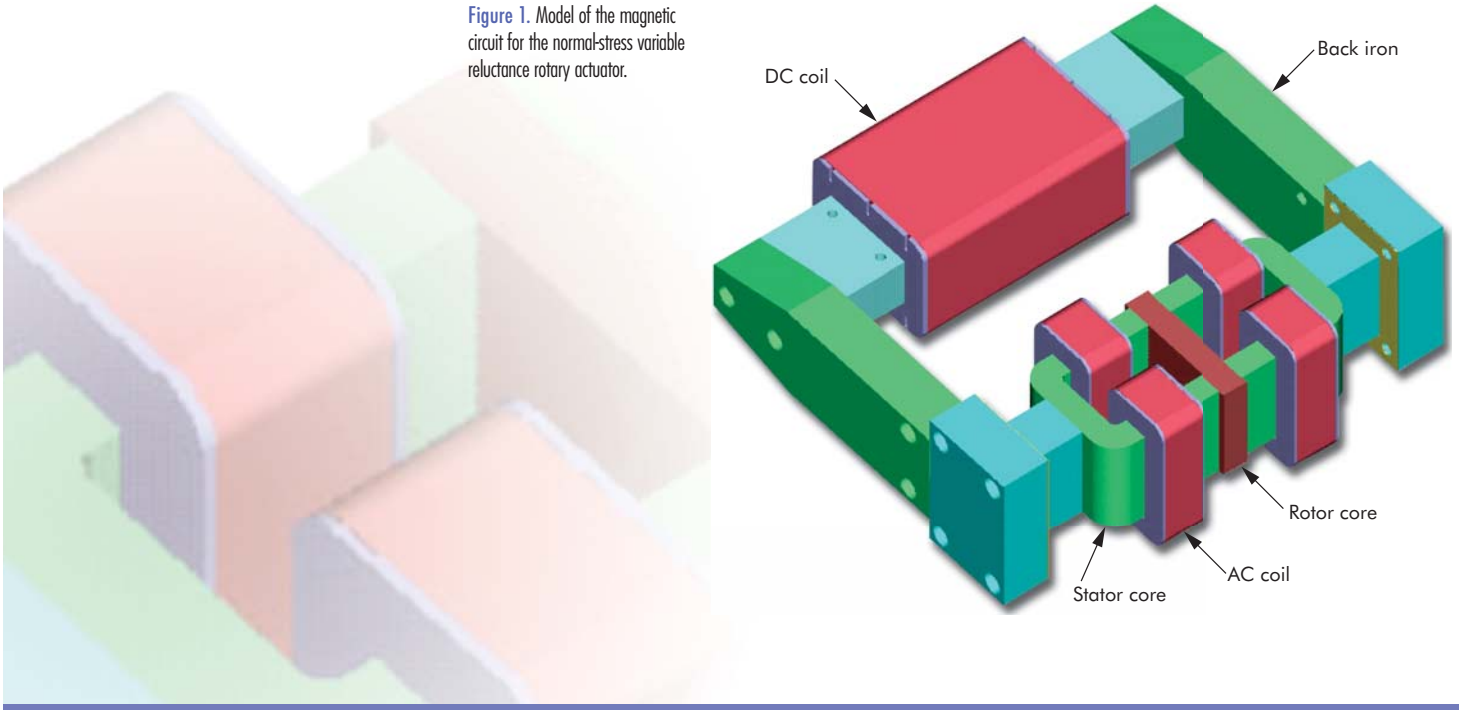

Figure 1. Model of the magnetic circuit for the normal-stress variable reluctance rotary actuator.

Project Goals

The goal of this project is to advance the state of the art in high-speed precision machine tools, specifically, to develop a FTS capable of producing a closed-loop motion of the tool tip at frequencies up to 10 kHz while producing optically smooth surfaces on diamond-turnable materials. Our original goal of a 5-μm PP stroke at 10 kHz (1000 g) was reduced to 2.5 μm PP (500 g) during a trade-off decision to have a more mechanically robust system with a higher likelihood of surviving anticipated tests for this prototype.

Relevance to LLNL Mission

High-energy-density experiments play an important role in corroborating the improved physics codes that underlie LLNL's stockpile stewardship mission. New and anticipated experiments to be conducted at NIF require extending LLNL's current capability for fabricating prescribed textured surfaces on a variety of diamond-turnable materials. 10-kHz bandwidth is an order of magnitude higher than commercially available FTS's and will enable reasonable production rates of the desired target surfaces and accommodate the surface cutting speed requirements of certain plastic target components.

FY2004 Accomplishments and Results

We developed software tools based on first-principle physics and closed-form engineering equations and used them to design and optimize the highly integrated mechanical-magnetic-electrical systems for the actuator and its payload. We completed and documented the detailed mechanical and electrical designs for the system, and procured all of the components. We presented two conference papers, and filed the second of two patent applications. As this work progresses, we will assemble the mechanical, magnetic, and electrical hardware; develop and integrate the control system; characterize the FTS performance with bench tests; and integrate the FTS with a diamond-turning machine to perform cutting tests on a workpiece.

Figure 1 shows a model of the magnetic circuit for this actuator. The rotor core is a rectangular prism suspended between two opposing C-shaped stator cores with nominal air gaps of 50 μm at the four pole faces.

Figure 2 shows a model of the rotor mounted to one of the stator housings via the outer ends of four of the eight flexures. Figure 3 shows a built-up model of the fully assembled 10-kHz rotary FTS.

Related References

1. Montesanti, R. C., and D. L. Trumper, "High Bandwidth Short Stroke Rotary Fast Tool Servo," *Proceedings of the American Society for Precision Engineering Meeting*, **30**, pp. 115-118, 2003.
2. Montesanti, R. C., and D. L. Trumper, "Design and Implementation of the Control System for a 2 kHz Rotary Fast Tool Servo," *Proceedings of the American Society for Precision Engineering Spring Topical Meeting on Control of Precision Systems*, pp. 28-33, April 2004.
3. Montesanti, R. C., and D. L. Trumper, "A 10 kHz Short-Stroke Rotary Fast Tool Servo," *Proceedings of the American Society for Precision Engineering 2004 Annual Meeting*, **34**, pp. 44-47, 2004.

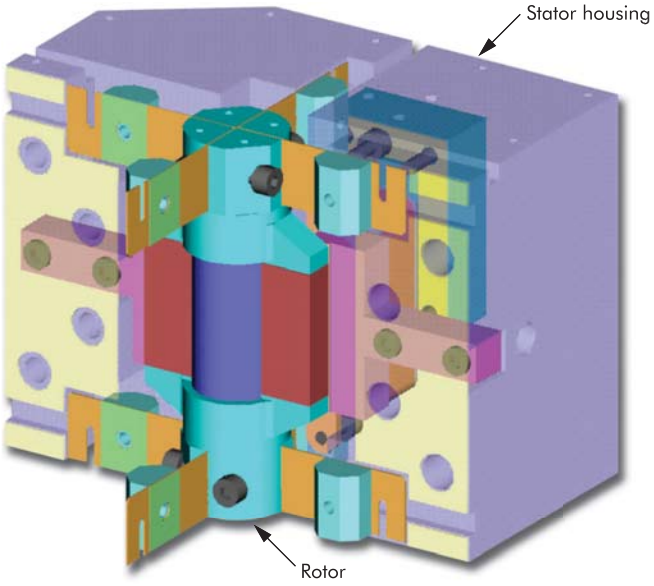

Figure 2. Model of the rotor mounted to one of two stator halves with flexures.

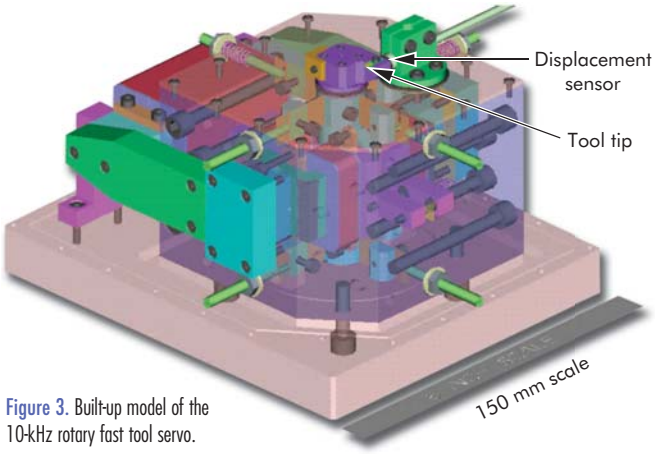

Figure 3. Built-up model of the 10-kHz rotary fast tool servo.


2
3
4

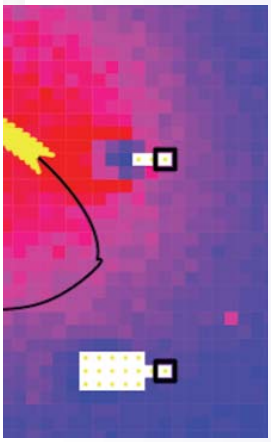

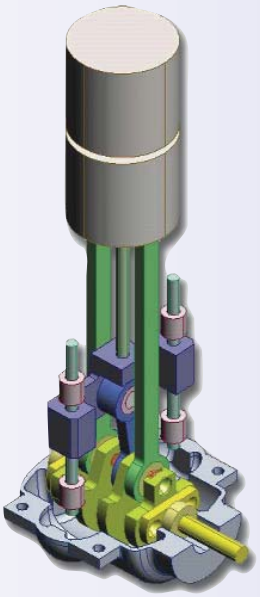

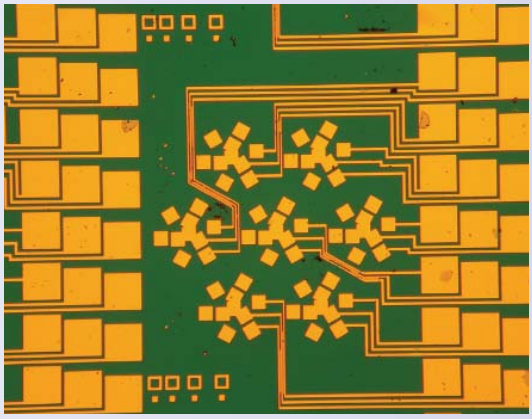

Center for
Complex Distributed Systems

LDRD

Dynamic Data-Driven Event Reconstruction for Atmospheric Releases

For more information contact **Gayle Sugiyama**
(925) 422-7266, sugiyama1@llnl.gov

For atmospheric releases, event reconstruction answers the critical questions – *How much material was released? When? Where?* and *What are the potential consequences?* Inaccurate estimation of the source term can lead to gross errors, time delays during a crisis, and even fatalities. We are developing a capability that seamlessly integrates observational data streams with predictive models to provide the best possible estimates of unknown source term parameters, as well as optimal and timely situation analyses, consistent with both models and data.

Our approach uses Bayesian inference and stochastic sampling methods (Markov Chain and Sequential Monte Carlo) to reformulate the inverse problem into a solution based on efficient sampling of an ensemble of predictive simulations, guided by statistical comparisons with data.

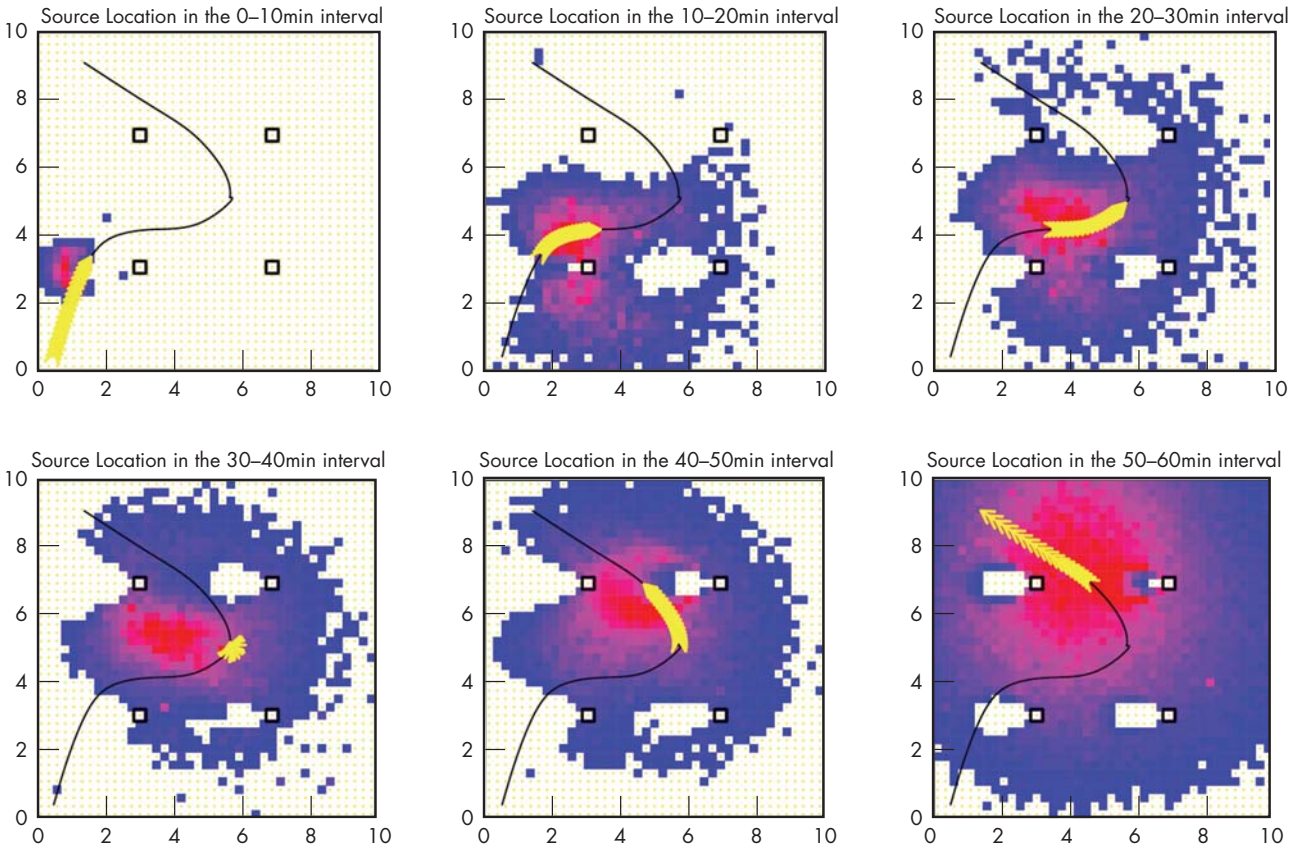

Example of event reconstruction for a release from a moving source. Color panels represent time evolution of probability distribution of the source location. Red represents high probability of source location, and yellow arrows represent the actual source location.

Project Goals

We are developing a flexible and adaptable data-driven event-reconstruction capability for atmospheric releases that provides quantitative probabilistic estimates of the principal source-term parameters, such as the time-varying release rate and location; predictions of increasing fidelity as an event progresses and additional data become available; and analysis tools for sensor network design and uncertainty studies. Our computational framework incorporates multiple stochastic algorithms, operates with a range and variety of atmospheric models, and runs on multiple computer platforms, from workstations to large-scale computing resources. Our final goal is a multi-resolution capability for both real-time operational response and high-fidelity multi-scale applications.

Relevance to LLNL Mission

This project directly contributes to the Laboratory's homeland and national security missions by addressing a critical need for atmospheric release event-reconstruction tools. It will support the rapidly growing number of operational detection, warning, and incident characterization systems being developed and deployed by the Department of Homeland Security (such as BioWatch, BWIC system, national BioSurveillance Initiative) and the Department of Energy (such as the Biological Warning and Incident Characterization System, chemical sensor networks, and the Department of Energy Nuclear Incident Response Team assets and deployments). The event-reconstruction and sensor-siting tools developed by this project are targeted for integration into the next-generation National Atmospheric Release Advisory Center (NARAC) and DHS's new Interagency Modeling and Atmospheric Analysis Center, based at LLNL.

FY2004 Accomplishments and Results

In FY2004, we: 1) implemented a 2-D prototype Bayesian Markov Chain Monte Carlo (MCMC) atmospheric event-reconstruction capability and tested it against a variety of scenarios and synthetic data; 2) developed a MCMC capability using the NARAC 3D Lagrangian particle dispersion code LODI, and tested it against field experiment data; 3) developed a Sequential Monte Carlo (SMC) methodology for time-dependent problems and tested it using synthetic data; 4) investigated optimization methods for determining proposal distributions and improving convergence; 5) evaluated the relative performance of MCMC and SMC methods using synthetic data; 6) designed a MCMC and SMC computational framework on massively parallel platforms; and 7) demonstrated the effectiveness of the SMC methodology for detecting moving sources using synthetic data.

Related References

1. Kosovic, B., G. Sugiyama, K. Dyer, W. Hanley, G. Johannesson, S. Larsen, G. Loosmore, J. K. Lundquist, A. Mirin, J. Nitao, and R. Serban, "Dynamic Data-Driven Event Reconstruction for Atmospheric Releases," *Second Sandia Workshop on Large-Scale PDE-Constrained Optimization,* Santa Fe, New Mexico, May 19-21, 2004.

2. Kosovic, B., G. Sugiyama, K. Dyer, W. Hanley, G. Johannesson, S. Larsen, G. Loosmore, J. K. Lundquist, A. Mirin, J. Nitao, and R. Serban, "Dynamic Data-Driven Event Reconstruction for Atmospheric Releases," *Eighth Annual George Mason University Transport and Dispersion Modeling Conference,* Fairfax, Virginia, July 13-15, 2004.

3. Sugiyama, G., K. Dyer, W. Hanley, G. Johannesson, B. Kosovic, S. Larsen, G. Loosmore, J. K. Lundquist, A. Mirin, J. Nitao, and R. Serban, "Markov-Chain Monte-Carlo and Sequential Monte-Carlo Approaches to Dynamic Data-Driven Event Reconstruction for Atmospheric Releases," *Second Workshop on Monte Carlo Methods*, Boston, Massachusetts, August 27-28, 2004.

FY2005 Proposed Work

Next year, we will: 1) implement a SMC atmospheric event-reconstruction capability based on NARAC operational models; 2) develop procedures and tools for input and model error quantification necessary for the event-reconstruction framework; 3) extend the event-reconstruction capability to handle complex terrain and an extended range of potential release types; 4) develop a multi-resolution capability for problems requiring multiple levels of models to accurately characterize the release event; 5) continue developing and testing efficient stochastic sampling and convergence algorithms; 6) explore methods for incorporating alternative input data types; and 7) enhance performance on massively parallel platforms for efficient event-reconstruction of complex atmospheric releases.

Low-Voltage, High-Precision MEMS SLM

For more information contact **Alex Papavasiliou**
(925) 423-1952, papavasiliou1@llnl.gov

The goal of this project is to make LLNL a leader in spatial light modulators (SLMs). By designing new lower voltage actuators, and bonding those actuators directly to controlling circuitry, we will overcome the fundamental limitations to the performance and scalability of MEMS SLMs (see Fig. 1).

SLMs are arrays of tiny movable mirrors that modulate the wavefronts of light. SLMs can correct aberrations in incoming light for adaptive optics or modulate light for beam control, optical communication, and particle manipulation. The first-generation MEMS SLMs have improved the functionality of SLMs while drastically reducing per-pixel cost, making arrays on the order of 1000 pixels readily available. By the nature of their designs, these MEMS SLMs are very difficult to scale above 1000 pixels, and have very limited positioning accuracy. By colocating the MEMS mirrors with CMOS electronics, we will increase the scalability and positioning accuracy. This requires substantial advances in SLM actuator design and fabrication (see Fig. 2).

Project Goals

The ultimate goal of this project is to make LLNL a leader in SLM technology. We will do that by demonstrating a small array (19 pixels) of MEMS mirrors that have an integrated closed-loop control system and a clear path to scaling that system up to thousands of pixels. We will also learn about bonding MEMS structures directly to controlling electronics.

Relevance to LLNL Mission

This work is relevant to a number of Laboratory projects, such as efforts in astronomy; nanolaminate deformable mirrors; laser control and beam-steering; and potentially in NIF preamplifiers. In biology, SLMs are useful for imaging and for particle manipulation.

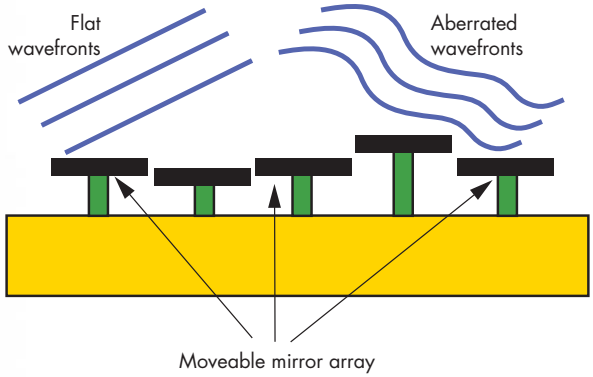

Figure 1. Schematic drawing of MEMS spatial light modulator.

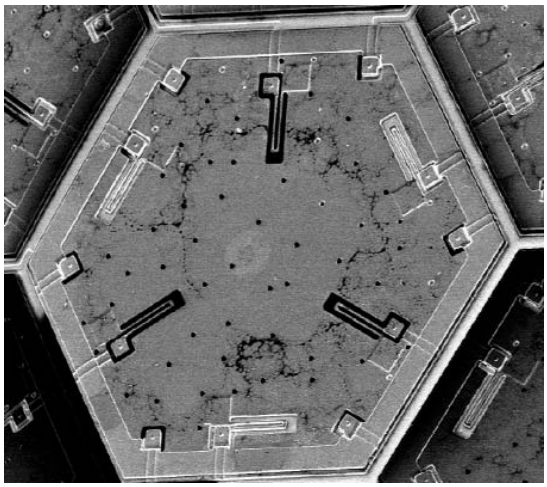

Figure 2. SEM of an actuator.

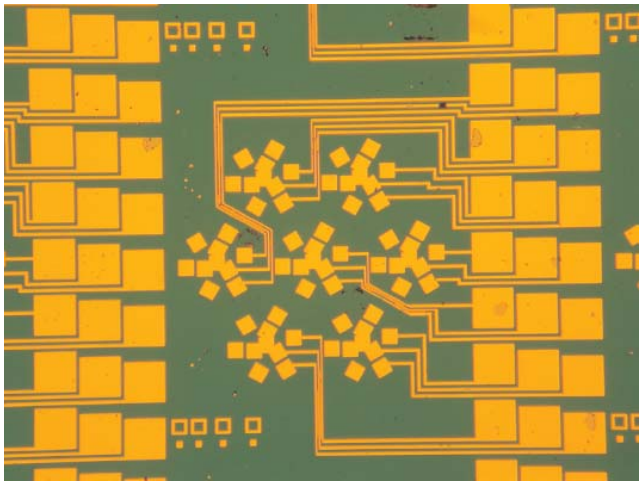

Figure 3. Microphotograph of dummy chip for bonding tests.

The bonding of MEMS to electronics has wide ranging applications, such as large-array chemical and biological sensors.

FY2004 Accomplishments and Results

We have made substantial progress in actuator design, fabrication, and electronics design.

We have created first-principles models of actuator structure; created optimal designs based on modeling work; designed a layout of the first-generation MEMS structures; fabricated the first-generation MEMS structures; demonstrated unbonded MEMS structures; and fabricated and delivered MEMS and dummy wafers to our bonding subcontractor (see Fig. 3).

We have moved toward a layout for the electronics chip that will eventually be bonded to the MEMS and control the SLM pixels. We have a schematic design for the analog circuits, and are poised to create a layout once software, technology files, and patent issues have been worked out.

Related References

1. Dimas, C. E., J. Perreault, S. Cornelissen, H. Dyson, P. Krulevitch, P. Bierden, T. Bifano, "Large-Scale Polysilicon Surface Micromachined Spatial Light Modulator," *Proceedings of Spie - the International Society for Optical Engineering*, **4983**, pp. 259-265, 2003.

2. Krulevitch, P. A., P. Bierden, T. Bifano, E. Carr, C. E. Dimas, H. Dyson, M. A. Helmbrecht, P. Kurczynski, R. S. Muller, S. S. Olivier, Y.-A. Peter, B. Sadoulet, O. Solgaard, E.-H. Yang, "MOEMS Spatial Light Modulator Development at the Center for Adaptive Optics," *Proceedings of Spie - the International Society for Optical Engineering*, **4983**, pp. 227-234, 2003.

3. Hickey, G. S., S. S. Lih, T. W. Barbee, Jr., "Development of Nanolaminate Thin-Shell Mirrors," *Proceedings of Spie - the International Society for Optical Engineering*, **4849**, pp. 63-76, 2002.

4. Cohn, M. B., K. F. Bohringer, J. M. Noworolski, A. Singh, C. G. Keller, K. Y. Goldberg, R. T. Howe, "Microassembly Technologies for MEMS." *Proceedings of Spie - the International Society for Optical Engineering*, **3511**, pp. 2-16, 1998.

FY2005 Proposed Work

In the second year of this project, we will concentrate on integrating simple electronics with MEMS. We will fabricate the electronics that are currently being designed. We will make improvements to the SLM technology, and use the bonding technology for second-generation MEMS devices.

Persistent Monitoring Platforms

For more information contact **Charles Bennett**
(925) 423-6131, bennett2@llnl.gov

We plan to build and test a model of the power plant for a stratospheric aircraft powered by thermal energy from the sun. Such an aircraft could maintain station over a designated ground location almost indefinitely, since it would not need fuel. We are developing a thermally-coupled system with an efficiency nearly an order of magnitude better than the state of the art (Helios), by creating the technology for a sun-tracking solar-heat collector, a thermal-storage reservoir, and a high-efficiency heat engine.

Project Goals

We will develop and validate the physics models to prove the principles involved in a solar thermal-powered aircraft, in preparation for constructing a prototype scale-model aircraft to demonstrate station-keeping capability at sea level. Successful demonstration of this technology would set the stage for construction of a stratospheric-altitude prototype capable of circumnavigating the globe.

We will also develop physics models for thermal transport, materials interactions, loss mechanisms, and engine performance in the stratosphere's environment.

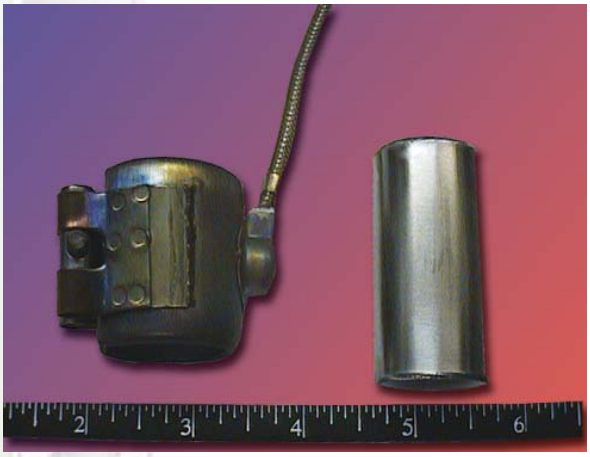

Figure 1. LiH experimental test capsule and heating unit.

Figure 2. LLNL's Jim Emig loading LiH into test capsule.

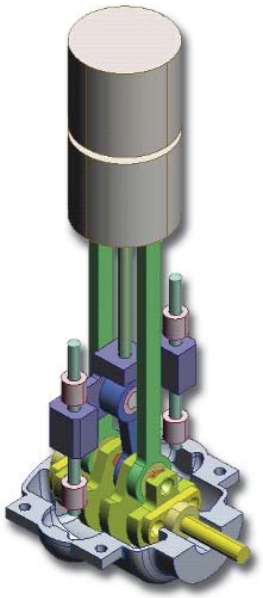

Figure 3. Conceptual design of our Stirling engine. Features include a power piston/cylinder wall, a displacer piston/cylinder wall, and crankcase feed-through journal bearing. There is virtually no limit to the operating altitude for the engine.

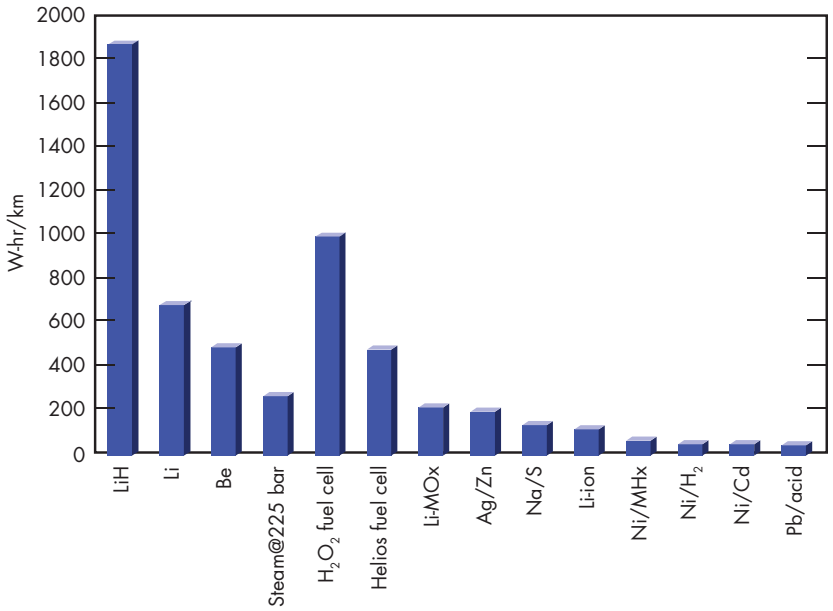

Figure 4. Chart showing LiH thermal energy compared to rechargeable batteries.

Relevance to LLNL Mission

Persistent surveillance, having essentially unlimited dwell-time over a region of interest, would enable the acquisition of a qualitatively new type of intelligence information for various national-security applications, such as countering the proliferation of weapons of mass destruction. Furthermore, inexpensive persistent surveillance has direct utility in border monitoring for homeland-security missions.

FY2004 Accomplishments and Results

We constructed a lithium hydride (LiH) thermal battery core, and developed a layered containment structure that can safely contain high-temperature, reactive LiH in equilibrium with a significant pressure of hydrogen gas (see Figs. 1 through 3). A thermal battery based on LiH has more than an order of magnitude higher specific energy capacity than the most advanced rechargeable electric batteries (see Fig. 4). We developed a comprehensive suite of physics models for each of the components in the thermal powered aircraft. The modeling study culminated in the submission of a patent application broadly covering the multiple aspects of a high-efficiency solar-powered aircraft.

FY2005 Proposed Work

For FY2005, we have two primary goals. One goal is to develop a heat engine whose thermal efficiency is at least 60% of the Carnot limit. To this end, we plan to closely couple computational fluid-dynamics models with experiments on a prototype Stirling engine. The second primary goal is to conduct laboratory experiments on the LiH thermal battery invention developed in the first year. We will use nondestructive evaluation techniques to monitor, in real time, the cooling characteristics of the thermal battery as it discharges, and compare the experimental observations with theoretical predictions.

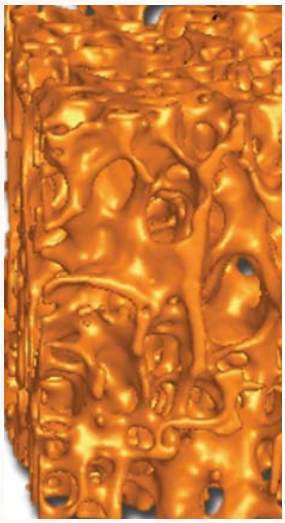

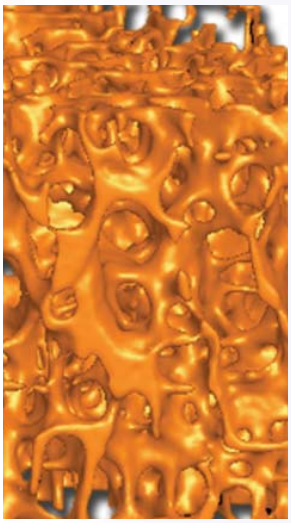

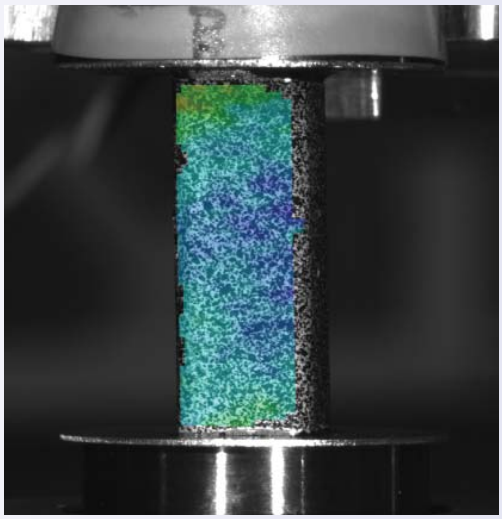

Other Technologies

Biomechanics of Spinal Fracture

For more information contact **John H. Kinney**
(925) 422-6669, kinney3@llnl.gov

Spinal fractures are the most common injuries associated with osteoporosis. The vertebra is composed of a latticework structure known as trabecular bone. We believe that most, if not all, of the tenfold decrease in the sustainable load of osteoporotic vertebrae can be explained by the age-related deterioration of trabecular architecture (see Figs. 1 and 2). In a departure from current thinking, we hypothesized that vertebral failure in older adults is initiated by loss of stability, or buckling.

Project Goals

Our goal was to test this hypothesis using advanced imaging and computational methods. Vertebrae from the skeletal archives of the Smithsonian Institution were imaged on the UC-Beamline at the Advanced Light Source, and geometric nonlinear finite-element analyses were used to simulate load displacement behavior from these "as-built" models. A positive test of the hypothesis will influence how osteoporosis is diagnosed and treated.

Relevance to LLNL Mission

The simulation effort is relevant to advanced simulation and computing in support of stockpile assessment, in which the ability to perform as-built, multiscale modeling is of the highest importance. The imaging tasks add further capabilities for NIF target characterization. Also, the application to nonlinear materials modeling of the osteoporotic fracture is relevant to LLNL's mission in bioscience to improve human health.

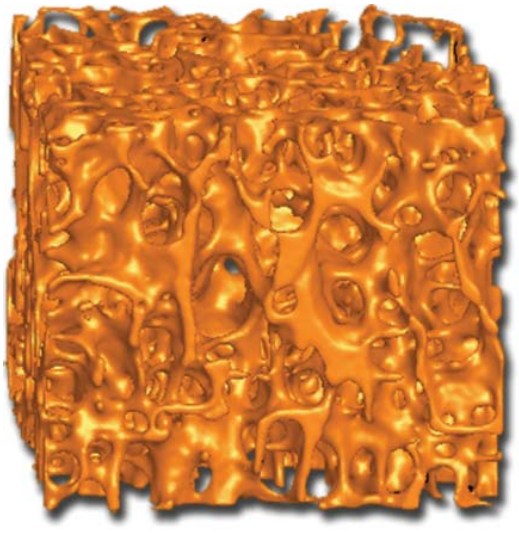

Figure 1. 3-D synchrotron micro-CT image of a 4-mm cube of trabecular bone from the interior of the vertebra of a 30-year-old female. The image shows bone of normal density and architecture: an open-celled foam with a significant number of plates aligned in the load-bearing direction.

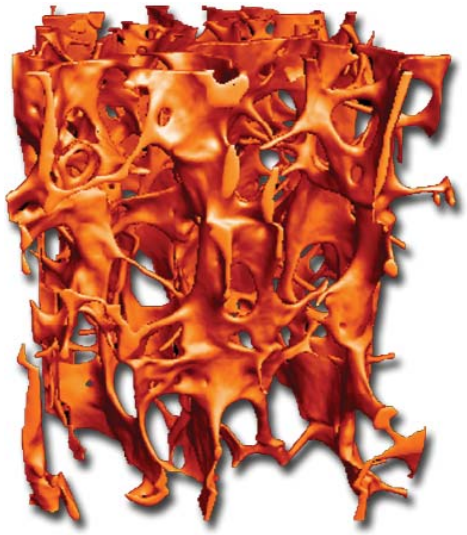

Figure 2. 3-D synchrotron micro-CT image of a 4-mm cube of trabecular bone from the interior of the vertebra of a 63-year-old male. The aged adult presents a markedly different trabecular architecture: fewer plate-like structures and many more high-aspect-ratio rod-like members.

FY2004 Accomplishments and Results

We discovered that there is a transition from strength-initiated failure to stability-initiated failure with age, where failure in osteoporotic vertebrae is mediated by instability of the individual trabecular members. We also uncovered evidence that osteoporotic vertebrae are hypersensitive to small imperfections. The small cavities caused by the cellular process of bone resorption are sufficient to destabilize the trabecular lattice under the right conditions. This provides a physical explanation of the clinical observation that bone remodeling is an independent predictor of fracture risk.

Figure 3 shows our results for tests on a 30-year-old female and a 63-year-old male. The distribution functions are superposed over the Euler hyperbola, as a function of applied stress (normalized to the yield stress of the tissue) and the slenderness ratio. At a slenderness ratio greater than the critical value, λ_c, failure occurs from elastic buckling of the trabecular members. At slenderness ratios less than λ_c, failure is initiated by yielding of the members. There appears to be an age-related increase in the fraction of trabecular members that have slenderness ratios greater than λ_c; the 30-year-old female has only a minor number of such members, while in the 63-year-old male, over 30% of the trabecular members are greater than λ_c.

The trabecular structures in Figs. 1 and 2 were meshed, and the stress-strain response was simulated on a parallel version of NIKE3D. The partitioning between the amount of nonlinear deformation from geometric nonlinear (elastic) response, and the nonlinear deformation from yielding, was examined as a function of the applied stress (normalized to the ultimate strength). In the 30-year-old female, the nonlinear deformation was entirely a result of tissue yielding, whereas, in the 63-year-old male the majority of the nonlinear deformation resulted from buckling of the trabecular members.

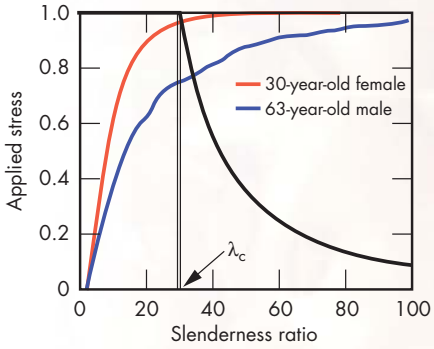

Figure 3. Graph showing the cumulative distribution functions of the slenderness ratios of the trabecular bone in two subjects of different ages. The critical value, λ_c, is indicated.

This complete reversal in the mechanisms of nonlinear deformation suggests that there may be a transition from stable lattice behavior to unstable lattice behavior, as a result of age-related loss of bone.

This work will change the diagnostic focus from simply measuring bone mass to considering factors that influence buckling, such as the aspect ratio of the trabeculae. Not only will risk estimates improve, but also it will be possible to select the optimal treatment strategies for an individual.

Related References

1. Kinney, J. H., and J. S. Stolken, "On the Importance of Geometric Nonlinearity in Finite-Element Simulations of Trabecular Bone Failure (Rapid Communication)," *Bone*, **33**, (494), 2003.
2. Kinney, J. H., and J. S. Stolken, "Response to Keaveny," *Bone*, **34**, (913), 2004.
3. Kinney, J. H., J. T. Ryaby, N. E. Lane, T. S. Smith, and J. S. Stolken, "An orientation Function for Trabecular Bone," *Bone*, in press.
4. Nalla, R. K., J. J. Kruzic, J. H. Kinney, and R. O. Ritchie, "Effect of Aging on the Toughness of Human Cortical Bone: Evaluation By R-Curves," *Bone*, **35**, pp. 1240–1246, 2004.
5. Nalla, R. K., J. S. Stolken, J. H. Kinney, and R. O. Ritchie, "Fracture in Human Cortical Bone: Local Fracture Criteria and Toughening Mechanisms," *Journal of Biomechanics*, in press.

Multiscale Characterization of bcc Crystals Deformed to Large Extents of Strain

For more information contact **Jeffrey Florando**
(925) 422-0698, florando1@llnl.gov

Experimental data are crucial in the process of construction and validation of multiscale crystal plasticity models, used in computer code simulations of materials deformed under extreme conditions such as high strain rate, pressure, and large extents of strain. The "6 Degrees of Freedom" experiment was designed specifically for validation of plasticity simulations and has provided data on the behavior of body-centered cubic (bcc) crystals that may well revolutionize how crystal plasticity models are developed and implemented in computer code simulations.

The experimental data and simulation efforts, however, have focused on relatively small extents of plastic deformation (0.5%). Both experiments and modeling must now be extended to large-strain deformations on the order of tens of percent. At these larger extents of strain, multiscale characterization tools can be better used to understand the fundamental behavior.

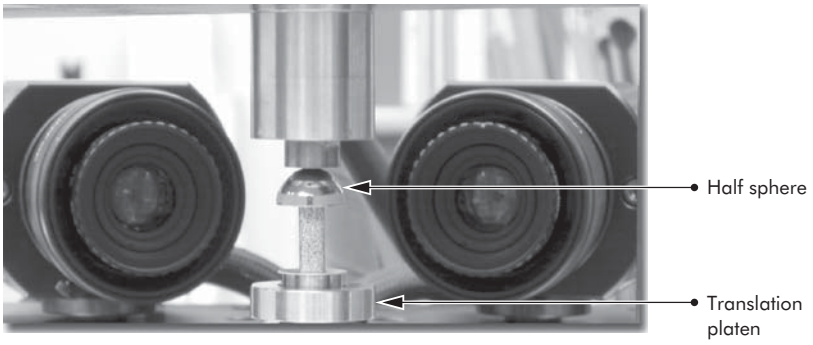

Figure 1. Photograph of the large-strain testing set-up.

Project Goals

Our goal is to develop large-strain experiments that will provide the essential data to enhance the multiscale modeling capability, through the creation of continuum strength models and the validation of future simulations. When completed, this work will increase the Laboratory's ability to develop predictive strength models for use in computer code simulations.

Relevance to LLNL Mission

Understanding and simulating the plastic, or nonreversible, deformation of bcc metals, is a major component of LLNL's Stockpile Stewardship Program and is intended to simulate future NIF experiments.

FY2004 Accomplishments and Results

Our accomplishments and results include:

Strain and slip system measurement. A commercial 3-D image correlation system was purchased and is being used in our deformation experiments to measure the strain nonuniformities in the sample. A picture of the set-up is shown in Fig. 1. Figure 2 shows a strain map of the image correlation result from a compression experiment performed on a single crystal Mo sample. Figure 2 also shows the corresponding stress and strain data in comparison with strain gage data. The close match between the two experiments verifies the accuracy of the image correlation technique. We have also performed a detailed analysis of the slip traces on the surface of the sample, and using that

information, have calculated the slip system activity that is consistent with the experimental data.

Stress State. A detailed FEM analysis has been performed on a deformed sample to examine the nonuniformities in the stress state. The analysis shows that at 2% strain the uniaxial stress in the sample varies by +/– 20%.

Large strain validation experiment. The development of a massively parallel dislocation dynamics code (ParaDis) has led to the ability to perform a dislocation-dynamics (DD) simulation to 3% strain. An experiment on a symmetrically oriented sample tested at 500 K to 10% strain has been conducted for the purpose of validating the simulation. The results of the experiment in comparison to the DD simulation show that while qualitatively the results appear similar, quantitatively, there is nearly a 4-× difference in the stress values. Although there is still large disparity between the simulation and the experiments, this comparison is the first step in increasing interactions between experimentalists and modelers to understand the necessary physical parameters required for future validation tests.

Related References

1. Bulatov, V. V., "Current Developments and Trends in Dislocation Dynamics," *J. Computer-Aided Mat. Design*, **9**, p. 133, 2002.
2. Lassila, D. H., M. M. Leblanc, and G. J. Kay, "Uniaxial Stress Deformation Experiments for Validation of 3-D Dislocation Dynamics Simulations," *J. Eng. Mat. Tech.*, **124**, p. 290, 2002.
3. Schmidt, T., J. Tyson, and K. Galanulis, "Full-Field Displacement and Strain Measurement Using Advanced 3D Image Correlation," *Photogrammetry: Part I, Exp. Techniques*, **27**, p. 47, 2003.

FY2005 Proposed Work

A second pair of cameras has been purchased and will be incorporated into our existing experimental set-up. We will continue to remachine and test single crystal Mo samples to achieve larger strains. Characterization of the deformed samples in collaboration with the University of California, Berkeley, will also continue. We will also begin performing experiments on Ta single crystals. The results of these experiments and characterizations will be compared with simulations to further the understanding of the deformation mechanisms in these materials and to begin validation of the DD code.

Accurate validation experiments out to large extents of strain are still required for the continued development of computer code simulation capabilities.

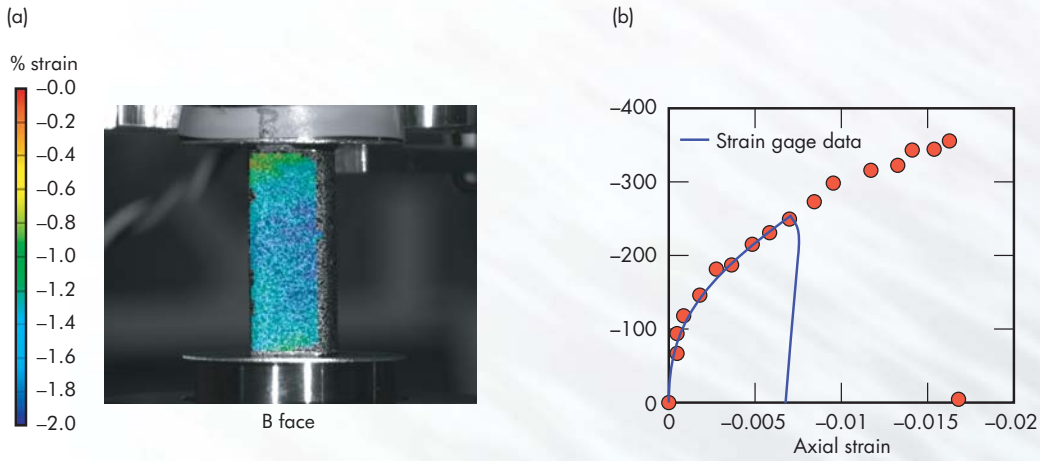

Figure 2. (a) Axial strain results using the image correlation system. (b) Corresponding stress/strain curve. The axial strains are calculated by averaging over an area similar to the active region of a strain gage.

Space-Time Secure Communications for Hostile Environments

For more information contact **James Candy**
(925) 422-8675, candy1@llnl.gov

Communicating in a complex environment is a daunting problem. Such an environment can be a hostile urban setting populated with a multitude of buildings and vehicles, or military operations in an environment with obstructive topographic features, or even a maze of buried water pipes servicing a city. These inherent obstructions cause transmitted signals to reflect, refract, and disperse in a multitude of directions, distorting them at network receiver locations.

These are the communications problems we solve using wave propagation physics (see Fig. 1). We develop time-reversal (T/R) communications using sensor arrays in a hostile environment, incorporating theory, simulation and experiments.

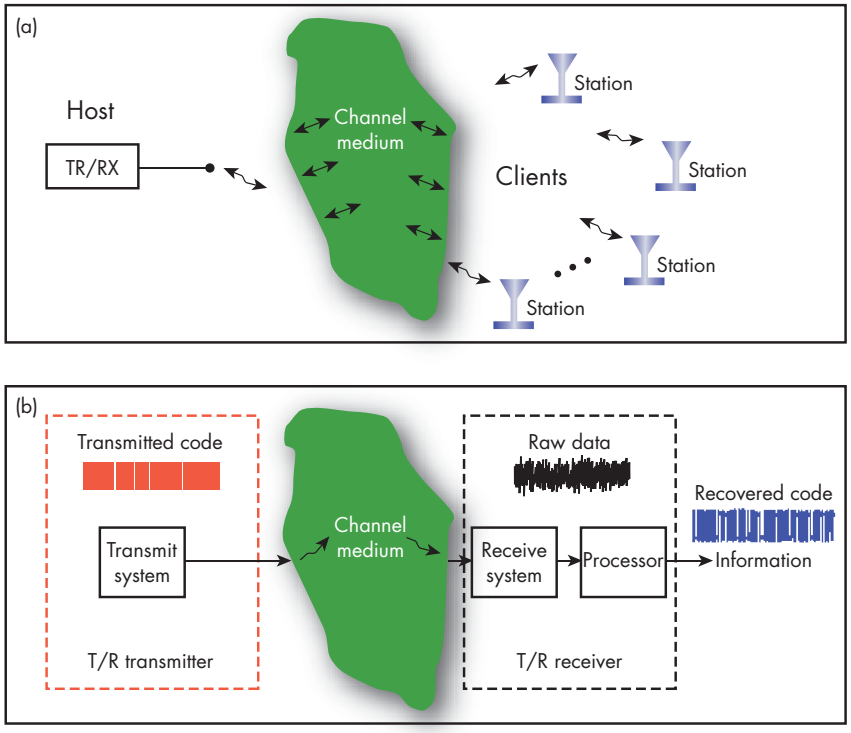

Figure 1. Representation of communications in a hostile environment: (a) the basic problem, including the host T/R, hostile medium, and client receiver stations; (b) T/R receiver solution, showing the transmitter, medium, and a particular T/R receiver structure extracting the coded information from the distorted received data.

Project Goals

Successful development and demonstration of T/R receiver performance will lead to the next generation advance for military and defense applications, as well as potential commercialization. Ultimately, our success will provide improved communications in noisy, distorted environments, with a potential breakthrough technology for both military and civilian (commercial) applications. This effort is aimed at developing a core competency in wireless communication networks, and falls within the advanced sensor and instrumentation competency area.

Relevance to LLNL Mission

Both the maintenance of communications in a strong multipath environment, and the protection of the communication against intercept, are important. Thus, there is a strong need for reliable channels in corrupting environments, with the additional feature that they be secure. Secure communications can be derived from T/R principles that will lead to novel applications, ranging from military applications (such as battlefield communications, urban warfare, tunnel complexes, and pipes) to the hostile urban environment. The T/R receiver technology also promotes protection of communication channels against intercept, and thus supports LLNL's national security mission as well as homeland defense applications.

FY2004 Accomplishments and Results

In FY2004, we accomplished the following: 1) completed the theoretical development of T/R multichannel receivers; 2) developed an eight-element T/R array capability; 3) performed experimental designs validating multichannel T/R receiver designs; 4) demonstrated a critical

theoretical development for future electromagnetics (EM) experiments, using 1-bit A/D conversions for T/R receivers; 5) conducted controlled experiments demonstrating T/R receiver performance; 6) designed a highly scattering medium (on an aluminum plate); 7) investigated the development (hardware) for an EM receiver design; and 8) initiated spin-off DARPA projects using related T/R concepts and team members.

Figures 2 and 3 show our controlled experimental set-up and sample results.

Related References

1. Candy, J., B. Guidry, A. Poggio, C. Robbins, and C. Kent, "Multichannel Time Reversal Communications in a Highly Reverberant Environment," *Journal of the Acoustical Society of America*, **115**, p. 2467, 2004.

2. Guidry, B., J. Candy, A. Poggio, A. Meyer, and C. Kent, "Experimental Design and Processing for Time-Reversal Communications in a Highly Reverberative Environment," *Journal of the Acoustical Society of America*, **114**, p. 2367, 2003.

3. Chambers, D., C. Kent, and A. Meyer, "Time-Reversal Communication Through a Highly Reverberant Medium," *Journal of the Acoustical Society of America*, **114**, p. 2468, 2003.

4. Chambers, D., J. Candy, S. Lehman, J. Kallman, and A. Poggio, "Time Reversal and the Spatio-Temporal Matched Filter," *Journal of the Acoustical Society of America*, **116**, p. 1348, 2004.

5. Candy, J., A. Meyer, A. Poggio, and B. Guidry, "Time-reversal Processing for an Acoustics Communications Experiment in a Highly Reverberant Environment," *Journal of the Acoustical Society of America*, **115**, pp. 1621-1631, 2004.

FY2005 Proposed Work

We will continue developing a fundamental theoretical basis for T/R communications by pursuing both simulations and laboratory evaluations. Evaluation of the techniques in a hostile environment will lead to 1) theoretical development; 2) simulation-based evaluation of the benefits of T/R; 3) controlled laboratory validation of the simulation results; 4) an operational brass-board design of an actual T/R receiver for applications, using the 1-bit A/D concept; 5) development of new T/R principles using 1-bit A/D converters; and 6) participation in T/R communications experiments in wideband EM and acoustic-pipe experiments.

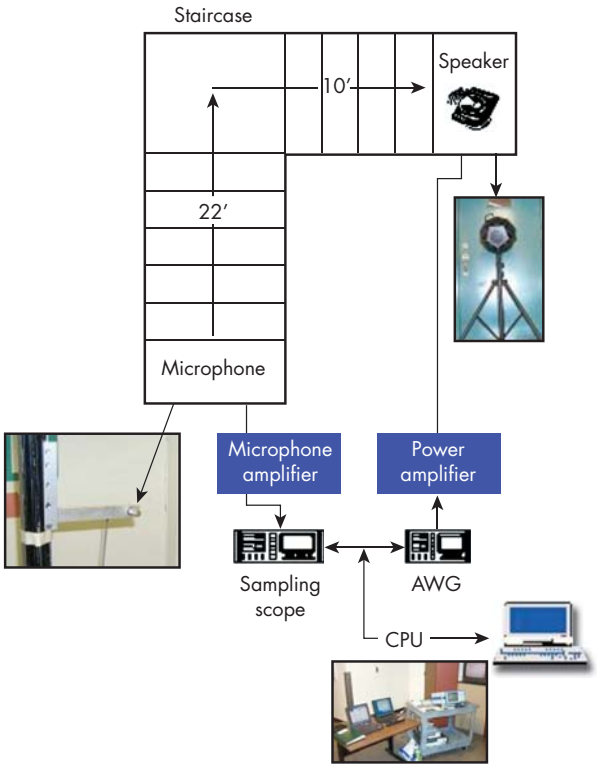

Figure 2. Controlled experimental set-up for T/R receiver designs: sound source (loud speaker), hostile medium (stairwell with obstructions), and microphone receiver with the T/R receiver implemented in software on the computer.

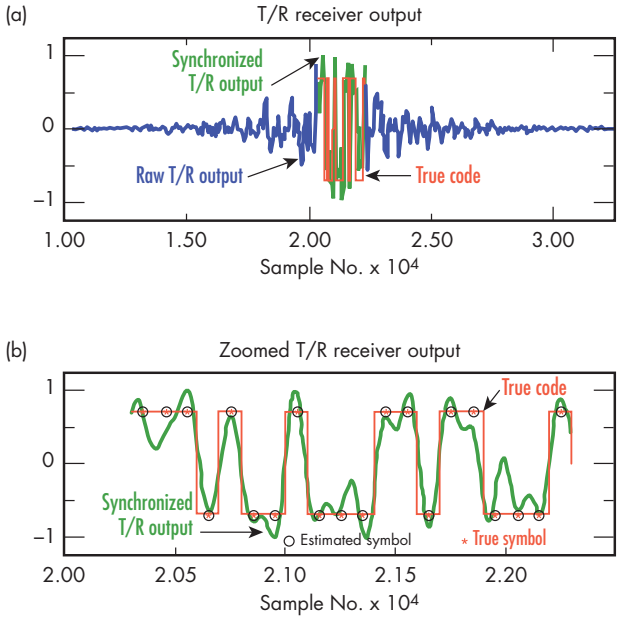

Figure 3. Time-reversal receiver output for the controlled stairwell experiment: (a) raw T/R receiver output, with synchronized code and true code superimposed; (b) zoomed synchronized T/R output, with both quantized code information extracted and true code superimposed. The estimated symbol and the true symbol are overlaid, demonstrating flawless T/R receiver operation.

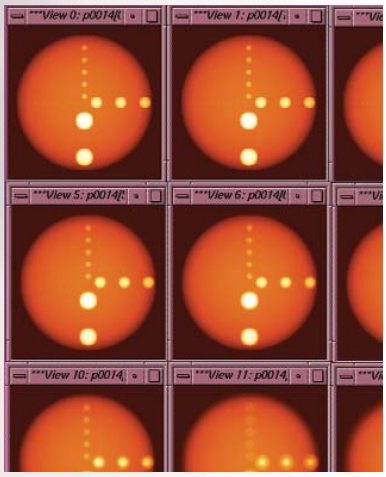
***View 0: p0014[t
***View 1: p0014[t
***View 5:: p0014[t
***View 6: p0014[t
***View 10: p0014
***View 11: p0014

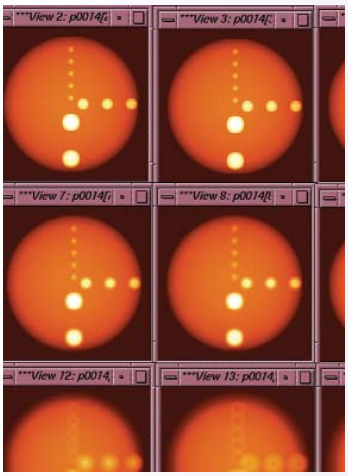

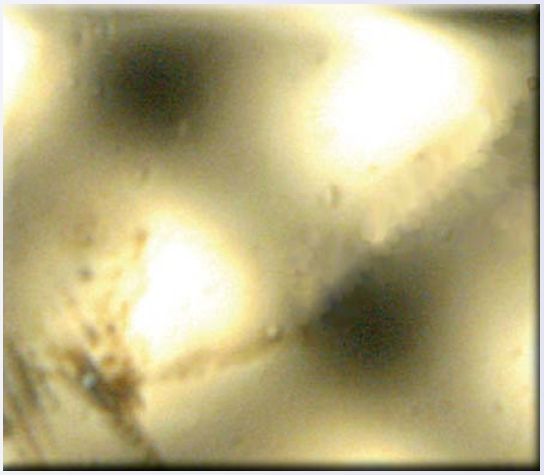

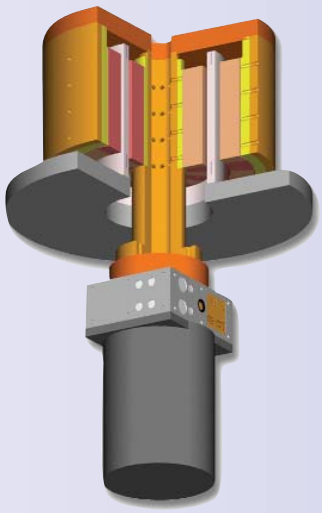

Author Index

Author Index

Manuscript Date April 2005
Distribution Category UC-42

This report has been reproduced directly from the best available copy.

Available for a processing fee to U.S. Department of Energy and its contractors in paper from
U.S. Department of Energy
Office of Scientific and Technical Information
P.O. Box 62
Oak Ridge, TN 37831-0062
Telephone: (865) 576-8401
Facsimile: (865) 576-5728
E-mail: reports@adonis.osti.gov

Available for sale to the public from
U.S. Department of Commerce
National Technical Information Service
5285 Port Royal Road
Springfield, VA 22161
Telephone: (800) 553-6847
Facsimile: (703) 605-6900
E-mail: orders@ntis.fedworld.gov
Online ordering: http://www.ntis.gov/products/

Or

Lawrence Livermore National Laboratory
Technical Information Department's Digital Library
http://www.llnl.gov/library/

This document was prepared as an account of work sponsored by an agency of the United States Government. Neither the United States Government nor the University of California nor any of their employees, makes any warranty, express or implied, or assumes any legal liability or responsibility for the accuracy, completeness, or usefulness of any information, apparatus, product, or process disclosed, or represents that its use would not infringe privately owned rights. Reference herein to any specific commercial products, process, or service by trade name, trademark, manufacturer, or otherwise, does not necessarily constitute or imply its endorsement, recommendation, or favoring by the United States Government or the University of California. The views and opinions of authors expressed herein do not necessarily state or reflect those of the United States Government or the University of California, and shall not be used for advertising or product endorsement purposes.

This work was performed under the auspices of the U.S. Department of Energy by the University of California, Lawrence Livermore National Laboratory under Contract W–7405–Eng–48.
ENG-04-0103-AD

ENGINEERING @ LLNL

Lawrence Livermore National Laboratory
University of California
P.O. Box 808, L-151
Livermore, California 94551
http://www-eng.llnl.gov/